Theses and Dissertations

December 2016

Experimental Investigation of Chicken Manure Pyrolysis and Gasification

Mohamed Hussein Hussein
University of Wisconsin-Milwaukee

Follow this and additional works at: https://dc.uwm.edu/etd

Part of the Mechanical Engineering Commons

EXPERIMENTAL INVESTIGATION OF CHICKEN MANURE PYROLYSIS AND

GASIFICATION

by

Mohamed S. I. Hussein

A Dissertation Submitted in

Partial Fulfillment of the

Requirements for the Degree of

Doctor of Philosophy

in Engineering

at

The University of Wisconsin-Milwaukee

December 2016

EXPERIMENTAL INVESTIGATION OF CHICKEN MANURE PYROLYSIS AND
GASIFICATION

by

Mohamed S. I. Hussein

The University of Wisconsin-Milwaukee, 2016
Under the Supervision of Professor Ryoichi Amano

The dependency on renewable resources of energy in power production is a necessary

step that mankind has to take if we want our advances in life and technology to resume.

In a century or two, fossil fuels will be depleted, and if we do not start to take action,

Energy will be the most expensive and rare item on our planet. Biomass is one of the

sources of renewable energy with an advantage of being the closest in characteristics to

fossil fuels. The evolved gases are similar to fossil fuel gases which make it the easiest

source to switch to, with the least infrastructure required. In this doctoral thesis, the

experimental study of the Pyrolysis and gasification of chicken manure is presented. Both

evolved gas analysis (EGA) and thermo-gravimetric analysis (TGA) have been

investigated in details using different gasifying agents. In EGA, the concentrations and

the mass flow rates of different evolved gases were presented and the mass flow rates

were used to calculate the energy and carbon conversion efficiencies. Different gases

including (N_2, air, CO_2, steam, and mixtures) were used as the gasifying agents, and the

effect of temperature 600-1000°C was tested. The effect of adding oxygen to steam

gasification at 900°C was studied and presented in details. In TGA, the degradation and

rate of degradation of the mass were analyzed with different gases (N_2, air, and CO_2) for

various heating rates (5-40°C/min.) using the extent of reaction, α. The order of reaction

model was then used to find the chemical kinetic parameters for the different gases.

TABLE OF CONTENTS

LIST OF FIGURES

LIST OF TABLES

LIST OF NOMENCLATURE

A	Pre-exponential constant in Arrhenius equation
DTA	Differential thermal analysis
DTG	Derivative Thermo-gravimetric
E	Energy
EGA	Evolved gas analysis
FTIR	Fourier Transform Infrared
GC	Gas chromatography
$K(T)$	Temperature dependent rate of reaction
m	Mass
n	Order of reaction
P&G	Pyrolysis and Gasification
R	Universal gas constant
t	Time
T	Temperature
TGA	Thermo-gravimetric analysis
v	Mass of volatile at any time
w	Mass of biomass
x	Conversion ratio (normalized converted mass)

Greek

α	Extent of reaction
β	Linear heating rate
Δ	Change

η	Efficiency

Subscripts

a	Activation
c	Converted / Carbon
f	Final
o	Initial
r	Residual
t	At time t

ACKNOWLEDGMENTS

Chapter 1 -   Introduction

1.1 Chicken manure in the state of Wisconsin

According to the United States Census Bureau in August 2014 the population of the United States is estimated to be 319 Million. If we know that the average consumption of chicken per capita is 84.6 Ib/year, the grow-out period for chicken is about 47 days and average chicken weight is 3.5 Ib, it can be estimated that the United States consume about 7792 Million chickens/year. The average chicken produces 2.5 Ib of dry manure throughout its grow out period. So, USA is producing 20,000 M Lb (8849 M kg) of chicken manure/year. The average calorific value of the chicken manure is 14 MJ/kg. In other words, the energy in the chicken manure is equivalent to the energy in 20 M barrels of Texas oil (Figure 1-1).
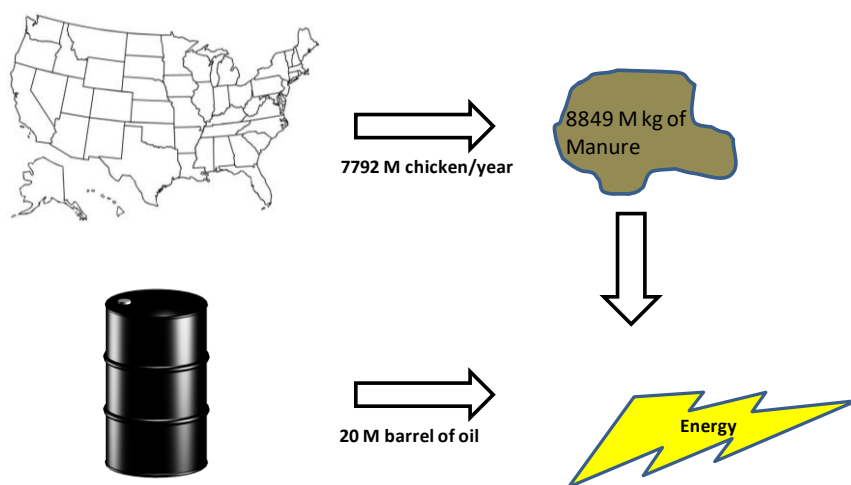
Figure 1-1: Available energy in chicken manure produced by chicken consumed in the United States per year

Chicken manure is mostly used as a fertilizer for it is rich in calcium, Nitrogen, and Phosphorous. But because of the dense chicken production, the production of the chicken manure exceeds the soil requirements. In the state of Maryland, it was found that the concentration of phosphorous in the soil is 60% higher than the levels required for plant growth, (Ridlington, 2016)[44] which made phosphorous, a soil pollutant. In order to avoid these risks, the manure should be transported to agricultural locations far from the chicken farms. Pathogens find chicken manure as a perfect environment to reproduce making the chicken manure a carrier for infection and diseases. Transportation requires special handling, disinfection, and extra costs. So how can we make use of the energy in the chicken manure?

1.2 Primitive usage of chicken manure as a source of energy

Manure has been used as a clay oven fuel for centuries, in some countryside and developing countries; it is still being used till this day. Manure is dried in the sun for several days to get rid of the moisture and most of the undesirable odors then used as a fuel in a similar manner as coal. Chicken manure can be burnt to generate heat, but in its solid state, it is considered as a low-quality solid fuel. And it cannot be easily used to produce electricity.

1.3 Pyrolysis and Gasification (P&G)

Anaerobic digestion provides a good solution, but the health issues are not resolved. Another way is Pyrolysis and gasification processes (Figure 1-2: Pyrolysis and gasification mechanisms). Pyrolysis is the decomposition of organic material at an elevated temperature in the absence of oxygen or halogens. The complex organic material

like manure decomposes into lighter organic gaseous and liquid fuels while solid carbon (char) is a bi-product of the process. Gasification process of the char can then take place at higher temperatures and in the presence of steam, carbon dioxide or a very fuel rich mixture of oxygen. Both the Pyrolysis and Gasification processes products can be used as fuels.
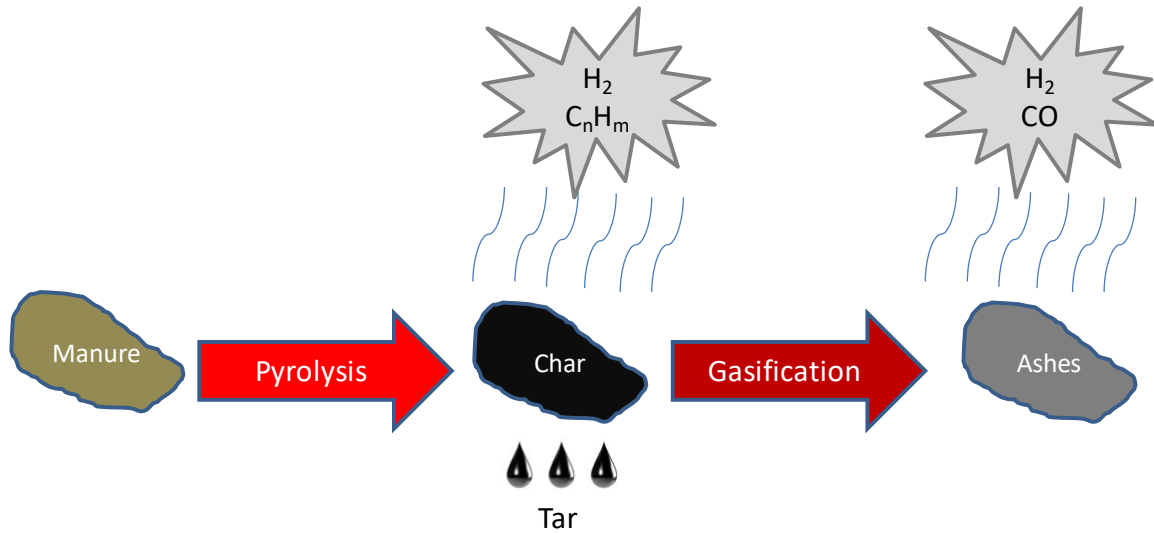
Figure 1-2: Pyrolysis and gasification mechanisms

The most practical way for disinfecting the chicken manure is by heating to a temperature higher than $90^{o}C$. But if the manure is heated to $200^{o}C$ (Pyrolysis) volatile organic compounds will evaporate and can be used as a fuel. And if an active gaseous agent was used and the temperature was increased above $600^{o}C$, we can gasify the leftover carbon from the Pyrolysis process and claim another portion of energy. The leftover ashes will be rich in calcium and other minerals that can still be used as a health-risk free fertilizer. Converting the chicken manure from its solid state to a gaseous fuel makes it easier to control the combustion and make it more possible to generate electricity from the higher quality gaseous fuel. The heat energy required for the Pyrolysis and Gasification processes can be generated by burning some of the evolving

gaseous fuel. So, the whole process is self-sustainable with the add-on of some excess gaseous fuel that can be used as needed.

Studying the different factors affecting the gasification process is critical. Some of the main factors are the temperature, gas flow rate, type of gas used, size of manure particles and the composition of the manure. In this study, a comprehensive study of the different factors will be carried out experimentally to determine the optimum operating conditions that would lead to faster conversion rates and higher quality gas produced.

1.4 Organization of Material

Chapter 1 gives a brief introduction to the importance of utilizing chicken manure as a source of energy then defines Pyrolysis and gasification

Chapter 2 presents a literature review of some of the previous work on Gasification and the techniques used for studying this process.

Chapter 3 gives a detailed description of the experimental setup, the different setups used, the test procedures, the data processing, and the cases studied.

Chapter 4 discusses the TGA and DTA for the different cases considered.

Chapter 5 details the EGA and its results for the different cases studied.

Chapter 6 Conclusion.

Chapter 2 -   Literature Review

2.1 Introduction:

Gasification is a series of sequential thermally driven chemical processes, where an organic material of complex chain of hydrocarbons is thermally degraded as it reacts with gaseous agents into simpler compositions including fuel ready for combustion. The organic materials used may be wood, plastics, animals manure..., etc. Meanwhile, the produced materials could be ashes, char (carbonaceous solids), oils, gases, and the produced gaseous fuel (syngas or synthesis gas). The chemical processes are usually arranged as follows: Drying, Pyrolysis, and Oxidation/Reduction (i.e. Gasification). The resultant fuel (CO and H_2) can be directly used in combustion for power generation.

Gasification as a biomass technology is considered as a renewable energy system because of the continuous availability of the organic materials in nature, the same as the solar and the wind energies. What would make biomass technology preferable over fossil fuels and the other renewable energy sources is that it makes it easier to utilize the currently installed equipment, like diesel engines, to generate power; clean fuel like hydrogen can be produced, and saves expenses of excavation and extraction compared to fossil fuels.

2.2 The history of gasification

Van Helmont (1609) also known as the pneumatic chemist was the first to discover that gases could be produced by thermal decomposition of wood or coal (*NETL, 2015*)[35]. Some other scientists developed the patents for the production of gases (e.g. town gas, water gas) for lighting and heating purposes. Others used the produced gases for the internal combustions engines

5

instead of steam during the late 1800s and the early 1900s using coke, coal, and wood (Breault, 2010)[7]. In World War I and II, because of the difficulties in securing permanent access to petroleum, wood and coal, gasifiers were heavily used (Dry, 1996)[13] to supply liquid vehicles fuels, especially in Germany (Reed, 1988)[43]. Gasification technology spread in Europe and several Asian and African countries during the 40s as the fuel supplier for the automobiles. After WW II, the petroleum was reachable and easily cleaned and derived from several fluids (gases, heavy and light liquids). Taking advantage of the less hazardous extraction, high calorific value and better flowing characteristics in processing and transportation, the industries started to rely on the petro-fuels more than the coal and solid organics. The concern was decreased except few investments (e.g. Sasol I) to share in the production of diesel, gasoline and chemical compounds using coal gasification (Hoogendoom, et al., 1981)[15]. After the oil trade embargo in 1973 and the obvious need to lessen the usage of the reserves, gasification regained interest to fulfill this energy gap. Individual efforts and governmental decisions of some countries contributed in reviving the technology in the transportation, appliances and power generation (NAS, 1983)[33]. One of the greatest companies in the scope, Sasol Synfuels, is operating two plants "Sasol II" and "Sasol III" since the mid-80s. The plants contain coal gasifiers that convert bituminous coal into synthesis gas of (CH_4, CO, and H_2) (Van Dyk, Keyser, & Coertzen, 2006)[51]. Recently much research on the gasification of Biomass has been conducted as a response to the fear of energy shortage in case of depletion of fossil fuels. (White, Catallo, & Legendre, 2011)[55], (Mermoud, Golfier, Salvador, Van De Steene, & Dirion, 2006)[30], (Song, Wu, Shen, & Xiao, 2012)[47]. Different studies on the G&P processes are discussed in the following sections.

2.3 Thermo-gravimetric analysis (TGA)

Thermo-Gravimetric Analysis (TGA), is the study of the effect of different thermal processes on the mass of substance. The various processes can be P&G, Evaporation, or any other chemical reaction. The sample is subjected to elevated temperatures and the mass of the sample and time are monitored while the different processes are taking place. If the first derivative of the mass-time curve is calculated (dm/dt) a derivative thermogravimetry (DTG) is derived which can provide the maximum reacting rates and the corresponding temperatures.

White et al.,2011 [55], did an extensive review of the different thermal analyses, the kinetics of Pyrolysis and different kinetics models, in their study, they referred to the famous Arrhenius rate expression that was used as the first step of almost any kinetics model,

$$k(T) = A \exp\left(\frac{-E_a}{RT}\right) \tag{2-1}$$

Even though A is slightly dependent on the temperature, it is usually considered as a constant. Two main techniques are then utilized to find the reaction kinetics; the isothermal and the non-isothermal techniques.

In the isothermal technique, the temperature is fixed, and the following canonical equation is used

$$\frac{d\alpha}{dt} = k(T)f(\alpha) = A \exp\left(\frac{-E_a}{RT}\right)f(\alpha) \tag{2-2}$$

where f(α) is a function depending on the reaction mechanism and dα/dt is the rate of the isothermal process, and the extent of reaction α is given by:

$$\alpha = \frac{w_o - w_t}{w_o - w_f} = \frac{v_t}{v_f} \tag{2-3}$$

In the non-isothermal technique eqn. (2.2) is written as:

$$\frac{d\alpha}{dT} = \frac{d\alpha}{dt} \cdot \frac{dt}{dT} \qquad (2\text{-}4)$$

$$\frac{d\alpha}{dT} = \frac{k(T)}{\beta} f(\alpha) = \frac{A}{\beta} \exp\left(\frac{-E_a}{RT}\right) f(\alpha) \qquad (2\text{-}5)$$

The reaction order models are often used where:

$$\frac{d\alpha}{dT} = k(T)(1-\alpha)^n \qquad (2\text{-}6)$$

In their review, they also discuss more kinetics models, and they show the results of these models on agricultural Biomass Pyrolysis. They also describe the different thermal degradation steps, starting by the evaporation of the free moisture followed by the decomposition of less stable polymers at lower rates than the more refractory components at higher temperatures. At a temperature around 400^oC only char residue is present after what they called the primary decomposition phase. Then at higher temperatures the second slow stage of aromatization takes place.

(Mansaray & Ghaly, 1999)[28] used eqn. (2.2) with the reaction order model to calculate the reaction kinetic parameters for the P/G of rice husk using a controlled environment of oxygen. The used equation was written as:

$$\frac{dX}{dt} = -A \exp\left(\frac{-E_a}{RT}\right) X^n \qquad (2.7)$$

Where X here is equal to (1-α) and was denoted as the weight of sample undergoing reaction. Four varieties of rice husk were tested using pure oxygen from ambient temperature to 700 ^{o}C at a heating rate 20 ^{o}C/min. The rate of thermal decomposition was higher in the first phase than the second phase. The different rates made it necessary to divided the kinetics into two discrete global reactions. The response of the four rice husk varieties was very similar. The TGA and

DTG analysis showed the two most critical phases of the gasification overlapping between 206-467 ^{o}C. An intermediate temperature was chosen on the TGA curves to separate these two regions. The highest degradation rates were observed at a temperature close to 290 ^{o}C for the four different varieties. Approximately 20% of the mass was a residue after the rate of reaction was almost zero. The kinetic parameters; activation energy, Arrhenius constant, and order of reaction were calculated from Eqn. 2.7. The authors then found a necessity for studying the effect of the heating rate on the kinetic parameters.

(Yanik, Stahl, Troeger, & Sinag, 2012)[59], studied the Pyrolysis of different algal biomass from the black sea, using the TGA method. They heated the biomass in a nitrogen environment to an 800°C temperature and monitored the change in the mass and the rate of mass conversion. The total percentage of weight conversion ranged between 55-70%, and the rate of conversion was highest between 250-450 ^{o}C, depending on the algae tested. The main contents of the algal biomass are carbohydrates and proteins whose degradation temperatures lies between 190-390°C which justifies their findings.

(Mermoud, Golfier, Salvador, Van De Steene, & Dirion, 2006)[30], studied the steam gasification of a single particle of charcoal at different temperatures, steam concentration, flow velocity and particle size both numerically and experimentally. The gasification time was proportional to the particle size and inversely proportional to the temperature and the steam concentration. They then utilized a particle mechanism to simulate the gasification process, and their results were acceptable up to 60% conversion. The mass fraction of the gas yields was calculated using the numerical model. For larger particle sizes, the numerical results were not accurate beyond 60% that they concluded to be due to asymmetry and fractures in the sample after certain conversion percentage.

Van de steen et al., 2011[50], studied the effect of changing the reacting gas on wood gasification. In their study, steam, carbon dioxide, and oxygen gasification at temperatures ranging between 800-1050°C, was analyzed both experimentally and numerically. It was found that the most important parameter was the particle thickness, and they were able to modify a particle mechanism using their experimental data. The conversion was faster as the temperature and the gas concentration increased. Oxygen showed the highest conversion rate while carbon dioxide had the lowest conversion rates.

(Wang, Guo, Wang, & Luo, 2011)[54], used the three most important components of biomass; hemicellulose, cellulose, and lignin as their samples and mixed the three components with different percentages. The samples were heated in a Nitrogen atmosphere from 30-800°C. The weight of the sample was measured over time. Hemicellulose decomposed in the lower temperature range 200-350°C with maximum conversion rate at 260°C, Cellulose in a higher range 260-430°C with maximum conversion rate at 360°C, while lignin in the highest range 200-500°C with maximum conversion rate at 370°C. For the mixture samples, the DTG curves showed more than one peak at the 260 and 370°C. It was also found that the presence of the three components promotes the gasification process due to the interaction between them.

Mermoud et al., 2006 [31], used steam in the gasification of large wood char particles. They implemented different Pyrolysis heating rates (2.6-900°C/min.) and studied the effect on mass, density, and porosity. The higher heating rate decreased the apparent density and increased the porosity. The apparent density followed a linear evolution versus the log of the heating rate. The ratio of the initial to final volume was approximately the same for different heating rates which means a higher volatile matter yield at higher heating rates. The gasification rate of the char prepared at the 900°C/min.; the heating rate was 2.6 times higher than the less porous char made

at the 2.6 ^{o}C/min. when both were gasified at the same 1200 K temperature with 20% by volume steam-nitrogen mixture gas.

2.4 Differential thermal analysis

Differential thermal analysis (DTA) is the time temperature recording of the difference between temperature of the tested sample and a reference substance as both being subject to the same uniform heating or cooling. DTA was first introduced by (Chatelier, 1887)[11] but was not employed extensively until the 1930's. Many applications on sodium sulfates, polyphosphates, clays, and soaps were conducted during this era by (Kracek, 1929)[26], (Norton, 1925)[36], (Partridge, 1941)[38], and (Vold, 1941)[53]. The sample is heated side to side to a reference substance usually an empty sample cell and the difference in temperature between the sample and the reference is recorded with time. In cases of higher energy consumption rates such as phase changes and endothermic reactions, or energy generation due to phase change or exothermic reaction, the difference in the temperature between the sample and the reference increases and after the reaction/transformation ends the difference decreases again leaving a peak in the temperature difference. The temperature equivalent to this peak is an indication of a certain characteristic of a reaction or substance such as boiling/melting points of a substance or can be used to find the required activation energy for a certain reaction.

Many factors affect the accuracy of the DTA from which are; heating/cooling rates, sample temperature uniformity, fluctuation in heating rate and fluctuation in desired temperature, (Vold M. J., 1949)[52].

In a more quantitative work ((Kissinger, 1957)[24]& (Kissinger H. E., 1956)[25]) it was found that the height and the location of the peaks are affected by the heating/cooling rates and

11

they are rarely located at the same temperature as the known characteristics of the substance. An ideal cooling rate would be infinitesimally small to allow the sample to reach the environment temperature, which at the same time will make the peak amplitude very small to detect.

(Murphy, 1958)[32] made a survey of the available bibliography on the DTA till the year 1958. In his work, he listed the different types of thermocouples and sample holders used. He also discussed the effect of heating rates, particle size and atmosphere control on the testing. Then he discussed the various equipment and analysis methods utilized in the different studies.

(Glass, 1954)[14] Determined the ranks of some coals using DTA. He investigated the plasticity of the coals by the number of endothermic and exothermic peaks in the DTA curve. As the rank carbon content of coal increases its rank increases. He classified the types of coal according to the DTA as; meta-anthracite, anthracite, low volatile, high volatile and sub-bituminous types of curves, which are arranged discerningly according to rank. He concluded that the most endothermic peaks at low temperature were an indication for the higher plasticity and lower grade of the coal.

(Bridgeman, Jones, Shield, & Williams, 2008)[8] used TGA/DTA to study the effect of torrefaction of different types of grass on their combustion characteristics. The DTA curves showed that the exothermic peaks occurred at approximately the same temperature, but the amplitude of the peak was higher as the torrefaction temperature increased.

2.5 Evolved Gas Analysis (EGA)

It is the detection of the evolved gases when a sample undergoes thermal decomposition/desorption. The gases can be detected using Fourier Transform Infrared spectrometer (FTIR), mass spectrometer or Gas Chromatographer (GC)

(Ahmed & Gupta, 2009)[2] carried out experiments on the P&G of paper for a temperature range 600-900°C. The Pyrolysis process started at 400°C while the gasification process started at a 700°C temperature. Gasification yielded more syngas than the Pyrolysis process and the higher the temperature, the higher the gas yield.

(Ahmed & Gupta, 2010)[1] studied the different gas yields from P&G of food wastes at two different temperatures 800 and 900°C, the syngas, hydrogen gas, energy yield and apparent thermal efficiency were calculated. They found that the gasification process gave more yield than the Pyrolysis process but at the expense of time. At the higher temperature (900 ^{o}C) the hydrogen and syngas yields were found to be higher than at the lower temperature.

(Song, Wu, Shen, & Xiao, 2012)[47] accounted six main reactions to the biomass P&G. The six reactions are the Pyrolysis of biomass into char, tar and gases. The tar then reacts with steam (tar decomposition). The char also reacts with steam (water gas reaction). At the same time char reacts with carbon dioxide to give carbon monoxide (also known as, Boudouard reaction). The carbon monoxide reacts with steam to give carbon dioxide and hydrogen (water-gas shift reaction) and finally methane from Pyrolysis can react with steam to give carbon dioxide and hydrogen (reforming reaction). They run a fluidized bed laboratory scale reactor using steam and biomass. The syngas composition was analyzed, and it was found that as the gasifier temperature increased the hydrogen and methane gases concentrations decreased in favor of the CO gas. The CO_2 gas concentration increased up to 800 ^{o}C after which it decreased again. On the other hand, all of the gas yields increased with the rise of the gasifier temperature, which was a result of the reduction in the biomass residuals.

(Collard, Blin, Bensakhria, & Valette, 2012)[12] Studied the effect of iron and nickel salts on the Pyrolysis mechanisms and yields of biomass. The iron salts yielded more char and less tar while the nickel salts yielded more hydrogen gas and aromatic tar.

2.6 Economics of biomass gasification

Economic review on the feasibility of applying the biomass technology G&P has been done by (Caputo, Palumbo, Pelgagge, & Scacchia, 2005)[10] Considerations for the capital cost, running cost (including the logistics), and revenue from power plants energy sale were taken into account. Also, biomass vehicles' transport costs, capacity, and density were studied to give a final map between economic constraints with the expected profit of biomass technology unspecified range of applications.

Chapter 3 - Experimental setup and procedures

In order to be able to determine the effect of different factors on the P&G process experimentally the following requirements should be accomplished:

- A high-temperature gas source is required. The supplied gas temperature should range between 150° and 1000^oC, which is a suitable range for both Pyrolysis and gasification. The gas temperature should be maintained as constant as possible.

- The biomass samples should be confined in an enclosure to be able to control the environment where the reaction takes place.

- The mass of the sample should be monitored continuously to assess the progress of the reaction.

- There should be a way to conclude the quality of the gas produced.

Two different test setups were used to acquire the experimental data:

3.1 Evolved gas analysis Experimental set up:

3.1.1 Experimental set up:

The set-up was built in the University of Maryland College Park and was used in the analysis of gas products from gasification of waste food, paper, plastics, and other biowastes. Figure 3-1: Schematic for the EGA apparatus and Figure 3-2 shows the experimental setup. A constant flow rate of N_2 was used for all of the experiments as a tracer gas. Because N_2 is not reacting, the mass of nitrogen into the apparatus will be equal to the mass of N_2 out, and thus it is possible to quantify all of the other gases using the known mass of N_2. In the case of Pyrolysis only, N_2 was used as the gas agent. While when different gases were used, The gases were mixed with the N_2 prior to heating. When steam was used, a H_2/O_2 flame was used to generate the

steam which was mixed with the N_2 prior to heating. The H_2/O_2 ratio was adjusted such that no concentrations of H_2 were detected at the gas chromatograph. The mixing section was then connected to a steel tube mounted inside two stages of electric tube furnaces. The first stage is a preheating section to ensure gases are at required temperature before being introduced to the biomass. The second section is the gasifier, where the biomass is to be located. A known mass of the chicken manure was first loaded into a quartz tube which was then inserted into the tube inside the furnace when a steady state condition was achieved. The quartz tube provides uniform temperature distribution for the whole biomass load. The electric heaters were controlled using accurate PID controllers and were capable of maintaining temperature up to $1200^{o}C$.
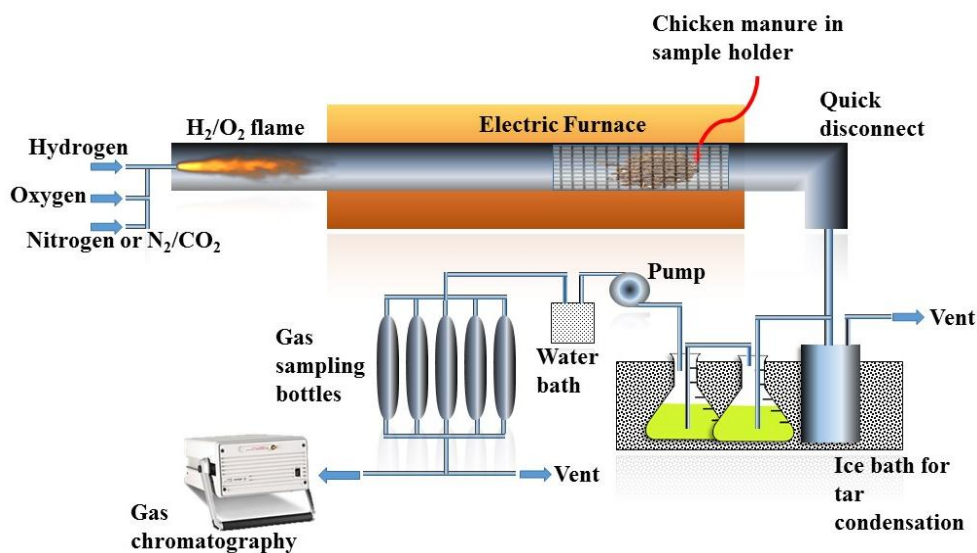
Figure 3-1: Schematic for the EGA apparatus

| a: Steam burner and electric heaters | b: Micro GC | c: Gas sampling bottles |
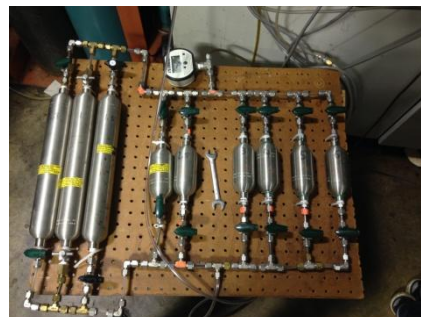
Figure 3-2: Pictures of the experimental setup

The steel tube connects to a quick connect elbow at the end of the heating section. The elbow is then connected to a flexible stainless steel pipe which is, in turn, delivers the gas products to a 3 stage condensation unit. The condensation unit consists of vented chamber and two glass beakers. All of the three elements of the condensation unit are submerged in an ice bath. The whole gas volume enters the vented chamber, Most of the gas is vented to the exhaust while a smaller portion of the gases passes through the two other stages of condensation for analysis. The gases are driven by a positive displacement pump through a gas dryer to make sure the sample gas is as dry as possible before it enters the gas analyzer. The gas chromatograph is capable of completing an analysis in 3 minutes. So, samples were stored in the gas sampling bottles during the first 5 minutes then were analyzed continuously every 3 minutes using the gas chromatograph. When the run was completed the gas samples inside the bottles were analyzed using the gas chromatograph.

The Gas analyzer was calibrated against standard gas mixtures, and the combined accuracy of the gas analysis is ±0.1%.

3.1.2 Test procedures:

The evolved gas analysis experiments were run according to the following procedures:

1. The electric furnaces were switched on until the required temperature was met.

2. The flow rate of agent gas/mixture of gases is started, and the gas was analyzed using the gas analyzer, then flow rates are adjusted to the required mixtures.

3. 35 gm of chicken manure sample is weighed on a delicate balance then loaded in a quartz cylinder.

4. When all the test conditions stabilize, The quick connect elbow is removed, and the sample is loaded inside the furnace then the elbow is reinstalled. The whole loading process took less than 10 seconds.

5. Time acquisition is started once the elbow is re-secured.

6. During the early five minutes, gas samples were collected in the sampling tubes.

7. After that samples are taken directly to the gas analyzer which samples every 3 minutes.

8. The test was continued until the concentrations of fuel gas components drop below 0.5%.

9. The test is stopped, and the gas samples stored in the sampling tubes are analyzed.

3.1.3 Test cases:

The following 29 cases shown in Table 3-1

Table 3-1: Test cases studied by evolved gas analysis:

Case	Gas agent	600°C	700°C	800°C	900°C	1000°C
0	N$_2$ only	x	x	x	x	x

1	N_2+CO_2	x	x	x	x	x
2	$N_2+21\%O_2$ (air)	x	x	x	x	x
3	$N_2+10\%$ O_2	x	x	x	x	x
4	N_2+steam	x	x	x	x	x
5	N_2+steam$+1\%O_2$				x	
6	N_2+steam$+2\%O_2$				x	
7	N_2+steam$+3\%O_2$				x	
8	N_2+steam$+4\%O_2$				x	

The same flow rate of N_2 was used in all of the experiments as a tracer gas. Because N_2 is an inert gas, it will leave the reaction in the same mass as it entered, then using the known mass of N_2, the masses of other gases were calculated using the measured concentrations from the gas analyzer.

The first case of each row was repeated to check repeatability. Some cases were repeated due to clogging in sampling pipes, human errors,….., etc.

3.1.4 Data processing:

The analyzer was calibrated to detect N_2, H_2, O_2, CO, CO_2, CH_4, C_2H_2, C_2H_4, C_2H_6, and C_3H_8. Any higher gaseous hydrocarbon present would be in an insignificant quantity, and liquid hydrocarbons would either precipitate on the tubes if not condensed. The gas analyzer provides raw data for the volume concentration of different gases. Using the known N_2 volume flow rate, the volumetric and mass flow rates of gases can be calculated as follows:

$$\dot{V}_x = \dot{V}_{N_2} \cdot \frac{C_x}{C_{N_2}}$$

(3- 1)

Where x is any given gas, $\dot{V}$ is the volume flow rate, and C is the mole (volume) concentration. The mass flow rate of any gas can then be found by multiplying the volume flow rate by the density of the gas as follows:

$$\dot{m}_x = \dot{V}_x \cdot \rho_x \tag{3-2}$$

Where $\dot{m}$, is the mass flow rate and ρ, is the gas density. The energy rate produced can be found by multiplying the mass flow rate by the heating value of the gas:

$$\dot{E}_x = \dot{m}_x \cdot HV_x \tag{3-3}$$

Where $\dot{E}$ energy rate produced in gas x and HV is the heating value. The total energy produced can then be found by numerically integrating the instantaneous values of energy rate:

$$E_x = (\dot{E}_{x,l} - \dot{E}_{x,l-1})\Delta t \tag{3-4}$$

The carbon conversion efficiency was used to evaluate the efficiency of conversion of the carbon content in the chicken manure into carbon in the product gas. The efficiency was used as an indication of the tar production as the current set up would not allow accurate measurements of the tar content. First the fraction of carbon by mass was evaluated for different product gases (ex: for $f_{CH4}=0.75$, $f_{CO}= 0.43,....$, etc) then the carbon fraction was multiplied by the mass of each product gas and then the sum of all carbon mass in all product gases was found as:

$$m_{c,gas} = \sum_{x=1}^{n}(\dot{m}_{x,l} - \dot{m}_{x,l-1})\Delta t \cdot f_x \tag{3-5}$$

Where m_c, is the total mass of carbon in product gases and f is the mass fraction of carbon in any product gas. Then the carbon efficiency was found as:

$$\eta_c = \frac{m_{c,gas}}{m_{c,manure}} \cdot 100\% \tag{3-6}$$

Where η_c, is the carbon efficiency.

The energy conversion efficiency was calculated from the total energy in the product gas and the total energy in the chicken manure:

$$\eta_E = \frac{\sum_{x=1}^{n} E_x}{m_{manure} \cdot HV_{manure}} \cdot 100\%$$

(3- 7)

3.2 The Shimadzu DTG-60AH:

3.2.1 Experimental set up:

The Shimadzu DTG-60AH, Figure 3-3: The Shimadzu DTG-60AH; the main device components to the left and the gas flow through the device to the right, will also be used as the experimental setup. The device can operate to a temperature 1500°C. It can perform simultaneous thermogravimetric (TGA) and differential thermal analysis (DTA). It consists of three main parts;

1. The furnace provides the heat needed for maintaining the sample surrounding at the required temperature.

2. The detectors are two long rods fitted with thermocouples and resting on a sensitive balance; the sample cells rest on the upper ends of the detectors.

3. The auto-sampler is a robotic system, which automatically loads and unloads the samples on the detectors. The sample is loaded on one of the detectors while an empty cell is loaded on the other sensor as a reference.
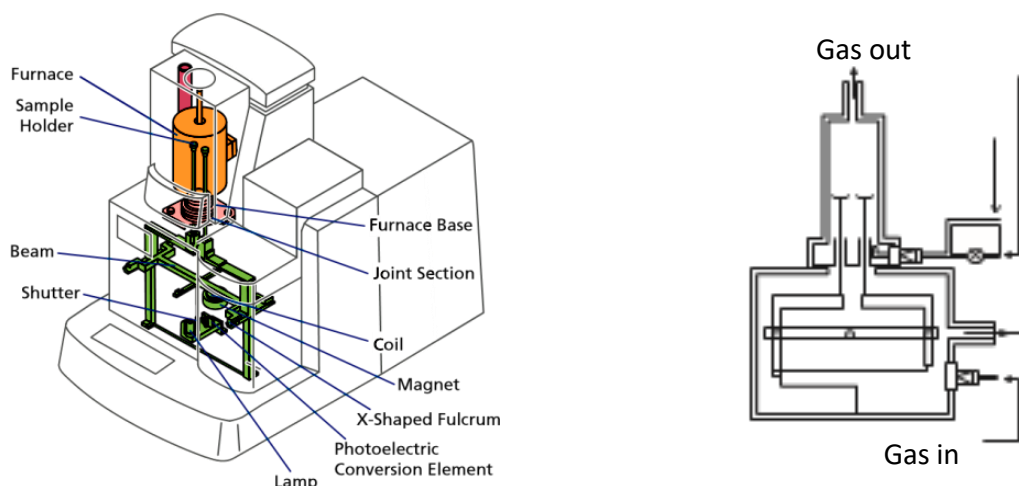
21

Figure 3-3: The Shimadzu DTG-60AH; the main device components to the left and the gas flow through the device to the right

The delicate balance detects the weight difference between the two detectors which corresponds to the sample weight while for differential thermal analysis the difference between the voltage readings of the two sensors is measured. Any dry, non-corrosive gas can be used with this device. The measurable mass range is ± 500 mg with a resolution of 0.001 mg and $\pm 1\%$ accuracy. The thermocouples are Pt-10%Pt/Rh thermocouples. The measurable range for the DTA is ± 1 to 1000 μV with a noise level ≤ 1 μV. The measurable range for temperature is room temperature to the maximum device temperature which is 1500°C. The Temperature uncertainty is ± 1 $^{\circ}$Cor ± 0.2 $^{\circ}$C if the instrument is calibrated as recommended by the manufacturer. Regular calibration was performed on the device all over the temperature range and at the operating gas flow rate to minimize the effect of gas turbulence on the readings. The sample is loaded on different material cells depending on the operating temperature. Aluminum cells are used for temperature below 600°C while Nickel was used for temperatures up to 1000°C. Other cell materials are available for higher temperatures such as Platinum for temperature up to 1200°C and Alumina up to 1500°C, which are more expensive and alumina has a high porosity, which makes it hard to clean if the sample melts inside the cell.

22

3.2.2 Test procedures:

The following test procedure was used as a standard procedure:

1. An empty test cell was loaded in the furnace, close the furnace, check for any zero error, and rest if necessary.

2. Open the furnace and fill the sample cell with chicken manure, then close the furnace.

3. Set the temperature program and start apparatus.

4. Mass, temperature, and DTA data were acquired at a rate of 1 Hz.

3.2.3 Test cases

The following 24 cases were studied:

Table 3-2: Test cases studied by DTA and TGA

Case	Gas agent	5°C/min	10°C/min	15°C/min	20°C/min	25°C/min	30°C/min	35°C/min	40°C/min
A	N_2	x	x	x	x	x	x	x	x
B	Air	x	x	x	x	x	x	x	x
C	CO_2	x	x	x	x	x	x	x	x

Each test was repeated at least two times. Ultra high pure gases were used for all tests.

3.2.4 Data processing

The raw data of mass, temperature and DTA were processed to produce values of the reaction extent (eq. 2-3) while the DTG values were found from:

$$\frac{d\alpha}{dt} = \frac{\alpha_t - \alpha_{t-1}}{\Delta t} \tag{3-8}$$

Eq. 2-5 and 2-6 were combined to give:

$$\frac{d\alpha}{dT} = \frac{k(T)}{\beta} f(\alpha) = \frac{A}{\beta} \exp\left(\frac{-E_a}{RT}\right)(1-\alpha)^n \tag{3-9}$$

If the natural log is taken for both sides:

$$\ln\left(\frac{d\alpha}{dT}\right) - n \ln(1-\alpha) = \ln\left(\frac{A}{\beta}\right) - \left(\frac{E_a}{RT}\right) \tag{3-10}$$

If $\ln\left(\frac{d\alpha}{dT}\right) - n \ln(1-\alpha)$ is sketched on the y-axis, while $\frac{1}{T}$ is sketched on the x-axis while plugging in different values for reaction order, n, we should get a straight line with $\left(-\frac{E_a}{R}\right)$ as the slope and $\ln\left(\frac{A}{\beta}\right)$ as the intersection with the y-axis. Using these values we can find the activation energy E_a and the exponent constant A.

Chapter 4 -   TGA and DTA

The thermo-gravimetric and the differential thermal analysis will be presented in this chapter. The extent of reaction α was calculated using equation (2-3) while $\frac{d\alpha}{dt}$ was calculated using equation (3-8). The Arrhenius reaction constant and the activation energy were found using the procedures discussed in Chapter 3 -.

4.1 Nitrogen Pyrolysis:

4.1.1 Extent of reaction (TGA):

When Nitrogen is used only Pyrolysis is expected. The three components in biomass are hemicelluloses, cellulose, and Lignin. The thermal degradation of hemicelluloses is known to peak at 240°C, Cellulose at 380°C, while lignin has more of a steady degradation with a small peak at high-temperature 600-800°C, (Yang, 2007)[58]

Figure 4-1 shows the extent of reaction of chicken manure when Nitrogen is used for different heating rates. The test was carried out for heating rates ranging from 5-40°C with a 5°C step. For figure clarity, only three heating rates were shown 5, 20, and 40°C. All different heating rates had the same trend. As the temperature increases the extent of reaction increases. When the heating rate increased, the progress of the extent of reaction seems to be delayed to a higher temperature. The faster heating rate does not allow the completion of each reaction before increasing the temperature, and thus the progress appear as delayed with respect to temperature. This delay in the response was similar for all different gas media tested. A similar behavior was observed for wood by (Poletto, 2010). The Pyrolysis reaction can be divided into three main

stages. A first ranges between the start of thermal cracking up to 250°C, a faster reaction between 250-360°C, and finally a steady reaction from 360°C to the end of reaction. These three distinct stages will be used to find the kinetics of reaction. Within the 370-700°C, the three main components' thermal degradation overlaps and the effect of heating rate on the extent of reaction is more obvious compared to other temperature ranges.
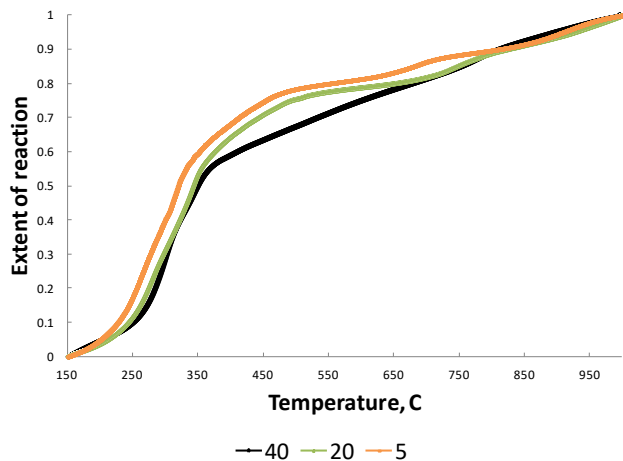
Figure 4-1 : The change in the extent of reaction with the temperature at different heating rates, case A.

The residual mass decreased slightly with the increase of the heating rate with an average residual mass of 28% of the total mass of the sample independent on the heating rate. Figure 4-2 shows the rate of change of extent of reaction of chicken manure when Nitrogen is used for different heating rates. The test was carried out for heating rates ranging from 5-40°C with a 5°C step. All different heating rates had the same trend. Three distinct peaks can be observed at temperatures: 250, 360, and 750°C. The magnitude of the peak is increased as the heating rate increased as well as the temperature at which the peak occurs. At the lower heating rate, the magnitude of the first peak was higher than the second, but as the heating rate increases, the magnitude of the first peak increased relative to the second. The three peaks are characteristic for the three main components: Hemicellulose, cellulose, and lignin respectively. The peaks are

26

slightly shifted from the exactly known values for the three compounds as the chicken manure contains other components like amino acids, fats,…etc. For the $40^{\circ}C$ another peak appears near the $150^{\circ}C$, which is due to the evaporation of any moisture in the sample. For other cases at $150^{\circ}C$ all the moisture has already evaporated from the sample.
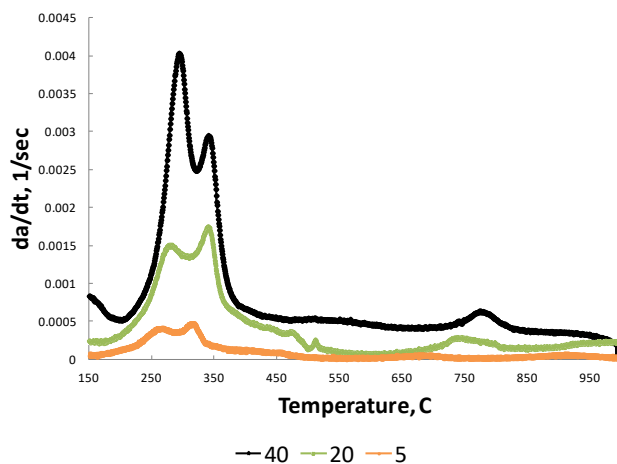
Figure 4-2 : The rate of change of the extent of reaction with temperature at different heating rates, case A.

4.1.2 Kinetics of reaction (TGA):

The values for the Arrhenius equation constant and the activation energy are shown in Table4-1.

Table4-1: Kinetic parameters for N_2 pyrolysis with different heating rates:

B ($^{\circ}$C/min)	n	Log(A/β)	E$_a$ (kJ/mole)
40 (250-360°C)	5	17.0	99.0
40(>360°C)	5	11.9	87.8

27

35 (250-360°C)	5	16.8	98.3
35(>360°C)	5	11.9	84.5
30 (250-360°C)	5	16.5	96.5
30(>360°C)	5	11.8	80.9
25 (250-360°C)	5	16	95.8
25(>360°C)	5	11.7	76.4
20 (250-360°C)	5	15.6	93.2
20(>360°C)	5	11.4	72.3
15 (250-360°C)	5	15.3	89.6
15(>360°C)	5	11.2	69.0
10 (250-360°C)	5	15	88.1
10(>360°C)	5	11	65.1
5 (250-360°C)	5	14.9	84
5(>360°C)	5	10.9	63.1

For the range 250-360°C, the average value for E_a= 91 kJ/mole and the average value for logA= 14.5 sec^{-1} .And for the range >360°C, the average value for E_a= 75.6 kJ/mole and the average value for logA= 10 sec^{-1}.

4.1.3 Differential thermal analysis (DTA):

Figure 4-3 shows the DTA of chicken manure when Nitrogen is used for different heating rates. The test was carried out for heating rates ranging from 5-40°C with a 5°C step. For figure clarity, only 3 heating rates were shown 5, 20, and 40°C. All different heating rates had the same trend. The reaction is relatively steady except for a large peak downwards for the endothermic

reaction due to the quick breakdown of cellulose and hemicelluloses below 350°C. When the heating rate increases the magnitude of the peaks increases as the furnace temperature is exceeding the sample temperature. The sample heats up slower with respect to temperature change. Thus the figure for 40°C looks different from the other two cases.
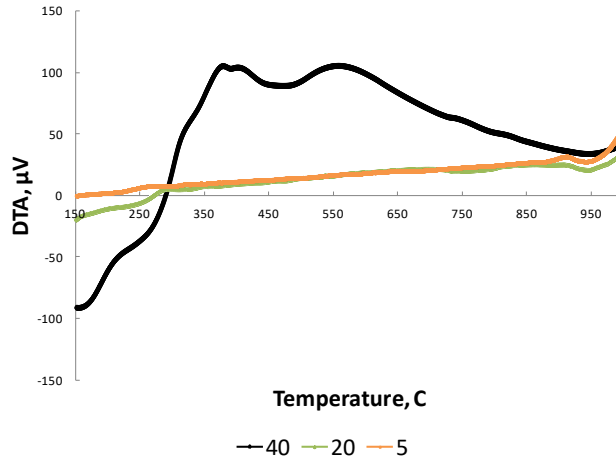
Figure 4-3 : The change of the DTA with temperature at different heating rates, case A

4.2 Air gasification:

4.2.1 Extent of reaction (TGA):

When air is used, gasification is expected due to the incomplete combustion of the gases and fixed carbon in the presence of O_2. Figure 4-4 shows the extent of reaction of chicken manure when air is used for different heating rates. The test was carried out for heating rates ranging from 5-40°C with a 5°C step. For figure clarity, only 3 heating rates were shown 5, 20, and 40°C. All different heating rates had the same trend. As the temperature increase the extent of reaction increase. When the heating rate increased, the progress of the extent of reaction seems to be delayed to a higher temperature. The air gasification reaction can be divided into 4

main stages. A first, ranges between the start of thermal cracking up to 250°C, a faster second reaction between 250-350°C, from 350 to 450°C another fast stage with a smaller slope than the previous region. Between 450 and 600°C a fluctuation in temperature due to self-ignition is detected. After 600°C the reaction tends to be slow, and the extent of reaction reaches more than 95% at 600°C.
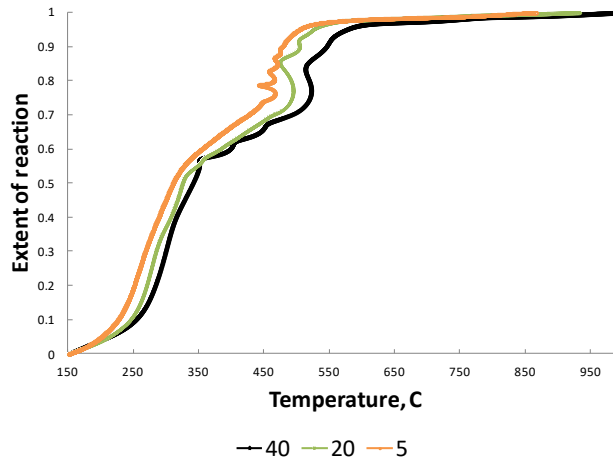
Figure 4-4 : The change in the extent of reaction with temperature at different heating rates, case B

The extra mass decreased slightly with the increase of the heating rate with an average remaining mass of 18% of the total mass of the sample.

Figure 4-5 shows the rate of change of extent of reaction of chicken manure when the air is used, for different heating rates. The test was carried out for heating rates ranging from 5-40°C with a 5°C step. For figure clarity, only three heating rates were shown 5, 20, and 40°C. All different heating rates had the same trend. Three distinct peaks can be observed at temperatures: 250, 360, and 500°C. The magnitude of the peak is increased as the heating rate increased as well as the temperature at which the peak occurs. The increase in the peak value is resulting from the faster change in temperature. The first two peaks are characteristic for Hemi-cellulose and

30

cellulose while the third peak is at the same temperature as the fluctuation in temperature and thus represents the ignition of chicken manure, which is another indication of self-ignition. A very small bump appears at 750°C for the 40°C/min., which is due to the degradation of the low residuals of lignin after combustion.
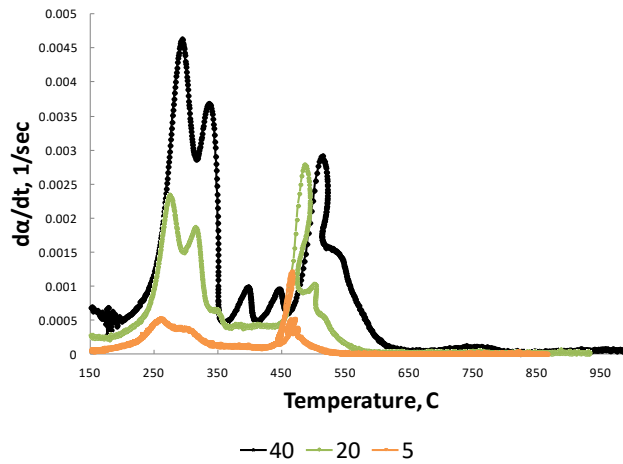
Figure 4-5 : The rate of change of the extent of reaction with temperature at different heating rates, case B

4.2.2 Kinetics of reaction (TGA):

The values for the Arrhenius equation constant and the activation energy are shown in Table4-2. Even though the reaction appeared more complicated than the N_2 pyrolysis; single kinetic reaction constants were calculated for the whole conversion reaction

Table4-2: Kinetic parameters for air gasification with different heating rates:

B ($^{\circ}$C/min)	n	Log(A/β)	E_a (kJ/mole)
40	3	10.2	69.0

35	3	10.3	67.9
30	3	10.9	70.3
25	3	10.3	67.6
20	3	10.9	70.8
15	3	10.1	64.5
10	3	10.1	66.7
5	3	11.2	70.3

The average value for E_a= 68.4 kJ/mole and the average value for logA= 9.3 sec^{-1} .

4.2.3 Differential thermal analysis:

It is shown in Figure 4-6 that the temperatures at which the peaks are formed are similar to the temperatures in Figure 4-5, 250, 360, and 500°C which corresponds to the peaks due to degradation of hemicellulose, degradation of cellulose, and ignition respectively. The fact that these peaks are positive (upwards) is due to the oxidation of some of the evolving gases rendering the reaction as exothermic. Fluctuation in temperature and DTA peaks were observed at a temperature of 500°C which can be due to the ignition of the sample. After 700°C no significant reaction was recorded, and the weight of the sample was stable.
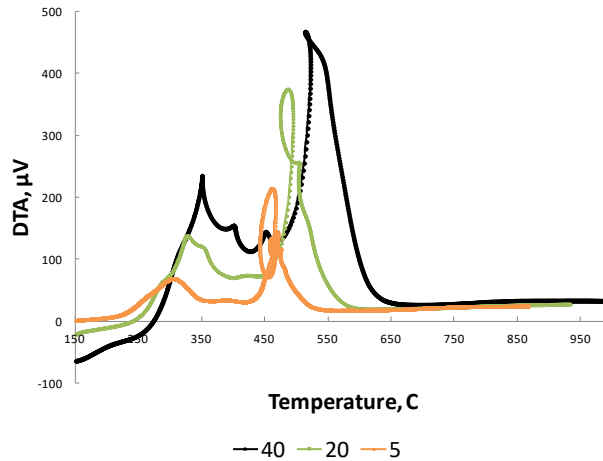
Figure 4-6 : The change of the DTA with temperature at different heating rates, case B

4.3 CO$_2$ gasification:

4.3.1 Extent of reaction (TGA):

When CO_2 is used gasification is expected. Figure 4-7 shows the extent of reaction of chicken manure when CO_2 is used for different heating rates. The test was carried out for heating rates ranging from 5-40°C with a 5°C step. For figure clarity, only three heating rates were shown 5, 20, and 40°C. All different heating rates had the same trend. As the temperature increase the extent of reaction increase. When the heating rate increased, the progress of the extent of reaction seems to be delayed to a higher temperature, while the higher heating rate tends to approach the maximum extent of reaction at a higher temperature. The gasification reaction can be divided into 4 main stages. A first, ranges between the start of thermal cracking up to 250°C, a faster reaction between 250-360°C, a steady reaction from 360 to 700°C, and finally a quick reaction at 700°C to the end of reaction. These four distinct stages will be used to find the kinetics of reaction.

33
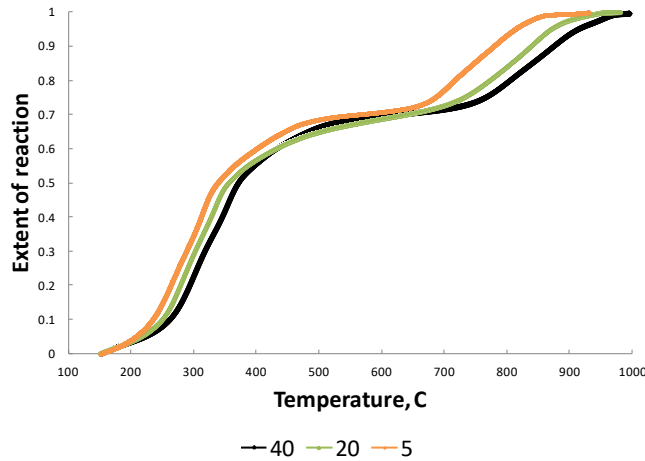
Figure 4-7 : The change in the extent of reaction with temperature at different heating rates, case C

The extra mass decreased slightly with the increase of the heating rate with an average remaining mass of 19% of the total mass of the sample.

Figure 4-8 shows the rate of change of extent of reaction of chicken manure when CO_2 is used for different heating rates. The test was carried out for heating rates ranging from 5-40°C with a 5°C step. For figure clarity, only three heating rates were shown 5, 20, and 40°C. All different heating rates had the same trend. Three distinct peaks can be observed at temperatures: 250, 360, and 700-800°C. The magnitude of the peak increased as the heating rate increased as well as the temperature at which the peak occurs. The first two peaks are characteristic for Hemi-cellulose and cellulose while the third peak is an overlap between the peak for lignin and the peak for the Boudard reaction between fixed carbon and CO_2 respectively. The peak value increases withthe heating rate due to the faster increase of the temperature with time.

34
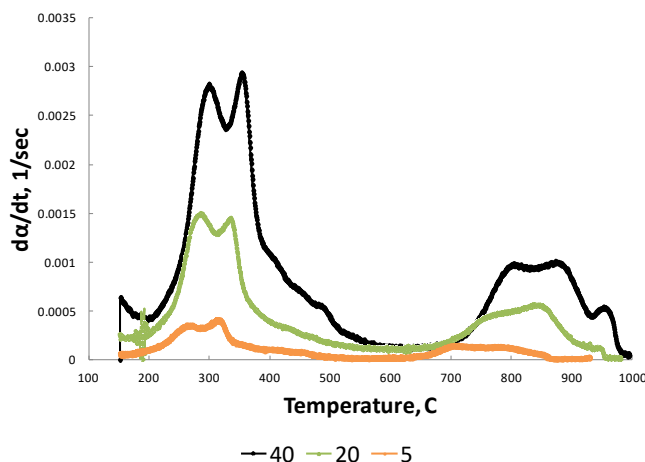
Figure 4-8 : The rate of change of the extent of reaction with temperature at different heating rates, case C

4.3.2 Kinetics of reaction (TGA):

The values for the Arrhenius equation constant and the activation energy are shown in Table4-3.

Table4-3: Kinetic parameters for CO_2 gasification with different heating rates:

B (^{o}C/min)	n	Log(A/β)	E_a (kJ/mole)
40 (250-360°C)	5	7.5	56.4
40 (360-630°C)	5	3.7	37.6
40 (>630°C)	5	62	519.7
35 (250-360°C)	5	8.0	56.4
35 (360-630°C)	5	2.9	32.6
35 (>630°C)	5	63.6	544.7
30 (250-360°C)	5	8.66	60.3
30 (360-630°C)	5	3.0	33.3

30 (>630°C)	5	68.1	561.5
25 (250-360°C)	5	8	57.1
25 (360-630°C)	5	3.0	30.5
25 (>630°C)	5	66.5	549
20 (250-360°C)	5	8.9	61.3
20 (360-630°C)	5	3.8	34.8
20 (>630°C)	5	67.25	551
15 (250-360°C)	5	9.1	61.5
15 (360-630°C)	5	3.5	32.9
15 (>630°C)	5	68	556
10 (250-360°C)	5	8.9	60.2
10 (360-630°C)	5	5.0	38.7
10 (>630°C)	5	68.1	523
5 (250-360°C)	5	9.8	63.2
5(360-630°C)	5	4.3	39
5(>630°C)	5	72.5	575.5

For the range 250-360°C, the average value for E_a= 59.6 kJ/mole and the average value for logA= 9.8 sec^{-1} , for the range 360-630°C, the average value for E_a= 34.9 kJ/mole and the average value for logA= 4.8 sec^{-1}, and for >630°C, the average value for E_a= 547.6 kJ/mole and the average value for logA= 68 sec^{-1}

4.3.3 Differential thermal analysis:

Figure 4-9 shows the DTA of chicken manure when CO_2 is used for different heating rates. The test was carried out for heating rates ranging from 5-40°C with a 5°C step. All different heating rates had the same trend. The reaction is relatively steady except for a large peak downwards for the endothermic reaction due to the fast breakdown of cellulose and hemicelluloses below 350°C. and another endothermic reaction of CO_2 with the fixed carbon in the chicken manure at a temperature greater than 700°C. When the heating rate increases, the magnitude of the peak increases. The faster rate of change in temperature does not allow enough time for thermal equilibrium between the reference and sample, and thus the peak value appears larger.
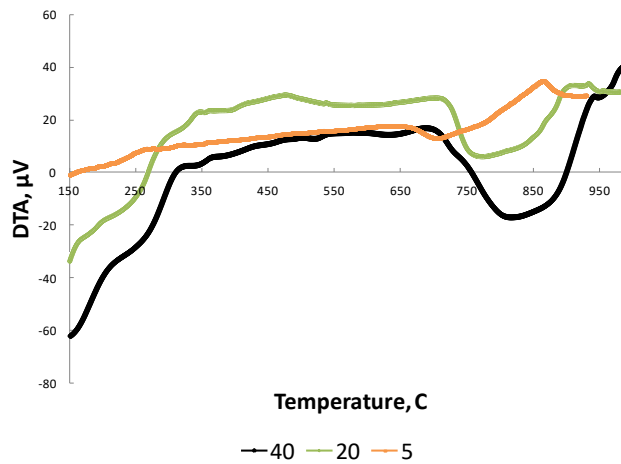
Figure 4-9 : The change of the DTA with temperature at different heating rates, case C

Chapter 5 -   Evolved gas analysis

The main governing chemical reactions are shown in Table Table 5-1: Chemical reactions governing Pyrolysis and gasification:. The first two equations are characteristic for CO_2 and air gasification, three and four are characteristic for steam gasification while the last equation takes place at the beginning of all cases. If a reaction is a characteristic to a certain case, then it is the dominant reaction, but it does not mean that each reaction happens exclusively with a certain agent.

Table 5-1: Chemical reactions governing Pyrolysis and gasification:

Char Oxidation:	$C + O_2 \Rightarrow CO_2$	(5-1)
Boudouard Reaction:	$CO_2 + C \rightleftharpoons 2CO$	(5-2)
Water-gas shift Reaction:	$CO + H_2O \rightleftharpoons CO_2 + H_2$	(5-3)
Water-gas Reaction:	$C + H_2O \rightleftharpoons CO + H_2$	(5-4)
Thermal cracking:	$C_nH_m \Rightarrow C + C_xH_y + H_2$	(5-5)
CO_2 dissociation:	$2CO_2 \rightleftharpoons 2CO + O_2$	(5-6)

The main composition of biomass is Hemi-cellulose, cellulose, and Lignin. Each has a range of decomposition temperature, and lignin has the highest range with temperatures exceeding 800^oC. When the P&G temperature is below the 800^oC, it can be assured that the residual mass is not only the ashes. Table 5-2 (Netherlands)[34] shows the proximate and ultimate analysis of chicken manure.

Table 5-2: Proximate and ultimate analysis of chicken manure[34]:

Proximate Analysis (wt. % dry)	
Volatile content	65.56

Ash content at 550 °C	21.65
Fixed carbon	12.8
Ultimate Analysis (wt. % dry)	
Carbon	35.59
Hydrogen	4.57
Nitrogen	4.98
Sulfur	1.45
Oxygen	35.52
HHV (in MJ/kg)	13.15

The gas concentrations were provided as raw data from the analyzer; mass flow rate was calculated using eq. (3- 1) and (3- 2), carbon conversion efficiency was calculated from eq. (3- 6); while the energy conversion efficiency was calculated from eq. (3- 8).

The gas which is referred to as syngas in this thesis is the mixture of CO, H_2, CH_4, C_2H_2, C_2H_4, C_2H_6, and C_3H_8. No significant concentrations of any higher hydrocarbon were detected. It is expected to get very low concentrations of H_2S , NH_3, and HCN but from literature, the expected quantities are in the order of ppm.

Please be noted that the concentrations of N_2 and O_2 are not shown in the figures as N_2 is non-reacting, while O_2 was not detected by any significant concentrations, and the main concern of the study is the useful gases (fuels).

It is worth mentioning that no higher temperatures were investigated as at approximately 1050°C, the ash melts and sticks to the reactor surface. The melting of ash is undesirable in the industry as it increases the maintenance time and cost.

5.1 Nitrogen Pyrolysis, Case 0

5.1.1 Evolved gas analysis at different temperatures

When Nitrogen is used as the gas agent, only Pyrolysis takes place. And eq. (5-5) will be the dominant equation. It should also be taken into consideration that components other than hydrocarbons are present in the chicken manure. Amino acids, fats, and other components are characterized by the presence of carboxylic groups (C=O-OH) which generates CO_2 when broken. Figure 5-1: The evolution of different gases at 600oC, case 0shows, (a) the mole fraction of different gas species in the product gas and (b) the mass flow rate of different species. Both (a) and (b) are for $600^{o}C$, when N_2 was used as the gas agent. It can be seen at the low temperature of $600^{o}C$ the useful gases (Fuels) evolution is limited and is very low compared to the CO_2 evolution. It was also observed that at this lower temperature, the tar production was very high, and it is a result of the incomplete thermal breaking of bonds. Tar can be used as a heavy-oil fuel but it is undesirable in the industry as it clogs pipes due to the high wax content. After 6 minutes of reaction, significant concentrations of H_2 started to evolve. Heavier hydrocarbons started evolution at earlier stages of the reaction (4 minutes) while CO was leading at as early as 2 minutes. The maximum peak of CO_2 is 25% of the total evolving gas volume after 5 minutes from the start of the reaction. CO peaks at the same time as the CO_2 with a peak value of 5%. H_2 peak is delayed to the eleventh minute with 5% magnitude. Other hydrocarbons contributes with lower percentage of the volume; 1.2%, 0.4% 0.25%, and 1.25% for CH_4, C_2H_6, C_2H_4, and C_3H_8 respectively.
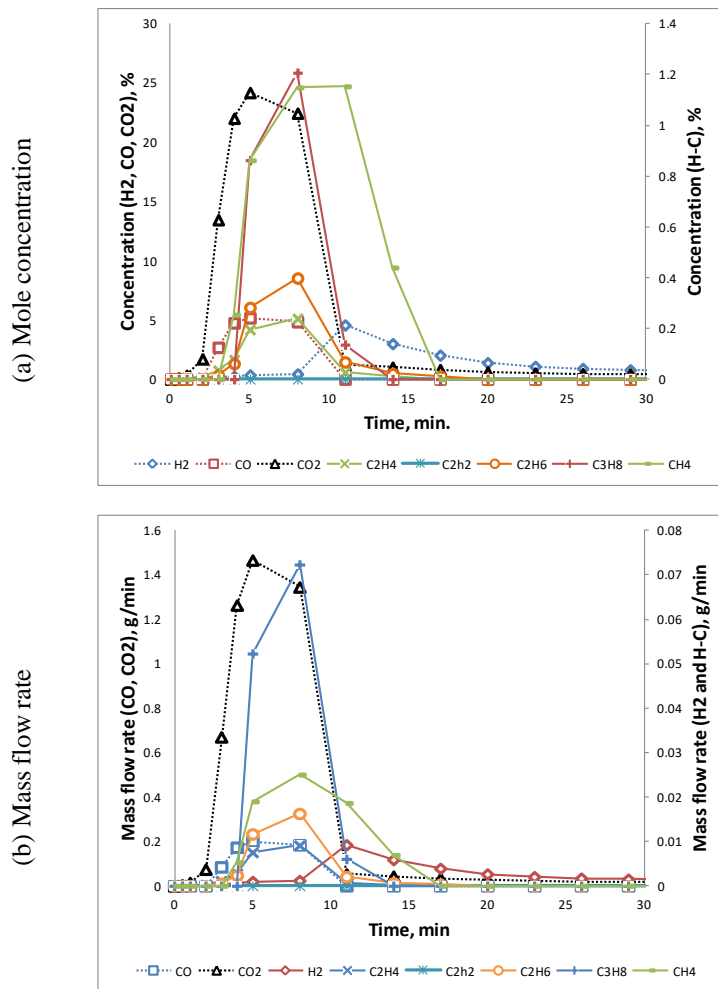
Figure 5-1: The evolution of different gases at 600°C, case 0

As the reaction temperature increases, higher flow rates of the product gases are observed in figures (Figure 5-2 : The evolution of different gases at 700oC, case 0) through Figure 5-5 : The evolution of different gases at 1000oC, case 0.

At 700°C, the high concentration of C_3H_8 is substituted by a high concentration of CH_4. When comparing with the gas evolution at 600°C, the gas peaks are higher, and the evolution time is prolonged, as more stable bonds can be broken at 700°C with a low reaction rate. The maximum peak of CO_2 is 30% of the total evolving gas volume after 5 minutes from the start of the reaction. CO peaks at the same time as the CO_2 with a peak value of 7%. H_2 peak is delayed

to the fourteenth minute with 8% magnitude. Other hydrocarbons contribute to a lower percentage of the volume; 6%, 1.6%, 1.1%, and 0.05% for CH_4, C_2H_6, C_2H_4, and C_3H_8 respectively.

(a) Mole concentration

(b) Mass flow rate
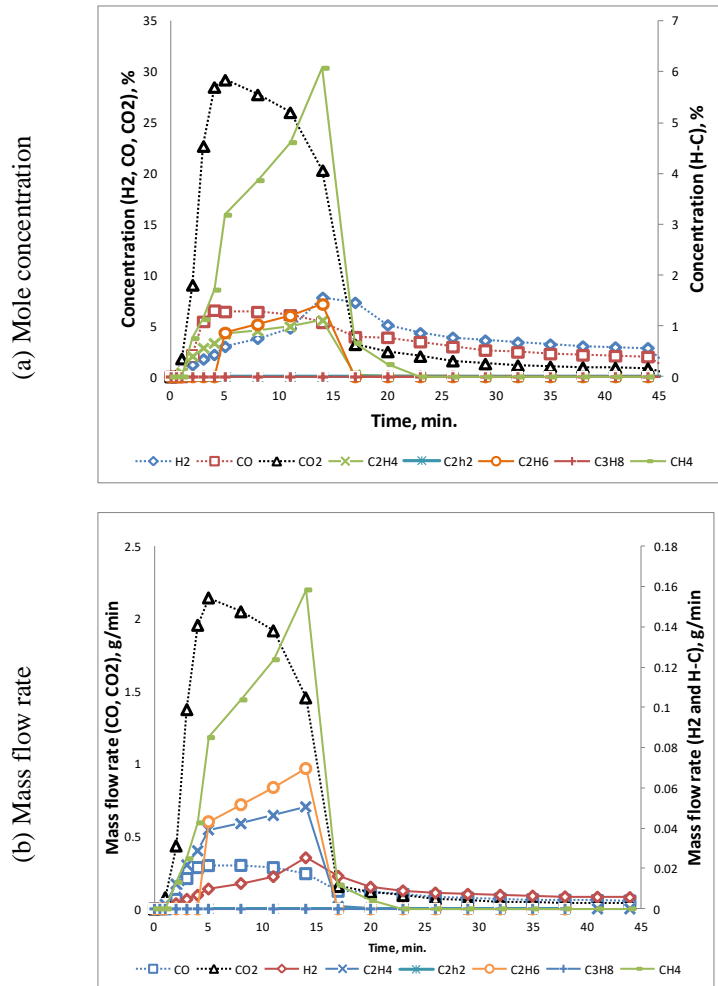
Figure 5-2 : The evolution of different gases at 700^oC, case 0

As the temperature further increase the peaks of gas species increases for lighter hydrocarbons (H_2, C_1 and C_2) while C_3H_8 concentration decreases. The composition of the syngas drastically changes depending on the reaction temperature with CO of the highest mass flow rate. At 600^oC, the gases with the highest flow rates after CO were C_3H_8 and CH_4. C_3H_8 diminishes at higher temperatures. At 700^oC, the maximum mass flow rate is for CH_4 followed

42

by C_2H_6, C_2H_4, then H_2. As the temperature increases further to 800^oC, the product gas species peak values are re-arranged with CH_4 leading, followed by C_2H_4, C_2H_6, then H_2. The peaks tend to occur at earlier times and the total reaction time is decreased. The maximum peak of CO_2 is 30% of the total evolving gas volume after 3 minutes from the start of the reaction. CO peaks at the same time as the CO_2 with a peak value of 8%. H_2 peak is delayed to the fifth minute with 17% magnitude. Other hydrocarbons contribute to lower percentage of the volume; 7%, 1.6%, and 2.5% for CH_4, C_2H_6, and C_2H_4 respectively.
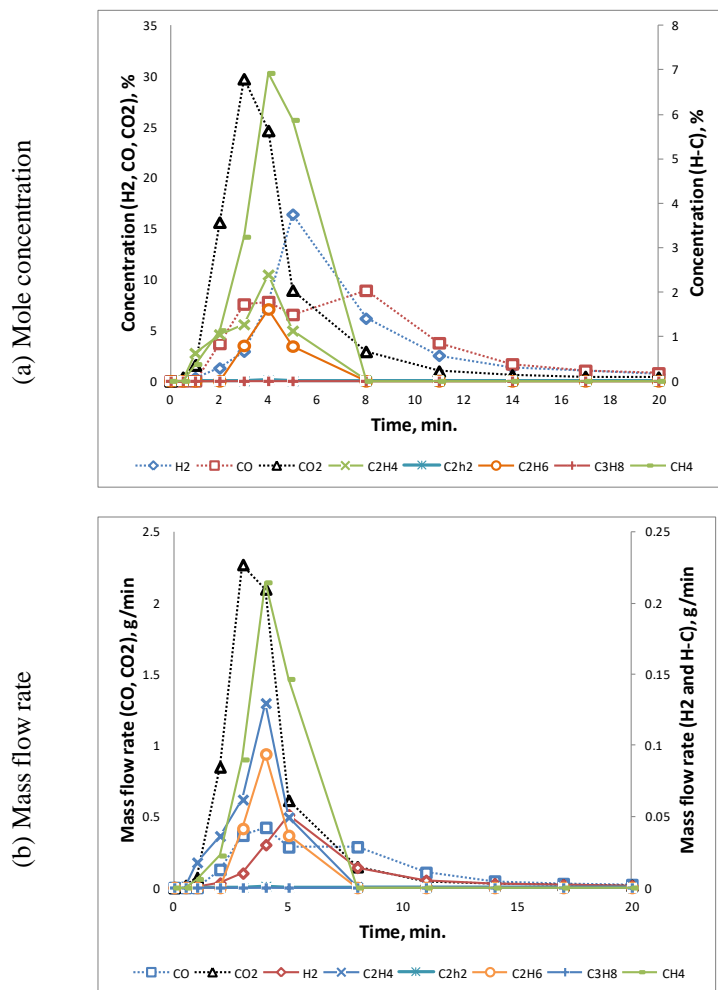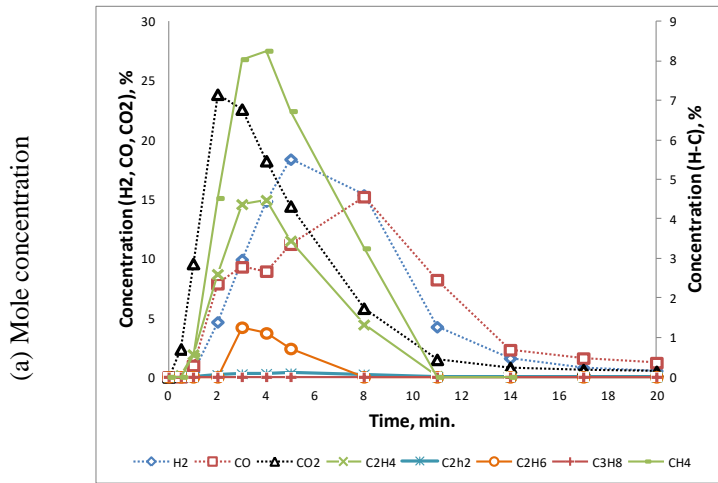

Figure 5-3 : The evolution of different gases at 800^oC, case 0

The total reaction time at $800^{\circ}C$ is 40% less than that at $700^{\circ}C$. Shorter reaction time improves the feasibility of the process as the same patch of biomass is subject to the high temperature for a shorter time and thus less energy required. Also, when the reaction time is higher, the reactor size should be increased, increasing the total reactor initial cost.

At $900^{\circ}C$, same as all temperatures CO_2 is produced at the highest flow rate. CH_4 is produced at the highest flow rate of all hydrocarbons followed by C_2H_4, H_2 then C_2H_6. All peaks tend to occur earlier, and the peak values increase. The maximum peak of CO_2 is 24% of the total evolving gas volume after 2 minutes from the start of the reaction. The largest peak of CO_2 occurred at $800^{\circ}C$ after which H_2 and CO evolution increased significantly decreasing the CO_2 concentration in the evolved gas. CO peaks value increased significantly to 15%. H_2 peak is 18% in magnitude. Other hydrocarbons contribute to lower percentage of the volume; 8%, 1.0%, and 4.5% for CH_4, C_2H_6, and C_2H_4 respectively.

(a) Mole concentration

(b) Mass flow rate
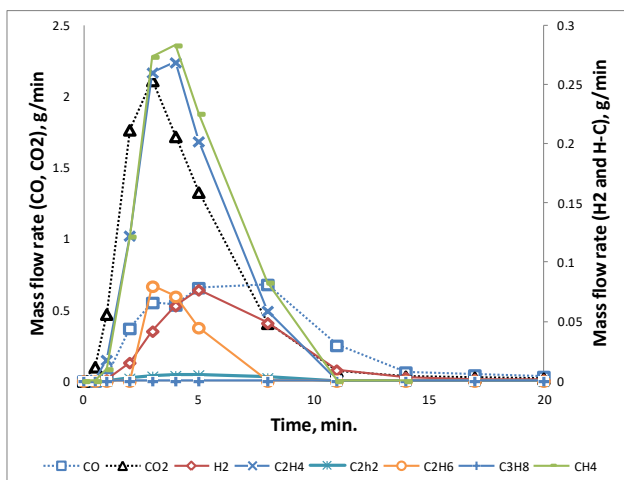
Figure 5-4 : The evolution of different gases at 900°C, case 0

The progress from 800°C to 900°C is similar to the progress from 900°C to 1000°C, increased peak value and shorter reaction time. The maximum peak of CO_2 is 23% of the total evolving gas volume after 2 minutes from the start of the reaction. CO peaks value increased significantly to 27% at the fourth minute. H_2 peak is 2% in magnitude. Other hydrocarbons contribute with lower percentage of the volume; 10.5%, 1.0%, and 6.1% for CH_4, C_2H_6, and C_2H_4 respectively.

(a) Mole concentration
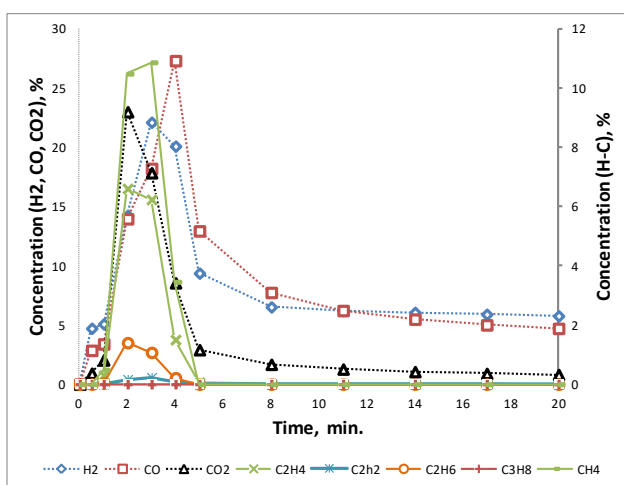
(b) Mass flow rate
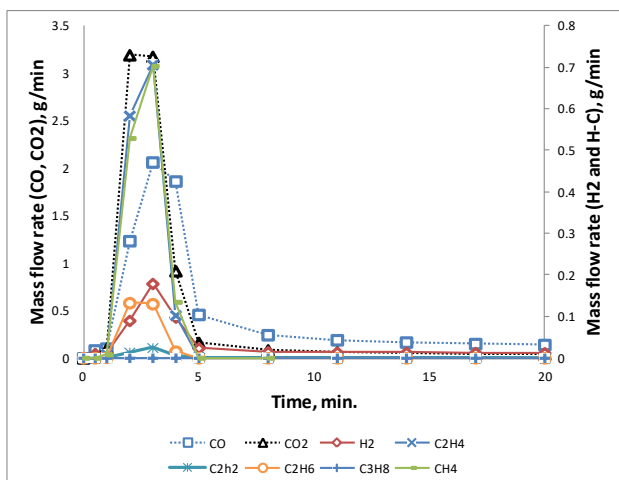
Figure 5-5 : The evolution of different gases at $1000^{\circ}C$, case 0

5.1.2 The effect of temperature on the evolution of different gases:

Figure 5-6. As the temperature increases the peak value increases, the peak is steeper, and the time at which the mass flow rate peaks occur is decreased. The mass flow rate of H_2 increased by 100% at $1000^{\circ}C$ compared to $900^{\circ}C$. At higher reacting temperature allows the chemical bonds to be thermally broken and thus generating smaller chain compounds like H_2.

Figure 5-6 : The effect of temperature on the evolution of H_2, case 0

46
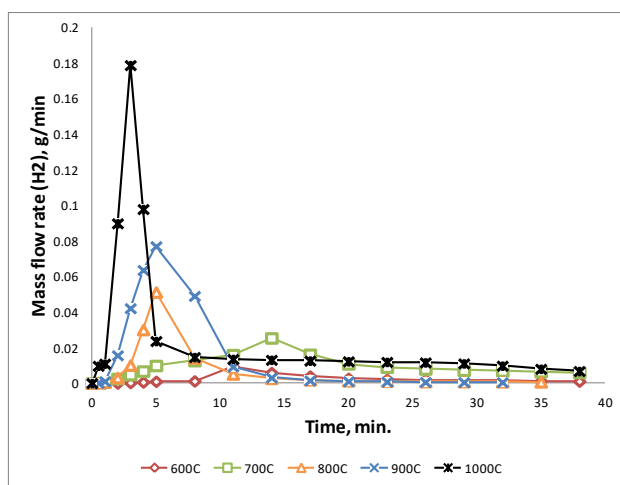
The mass flow rate of CO follows a similar trend as that of H_2. The peak value at 1000^oC is 3 times larger than that at 900^oC. The sharp increase in CO mass flow rate is a result of thermal deterioration of CO_2, and can be a result of the reaction of CO_2 generated from the thermal degradation of carboxylic bonds with the fixed carbon present in the chicken manure, eq. (5-2). This can be justified by the steady CO generation (Figure 5-7) after the Pyrolysis process. Another justification can be postulated from Figure 5-8 : The effect of temperature on the evolution of CO2, case 0where the mass flow rate of CO_2 increased by 50% while the mass flow rate of CO increased by 300%.
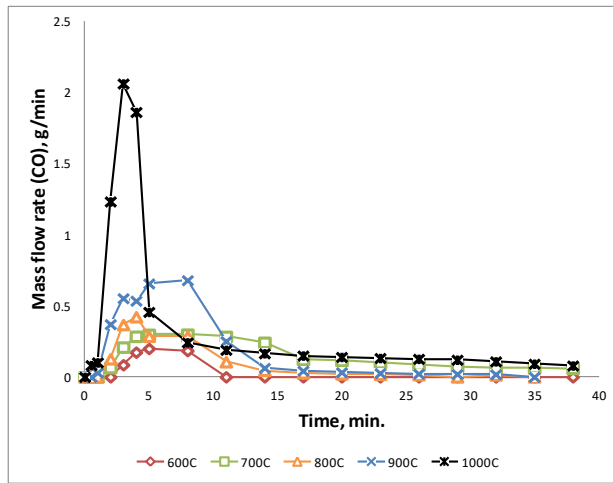
Figure 5-7 : The effect of temperature on the evolution of CO, case 0

The mass flow rate of carbon dioxide contributed by 50% of the total mass flow rate of the product gas all the time. Similar to other gases the higher the temperature, the higher the mass flow rate peak and the earlier the maximum flow rate is occurring.
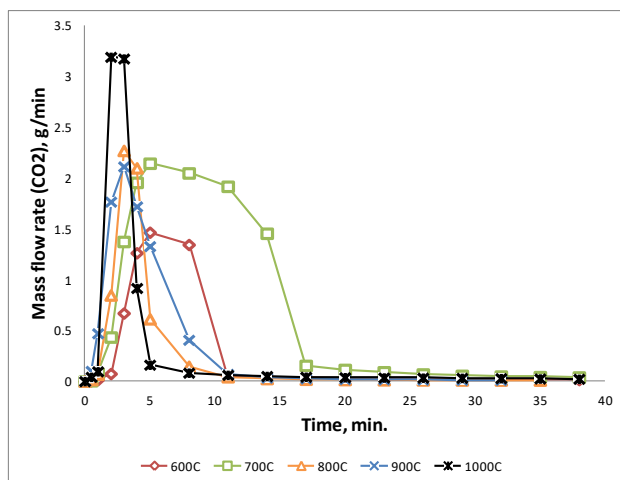
Figure 5-8 : The effect of temperature on the evolution of CO_2, case 0

Figure 5-9 shows the total mass evolution of syngas, the mass flow rate peaked at 4 g/min. after 3 minutes from the start of the reaction, at 1000^oC. The peak is 3 times the peak at 900^oC which is similar to the CO behavior. The bulk mass of the gas is CO which contributed in the highest mass fraction of all other gases at all the 5 different temperatures.
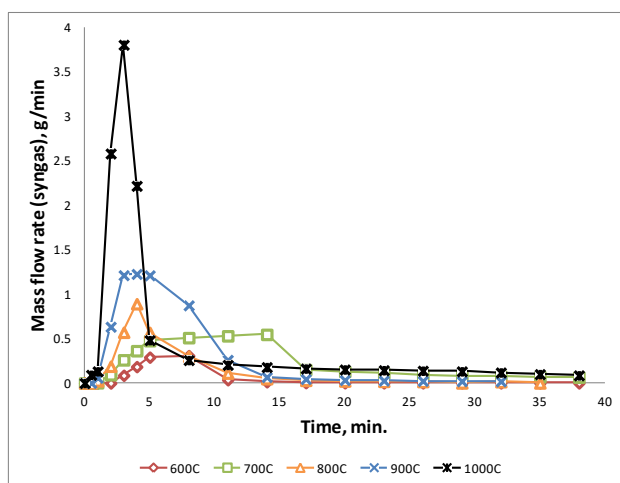
Figure 5-9 : The effect of temperature on the evolution of syngas, case 0

5.1.3 Conversion efficiency:

In order to assess the conversion process of both carbon and energy, conversion efficiencies were calculated using eq. (3- 6) and (3- 7) respectively.

Figure 5-10, shows the calculated values for carbon and energy conversion efficiencies, both efficiency increased with the temperature especially as the temperature increases from $900^{o}C$ to $1000^{o}C$. Given that chicken manure has a 12.8% fixed carbon, it is not possible to reach a 100% efficiency for energy or carbon conversion using N_2. The low carbon conversion efficiency at low temperatures indicate a high tar production, and thus less energy converted into gaseous form.
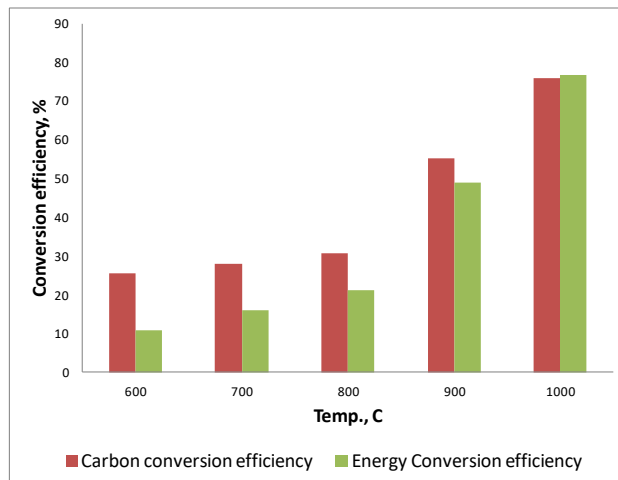
Figure 5-10 : Carbon and energy conversion efficiencies at different temperatures, case 0

5.2 CO_2 gasification, Case 1

5.2.1 Evolved gas analysis at different temperatures

When CO_2 is used as the gas agent gasification of the fixed carbon in the chicken manure is expected as a result of eq. (5-2). At $600^{o}C$, no improvement in the gas production from the case of N_2 is expected. Equation (5-2) is active only at a higher temperature which makes the

600°C similar to N_2 pyrolysis at the same temperature. Figure 5-11, shows (a) the mole fraction of different gas species in the product gas and (b) the mass flow rate of different species. It can be seen at the low temperature of 600°C the useful gases (Fuels) evolution is limited and is very low compared to the CO_2 evolution. The tar production is high while the gas conversion is low. During the first 4 minutes, no gas evolution was detected, which means that during this time only condensable products were produced. After the first 4 minutes CO, CH_4, C_2H_4, and C_2H_6 starts to evolve while H_2 is delayed till the fifth minute. CO was produced at the highest flow rate followed by CH_4, C_2H_6, then H_2 and C_2H_4. The maximum peak of CO_2 is 50% of the total evolving gas volume after 5 minutes from the start of the reaction. CO peaks at the same time as the CO_2 with a peak value of 5%. H_2 peak is delayed to the eleventh minute with 5% magnitude. Other hydrocarbons contribute to lower percentage of the volume; 1.3%, 0.4%, and 0.25% for CH_4, C_2H_6, and C_2H_4 respectively. It can be seen that the values of the peaks are very similar to the N_2 cases except for CO_2 which increased as a result of the introduced amount of the agent.

(a) Mole concentration

(b) Mass flow rate
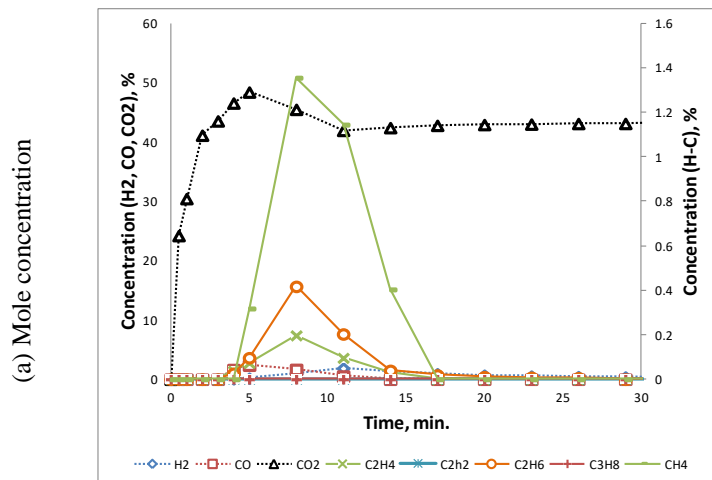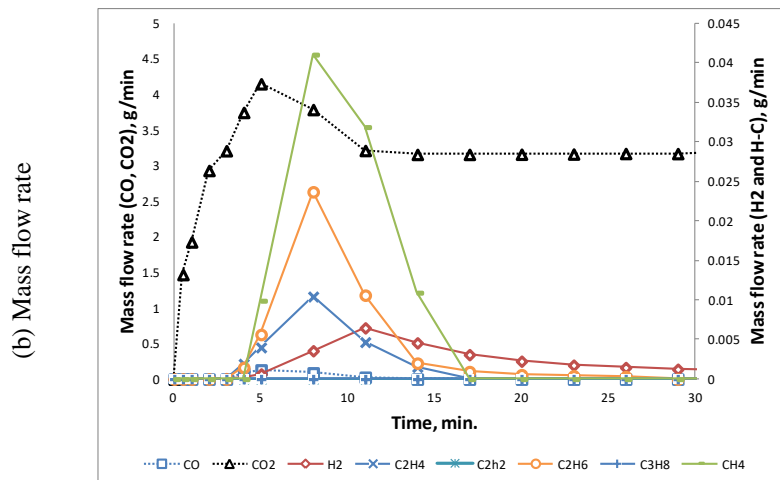
Figure 5-11: The evolution of different gases at $600^{o}C$, case 1

As the reaction temperature increases, the higher flow rate of the product gases is observed in Figures Figure 5-11 through Figure 5-15.

At $700^{o}C$, a slow rate Boudard reaction (5-2) starts at the fifth minute. The total reaction time was increased, and the generated mass flow rates were very low compared to CO_2. C_2H_6, H_2, and C_2H_4 were detected during the Pyrolysis stage (10 minutes), after which the syngas consisted of mainly CO. The maximum peak of CO_2 is 54% of the total evolving gas volume after 5 minutes from the start of the reaction. CO evolution is very steady but at a low concentration of 5% for the whole reaction time. H_2 peaks at 9 minutes with 5% magnitude. Other hydrocarbons contribute with a lower percentage of the volume; 3.5%, 1.0%, and 0.6% for CH_4, C_2H_6, and C_2H_4 respectively.

(a) Mole concentration

(b) Mass flow rate

Figure 5-12 : The evolution of different gases at 700°C, case 1

As the temperature further increase the peaks of gas species increases for lighter hydrocarbons (H_2, C_1 and C_2). The maximum peak of CO_2 is 55% of the total evolving gas volume after 4 minutes from the start of the reaction. At the eleventh minute CO concentration peaks to 10% then the production of CO steadily declined to the end of the reaction. H_2 peaks at 6 minutes with 6% magnitude. Other hydrocarbons contribute to a lower percentage of the volume; 2.7%, 0.1%, and 0.7% for CH_4, C_2H_6, and C_2H_4 respectively. The composition of the syngas changes depending on the reaction temperature with CO of the highest mass flow rate. At 600°C, the gases with the highest flow rate were CO, CH_4 then C_2H_6. At 700°C, the maximum

mass flow rate is still for C_2H_6 followed by C_2H_4, then H_2. As the temperature increases further to 800^oC, the product gas species peak values are re-arranged with C_2H_4 leading, followed by H_2. The peaks tend to occur at earlier times and the total reaction time is decreased.
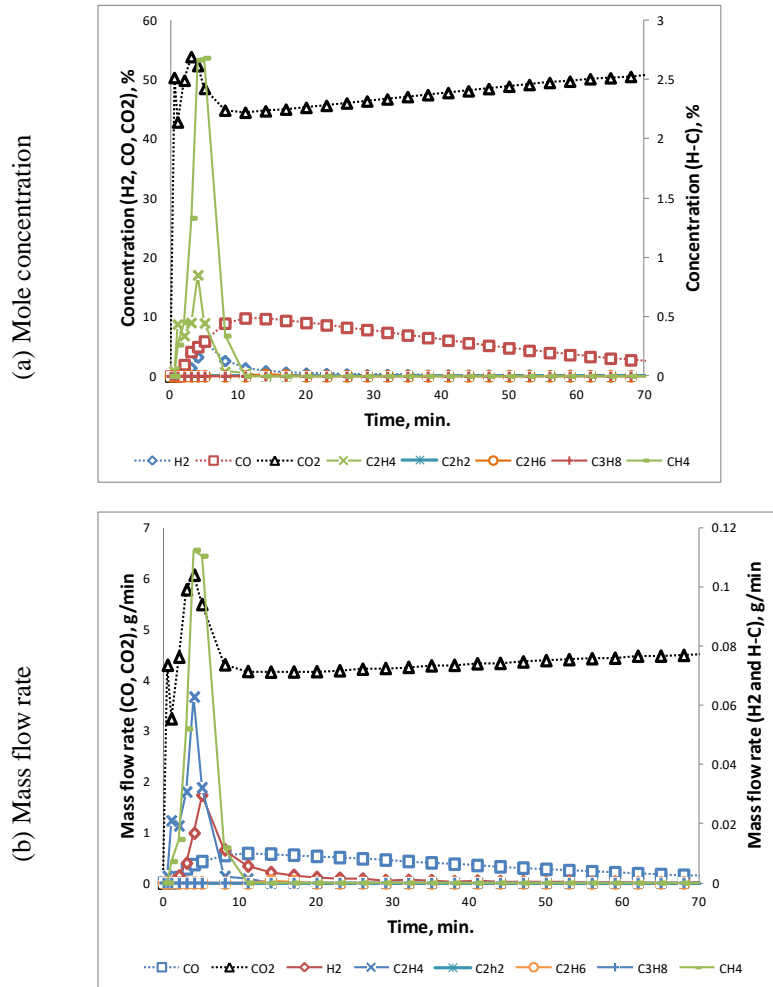
Figure 5-13 : The evolution of different gases at 800^oC, case 1

At 900^oC, same as all temperatures CO is produced at the highest flow rate. CH_4 is produced at the highest flow rate of all hydrocarbons followed by C_2H_4 then H_2. All peaks tend to occur earlier, and the peak values increase. The maximum peak of CO_2 is 55% of the total evolving gas volume after 4 minutes from the start of the reaction. At the ninth minute CO concentration peaks to 18% then the production of CO steadily declined to the end of the

reaction. H_2 peaks at 5 minutes with 8% magnitude. Other hydrocarbons contribute to a lower percentage of the volume; 5%, 0.9%, and 2.1% for CH_4, C_2H_6, and C_2H_4 respectively.
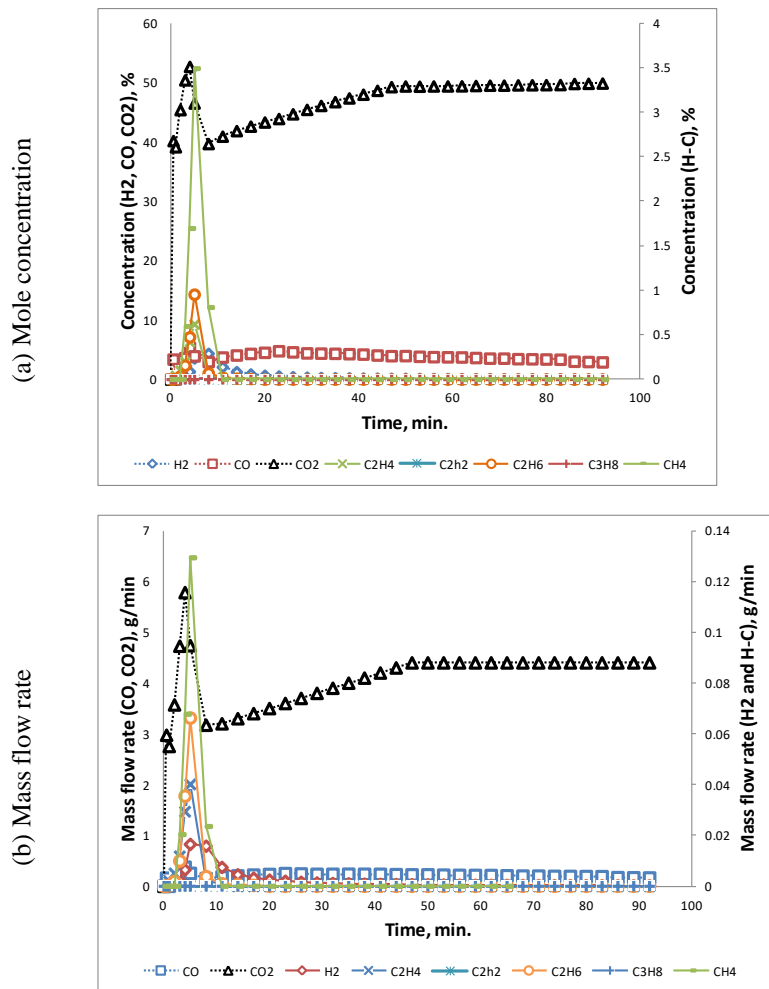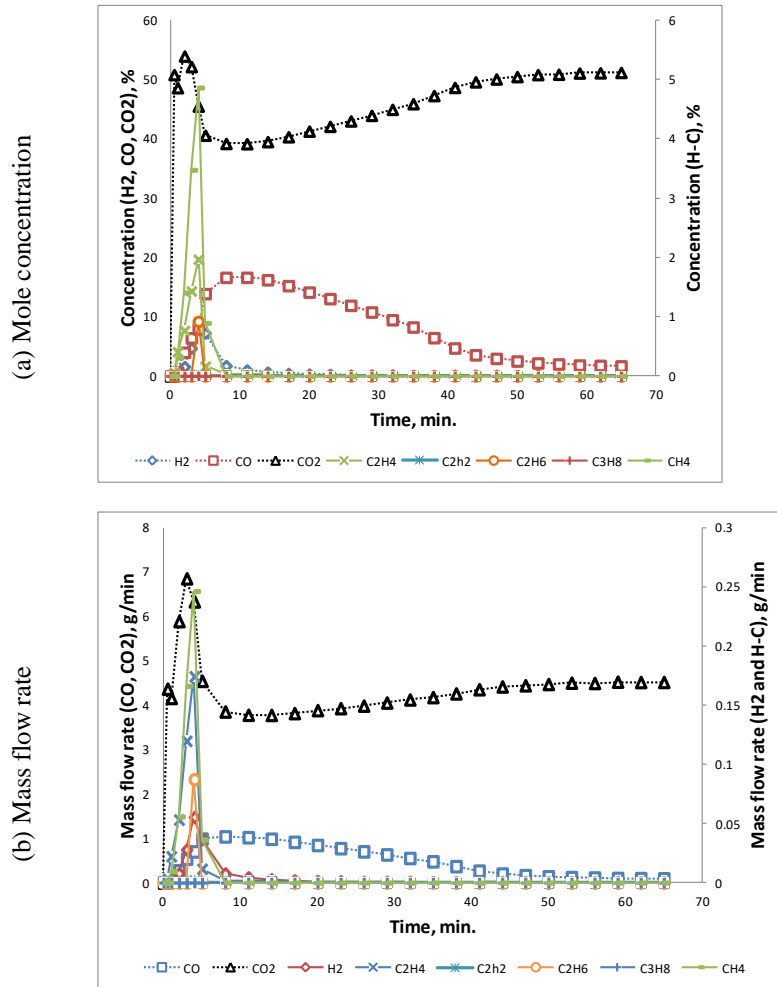

Figure 5-14 : The evolution of different gases at 900°C, case 1

The progress from 800°C to 900°C is similar to the progress from 900°C to 1000°C, increased peak value and shorter reaction time. The maximum peak of CO_2 is 50% of the total evolving gas volume after 2 minutes from the start of the reaction. At the fifth minute CO concentration peaks to 25% then the production of CO steadily declined to the end of the

reaction. H_2 peaks at 4 minutes with 14% magnitude. Other hydrocarbons contribute with a lower percentage of the volume; 7.6%, 1.2%, and 3.5% for CH_4, C_2H_6, and C_2H_4 respectively.

(a) Mole concentration

(b) Mass flow rate
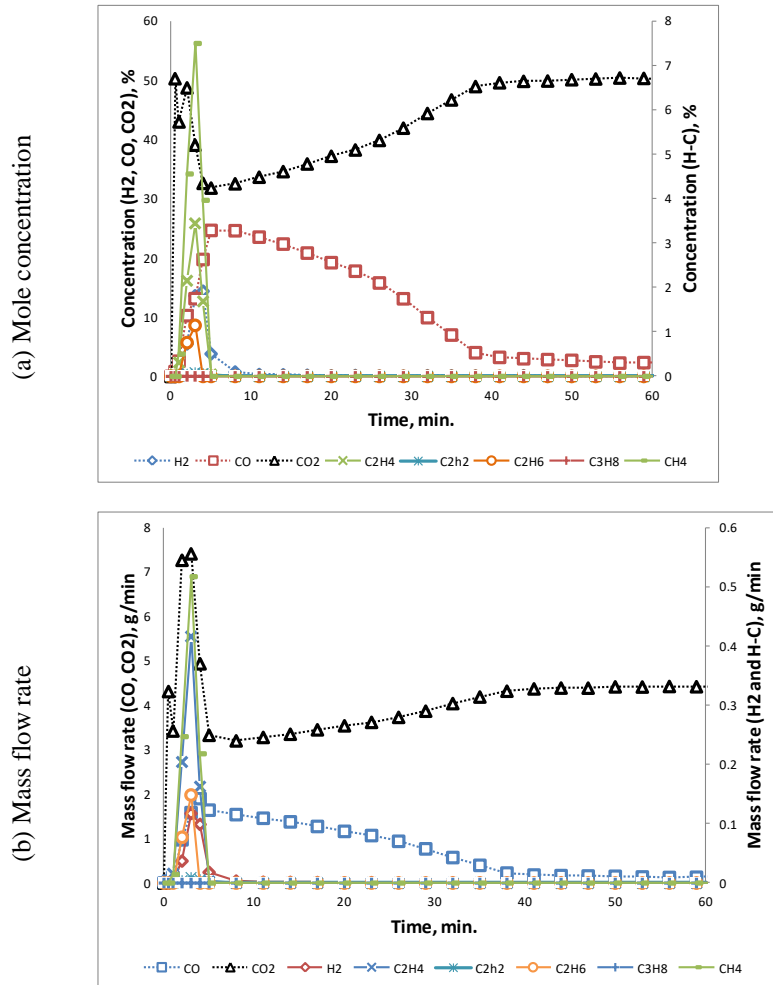
Figure 5-15 : The evolution of different gases at 1000°C, case 1

5.2.2 The effect of temperature on the evolution of different gases:

In Figure 5-16, as the temperature increases the peak value increases, the peak is steeper, and the time at which the mass flow rate peaks occur is decreased. The mass flow rate of H_2 increased by 200% at 1000°C compared to 900°C. Higher reacting temperature allows the chemical bonds to be thermally broken and thus generating smaller chain compounds like H_2.
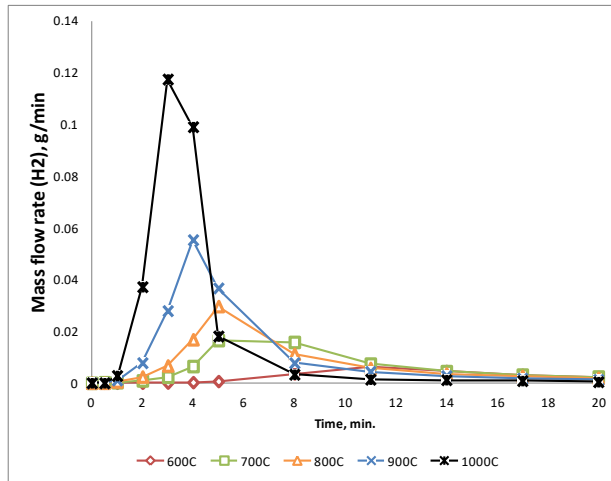
Figure 5-16 : The effect of temperature on the evolution of H_2, case 1

The mass flow rate of CO follows a similar trend as that of H_2. The peak value at 1000^oC is 2 times larger than that at 900^oC. The sharp increase in CO mass flow rate is a result of eq. (5-2). The production of CO was characterized by a sharp increase at the start of the reaction until it reaches a peak after which the CO flow rate declines steadily. Gasification reaction of the fixed carbon in the biomass are characterized by lower reaction rates as compared to the Pyrolysis reaction, which explains the slow, steady declining mass flow rate of CO
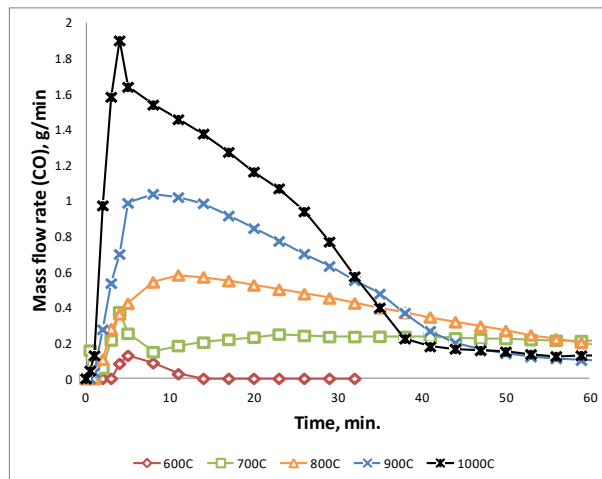
Figure 5-17 : The effect of temperature on the evolution of CO, case 1

56

The mass flow rate of carbon dioxide contributed by 50% of the total mass flow rate of the product gas all the time. Similar to other gases the higher the temperature, the higher the mass flow rate peak and the earlier the maximum flow rate is occurring. The CO_2 peak is due to the Pyrolysis stage after which the mass flow rate drops below the introduced CO_2 in the agent (4.4 gm/min) due to the reaction of CO_2 with the fixed carbon. The flow rate of CO_2 then increases to reach the 4.4 gm/min near the end of the reaction.
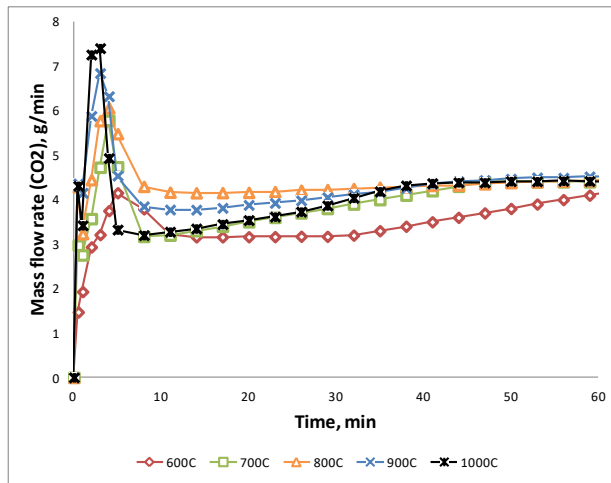
Figure 5-18 : The effect of temperature on the evolution of CO_2, case 1

Figure 5-9 : The effect of temperature on the evolution of syngas, case 0shows the total mass evolution of syngas. The peak at 1000^oC is 2.5 times the peak at 900^oC which is similar to the CO behavior. The bulk mass of the gas is CO which contributed in the highest mass fraction of all other gases at all the 5 different temperatures.

57
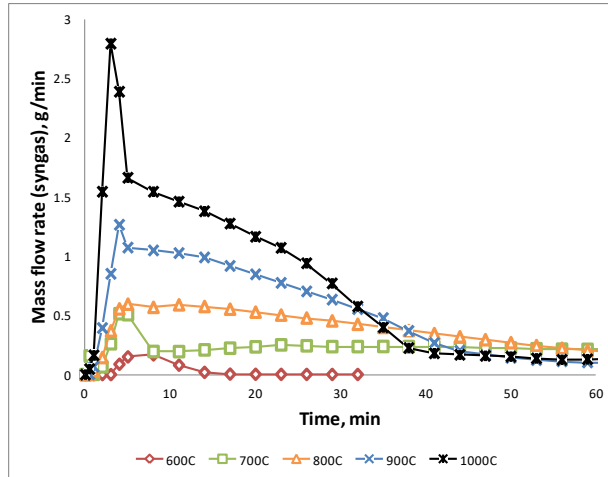
Figure 5-19 : The effect of temperature on the evolution of syngas, case 1

5.2.3 Conversion efficiency:

Figure 5-20 shows the calculated values for carbon and energy conversion efficiencies, both efficiency increased with the temperature. Both efficiencies increased significantly as the temperature reached 700°C, this is a result of the Boudard reaction which needs high temperatures produce CO from fixed carbon, eq.(5-2).
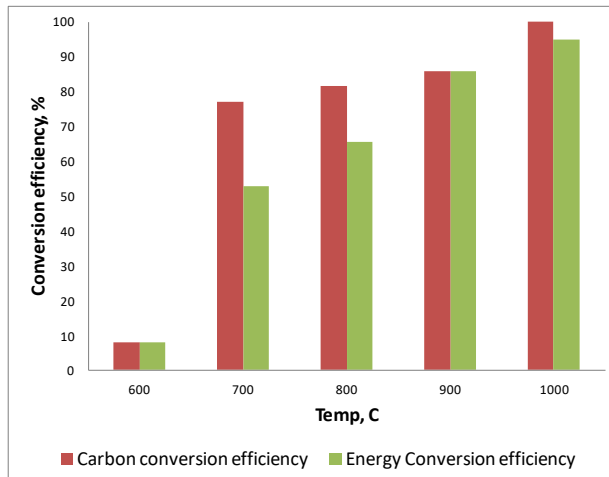
Figure 5-20 : Carbon and energy conversion efficiencies at different temperatures, case 1

5.3 Air gasification, Case 2

5.3.1 Evolved gas analysis at different temperatures

When air is used as the gas agent, gasification of the fixed carbon in the chicken manure is expected as a result of eq. (5-1) and (5-2). At $600^{\circ}C$, there is a slight improvement in the gas evolution when compared to the previous cases. The improvement is due to the combustion of some of the evolving gas/tar in exothermic reactions. The exothermic reactions provide more heat than the previous cases, allowing better breakdown of chemical bonds. Figure 5-21, shows (a) the mole fraction of different gas species in the product gas and (b) the mass flow rate of different species. The magnitude of the CH_4, is twice the magnitude of the same peak for other cases at the $600^{\circ}C$. The maximum peak of CO_2 is 19% of the total evolving gas volume after 6 minutes from the start of the reaction. CO peaks at the same time as the CO_2 with a peak value of 5%. H_2 peak is delayed to the eleventh minute with 3% magnitude. Other hydrocarbons contributes with lower percentage of the volume; 2.7%, 0.7%, 0.8% and 0.25% for CH_4, C_2H_6, C_2H_4, and C_3H_8 respectively.

Even though the gas evolution has been improved compared to other cases, the absolute value of the peaks is still low. The tar production is high while the gas conversion is low. During the first 2 minutes, no syngas evolution was detected, which means that during this time only condensable products were produced. After the first 2 minutes CO, CH_4, C_2H_4, C_2H_6, and C_3H_8 starts to evolve while H_2 is delayed till the fifth minute. CO was produced at the highest flow rate followed by C_3H_8, CH_4, C_2H_4, C_2H_6 then C_2H_4, and H_2. After 20 minutes of the reaction mainly CO_2 is evolving from the combustion of fixed carbon while the syngas evolution is minimal.

59
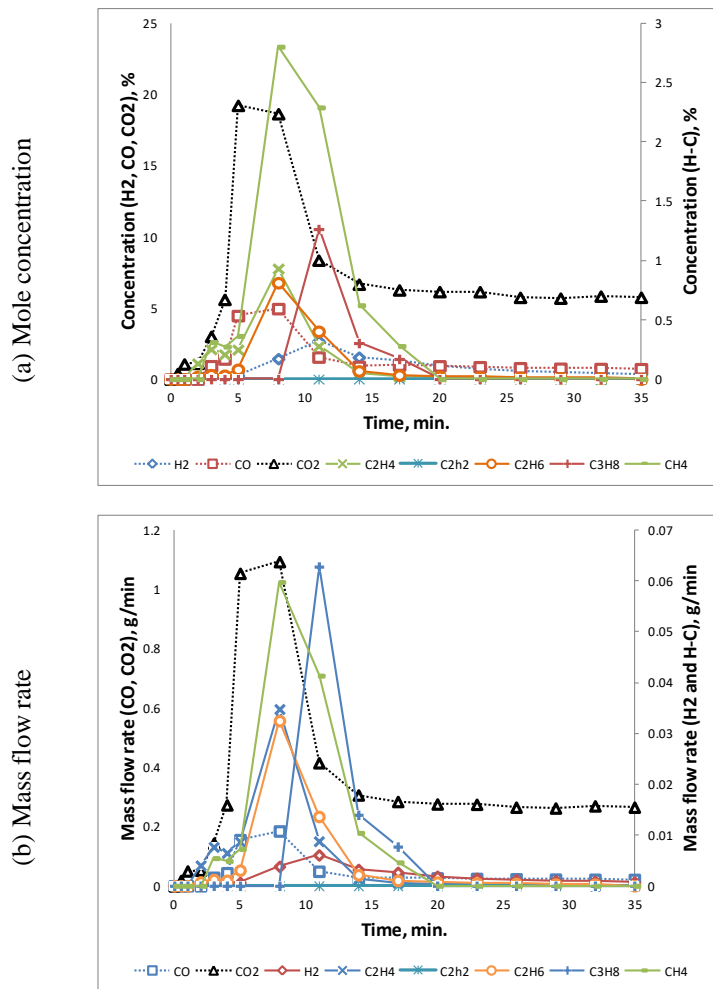
Figure 5-21: The evolution of different gases at 600°C, case 2

As the reaction temperature increases, the higher flow rate of the product gases is observed in Figure 5-21through Figure 5-15.

At 700°C, the peak at the beginning of the reaction is a combination of Pyrolysis and gasification then the slower after the first 5 minutes only char is reacting with oxygen in air to give CO_2 and CO. The maximum peak of CO_2 is 25% of the total evolving gas volume after 5 minutes from the start of the reaction. CO peaks at the same time as the CO_2 with a peak value of 7%. H_2 peak is delayed to the seventh minute with 8% magnitude. Other hydrocarbons contribute

to a lower percentage of the volume; 6.5%, 1.5%, and 2.2% for CH_4, C_2H_6, and C_2H_4 respectively.
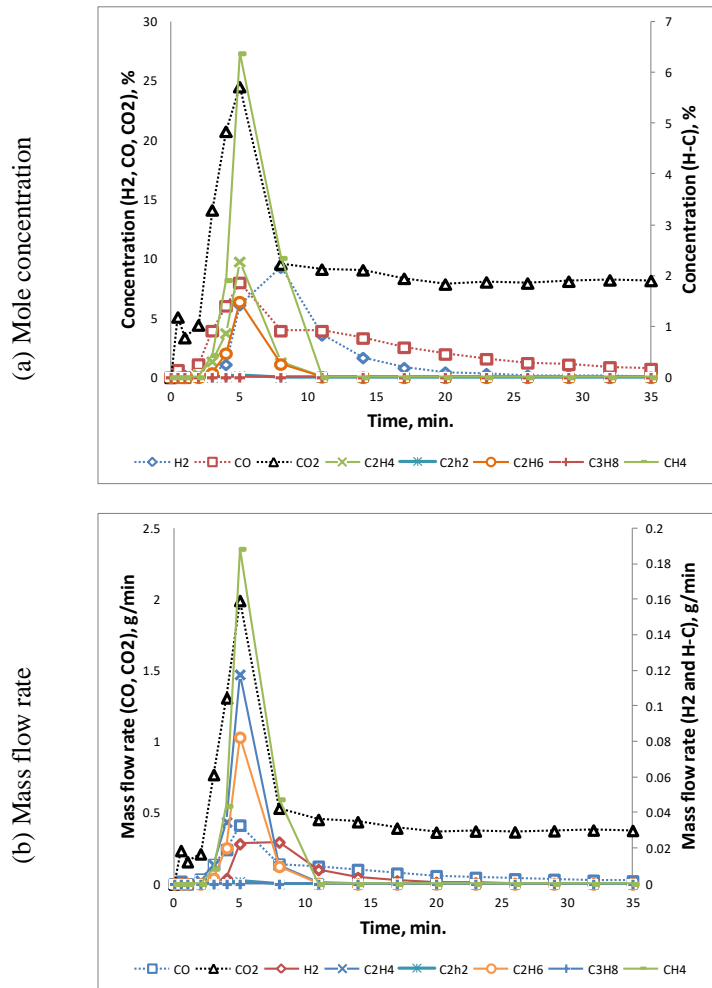
Figure 5-22 : The evolution of different gases at $700^{\circ}C$, case 2

The composition of the syngas during the Pyrolysis stage varies with the reaction temperature. As the temperature increases, lighter hydrocarbons evolve at higher flow rates while heavier hydrocarbon like C_3H_8 flow rate declines. After the Pyrolysis stage, only CO is detected at a significant concentration. The maximum peak of CO_2 is 27% of the total evolving gas volume after 4 minutes from the start of the reaction. CO peak is at 7 minutes which is an overlap between the generated CO in Pyrolysis and gasification; the peak value was 14%. H_2

peak is delayed to the seventh minute with 8% magnitude. Other hydrocarbons contribute to a lower percentage of the volume; 6.5%, 1.5%, and 2.2% for CH_4, C_2H_6, and C_2H_4 respectively.

(a) Mole concentration

(b) Mass flow rate
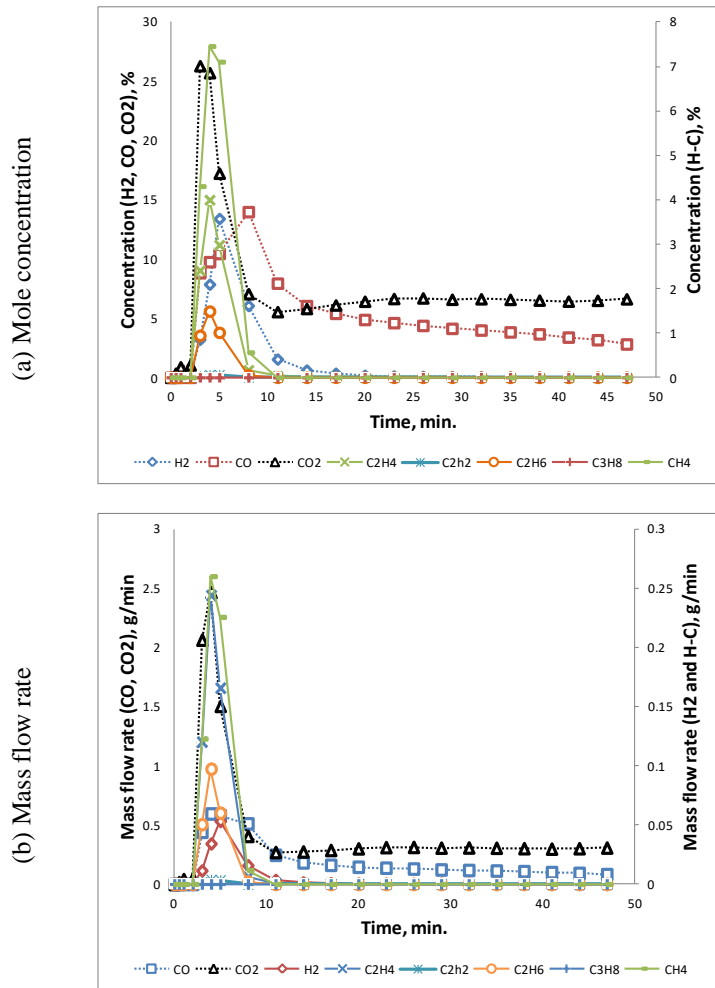
Figure 5-23 : The evolution of different gases at 800^oC, case 2

At 900^oC, CO is produced at the highest flow rate. CH_4 is produced at the highest flow rate of all hydrocarbons followed by C_2H_4, C_2H_6, then H_2. All peaks occur earlier, and the peak values increased. The maximum peak of CO_2 is 27% of the total evolving gas volume after 3 minutes from the start of the reaction. CO peak is at 4 minutes which is an overlap between the generated CO in Pyrolysis and gasification; the peak value was 15%. H_2 peak at the fourth

62

minute with 15% magnitude. Other hydrocarbons contribute to a lower percentage of the volume; 8.5%, 1.2%, and 4.8% for CH_4, C_2H_6, and C_2H_4 respectively.
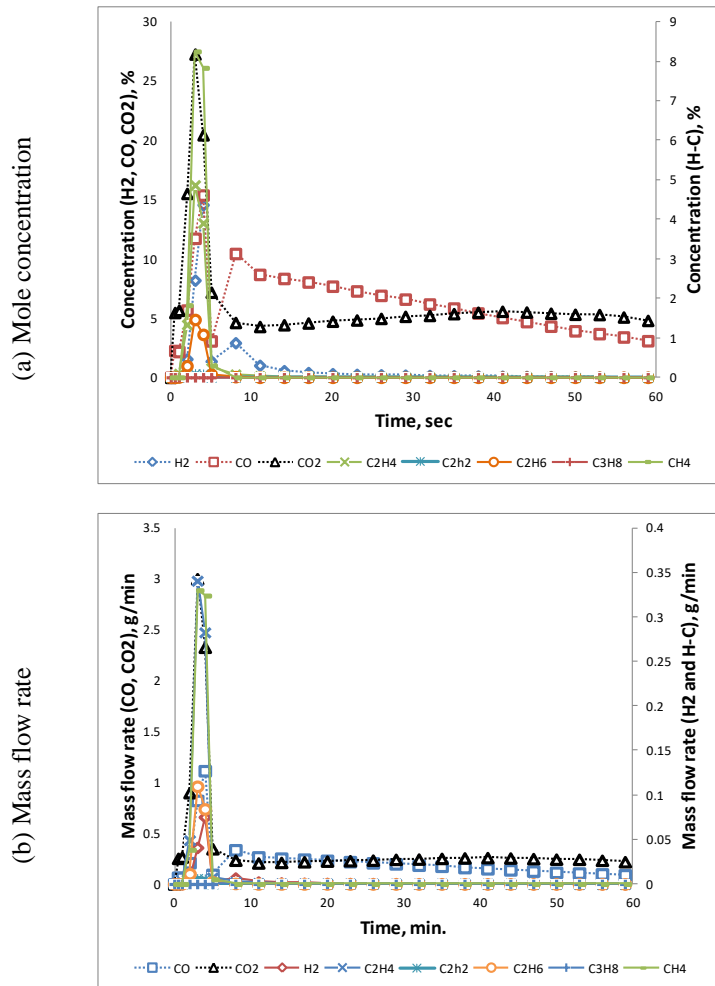
Figure 5-24 : The evolution of different gases at 900^oC, case 2

At 1000^oC the concentration of CO exceeds the concentration of CO_2 for the first time in all of the cases. The high concentration of CO is due to the dissociation of CO_2, and the incomplete combustion of fixed carbon with oxygen in the air.

(a) Mole concentration
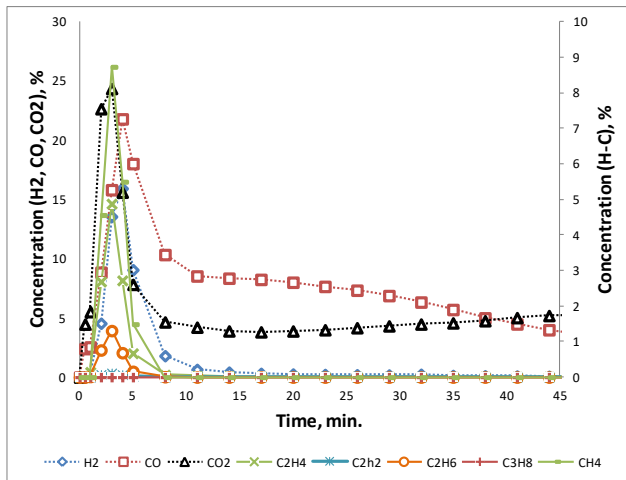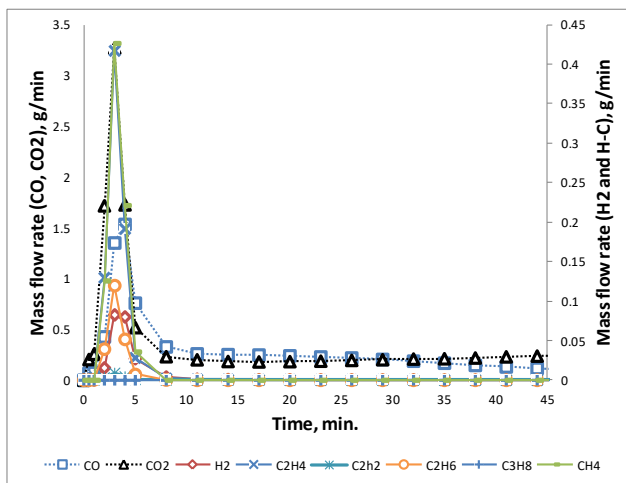
(b) Mass flow rate

Figure 5-25 : The evolution of different gases at 1000°C, case 2

5.3.2 The effect of temperature on the evolution of different gases:

As the temperature increases the peak value increases, the peak is steeper, and the time at which the mass flow rate peaks occur is decreased. The rate of increase in the peak value of temperature is lower than other gaseous agents due to the combustion of a fraction of the product H_2 by excess O_2 in air.
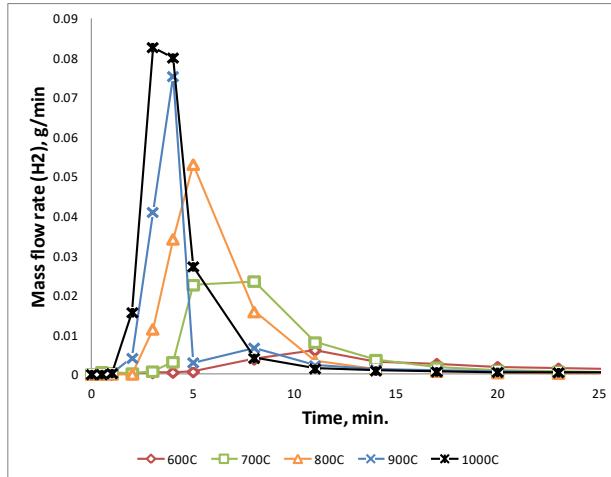
Figure 5-26 : The effect of temperature on the evolution of H_2, case 2

The mass flow rate of CO follows a similar trend as that of H_2. The peak value increases with temperature. A large peak due to Pyrolysis then a steady lower flow rate from gasification.
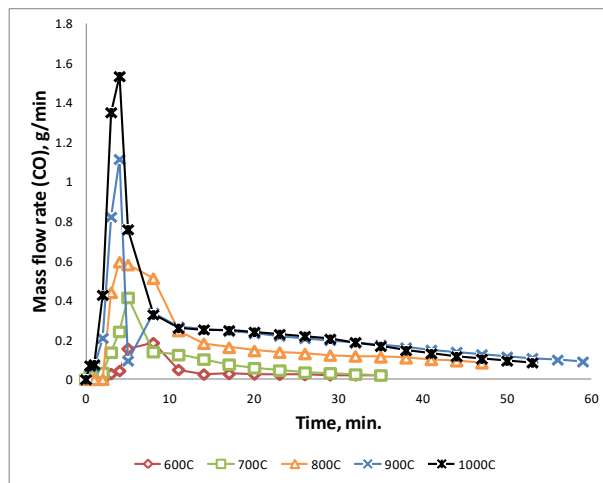
Figure 5-27 : The effect of temperature on the evolution of CO, case 2

The mass flow rate of carbon dioxide contributed by at least 50% of the total mass flow rate of the product gas all the time. Similar to other gases the higher the temperature, the higher the mass flow rate peak and the earlier the maximum flow rate is occurring. As the temperature increases from 900°C to 1000°C the mass flow rate peak only increased by 16%.
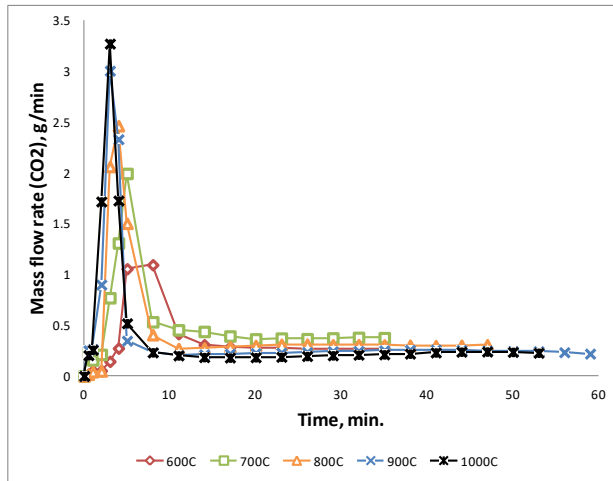
Figure 5-28 : The effect of temperature on the evolution of CO_2, case 2

Figure 5-29 shows the total mass evolution of syngas. Unlike other cases, the increase in mass flow rate with temperature is steady, and there is no sudden increase from one temperature to the other.
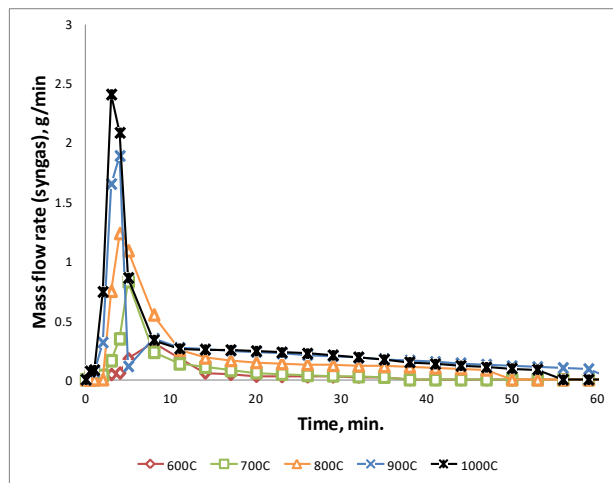
Figure 5-29 : The effect of temperature on the evolution of syngas, case 2

5.3.3 Conversion efficiency:

Figure 5-30 shows the calculated values for carbon and energy conversion efficiencies, both efficiencies increased with the temperature. The total energy conversion at high temperatures is lower than the previous cases, because of the oxidation of some of the product gases in the presence of oxygen.
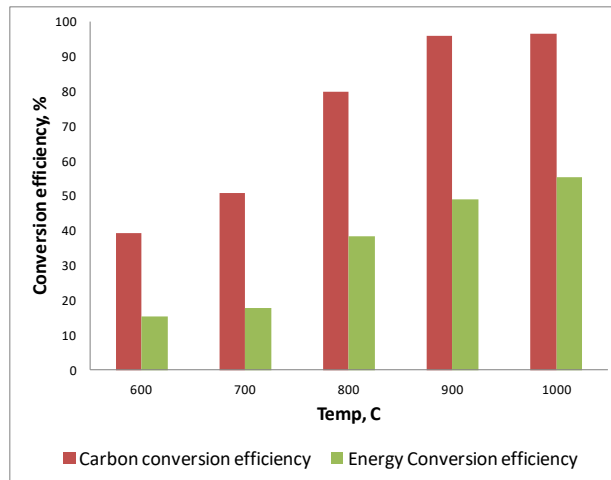
Figure 5-30 : Carbon and energy conversion efficiencies at different temperatures, case 2

5.4 10% Oxygen, Case 3

Case 2 showed improvement in the reaction rates (total reaction time decreased) but on the expense of energy conversion. The concentration of O_2 was halved in case 3 to gain the improvement in reaction time and decrease the loss of energy due to the complete combustion of some of the evolving gases.

5.4.1 Evolved gas analysis at different temperatures

Figure 5-1: The evolution of different gases at 600oC, case 0shows, (a) the mole fraction of different gas species in the product gas and (b) the mass flow rate of different species. Both (a) and (b) are for $600^{o}C$, when N_2 + 10% O_2 was used as the gas agent. The mass flow rates of

syngas components are lower as compared with higher temperatures. CO is the first to evolve after 3 minutes, and its peak is the highest amongst all of the syngas components. The mass flow rate of CO is three times higher than any other syngas species. CH_4 is the second most produced gas followed by C_2H_4, C_2H_6, H_2, and C_2H_2. The evolution of H_2 and hydrocarbons is only detected at the early Pyrolysis stage. The value of the peak of CO_2 is 26% of the total evolving gas volume after 5 minutes from the start of the reaction. CO peaks at the same team as CO_2 with a peak magnitude of 6%. H_2 peak a while after CO seventh minute with 4% magnitude. Other hydrocarbons contribute with a lower percentage of the volume; 3.8%, 0.8%, and 1.5% for CH_4, C_2H_6, and C_2H_4 respectively.

(a) Mole concentration

(b) Mass flow rate

Figure 5-31: The evolution of different gases at 600°C, case 3

As the reaction temperature increases, higher flow rates of the product gases are observed in Figures Figure 5-32 through Figure 5-35.

At 700°C, the relatively high concentration of C_2H_6 does not increase while concentrations of lighter hydrocarbons increases. When comparing with the gas evolution at 600°C, the gas peaks are higher, earlier, while the evolution time remains the same. The value of the peak of CO_2 is 35% of the total evolving gas volume after 4 minutes from the start of the reaction. CO peaks at the same time as CO_2 with a peak magnitude of 8%. H_2 peak a minute after CO with 7% magnitude. Other hydrocarbons contribute to a lower percentage of the volume; 6.5%, 1.2%, and 1.8% for CH_4, C_2H_6, and C_2H_4 respectively.

(a) Mole concentration

69

(b) Mass flow rate
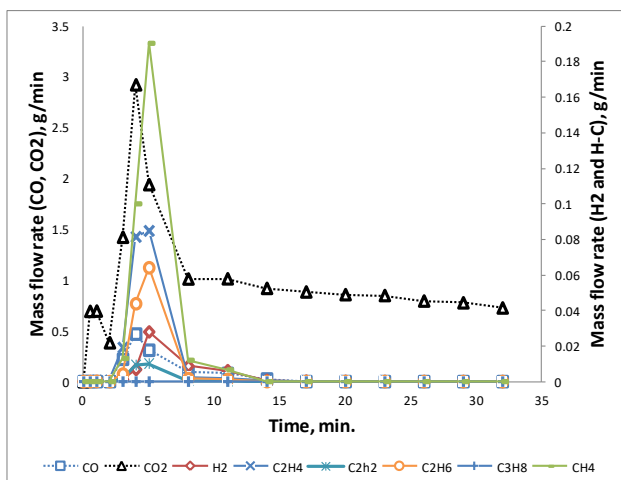
Figure 5-32 : The evolution of different gases at 700°C, case 3

As the temperature further increase the peaks of gas species increases for lighter hydrocarbons (H_2, C_1 and C_2) while C_2H_6 concentration decreases. The composition of the syngas changes depending on the reaction temperature with CO of the highest mass flow rate. The mass fraction of lighter gases increases as the temperature increases. The value of the peak of CO_2 is 30% of the total evolving gas volume after 4 minutes from the start of the reaction. CO peaks at the same time as CO_2 with a peak magnitude of 10%. H_2 peaks a minute after CO with 12% magnitude. Other hydrocarbons contribute to a lower percentage of the volume; 8.5%, 1.1%, and 4% for CH_4, C_2H_6, and C_2H_4 respectively.

(a) Mole concentration

70
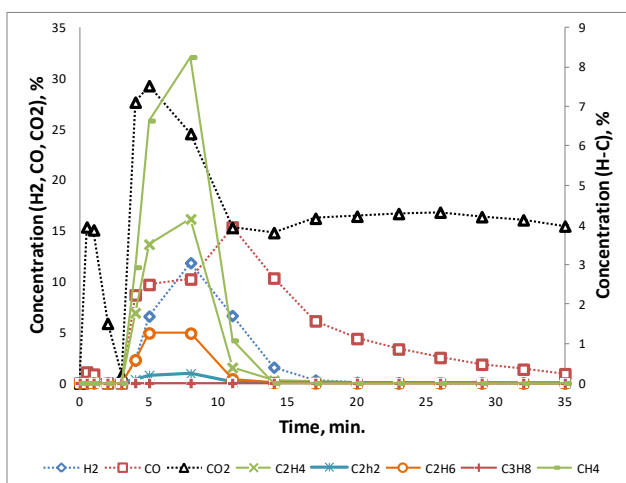
(b) Mass flow rate
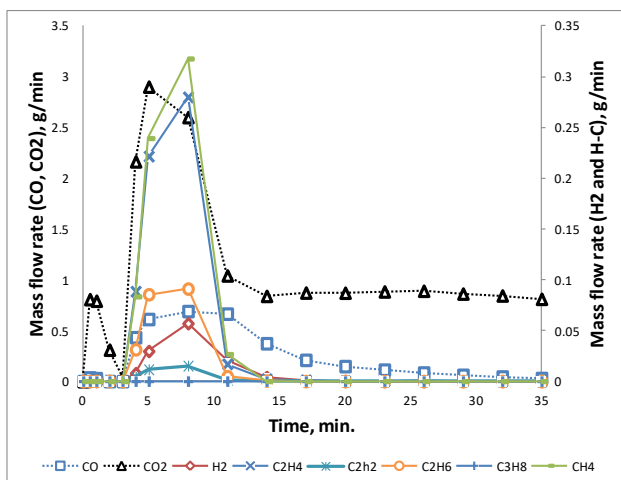
Figure 5-33 : The evolution of different gases at 800°C, case 3

At 900°C CO is produced at high concentrations comparable to that of CO_2. The Pyrolysis stage is shorter and H_2 concentrations up to 13% was detected. CO is the main syngas components followed by CH_4, C_2H_4, C_2H_6, and H_2. The value of the peak of CO_2 is 28% of the total evolving gas volume after 3 minutes from the start of the reaction. CO peaks a minute after CO_2 as a result of the gasification process with a peak magnitude of 22%. H_2 peaks at the same time as CO with 12% magnitude. Other hydrocarbons contribute with a lower percentage of the volume; 7.5%, 1.0%, and 3.3% for CH_4, C_2H_6, and C_2H_4 respectively.
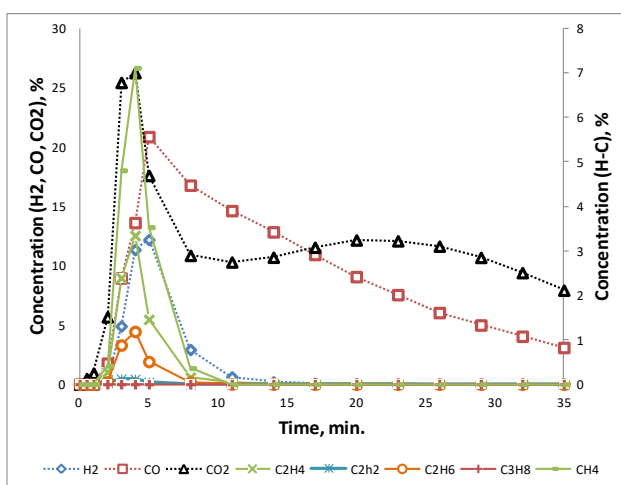
(a) Mole concentration
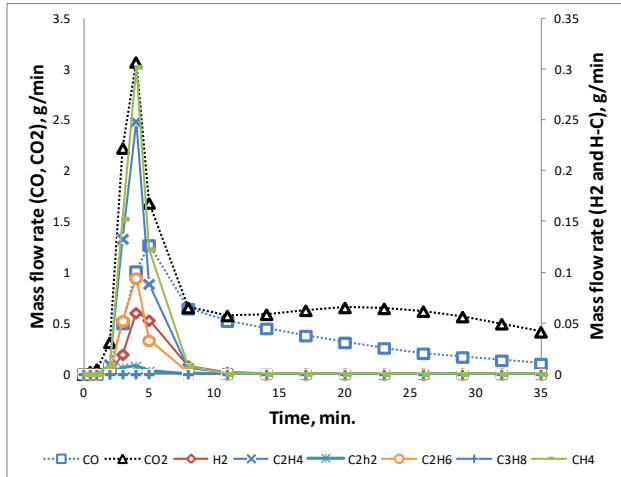
Figure 5-34 : The evolution of different gases at 900$^{\text{o}}$C, case 3

At 1000$^{\text{o}}$C, during the fifth of reaction, the syngas consists mainly of CO (25%), H$_2$ (18%), and CH$_4$ (12%) while the concentrations of heavier hydrocarbons are less than (10%) combined. On the other hand, the mass flow rate of C$_2$H$_4$ is higher than that of CH$_4$ because C$_2$H$_4$ has a higher molecular weight. The value of the peak of CO$_2$ is 25% of the total evolving gas volume after 3 minutes from the start of the reaction. CO peaks 2 minutes after CO$_2$ as gasification overlaps with pyrolysis with a peak magnitude of 25%. H$_2$ peak a minute after CO$_2$ with 17% magnitude. Other hydrocarbons contribute with a lower percentage of the volume; 12%, 0.7%, and 7.5% for CH$_4$, C$_2$H$_6$, and C$_2$H$_4$ respectively.
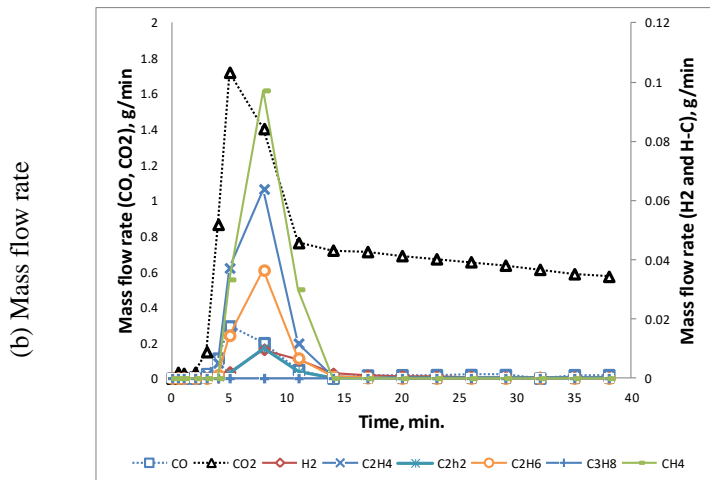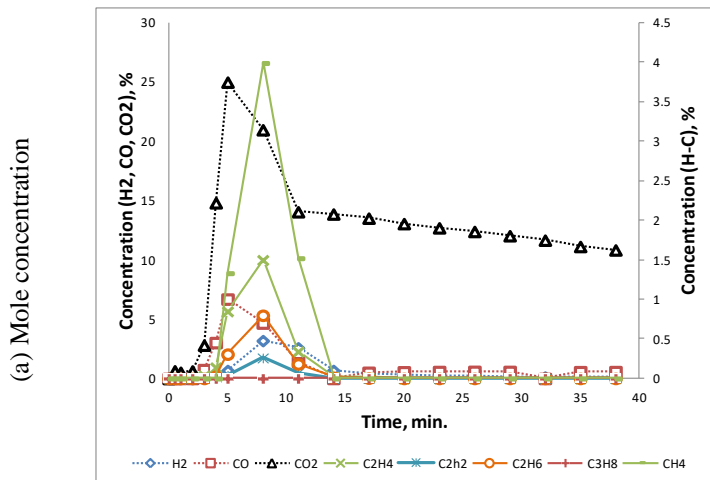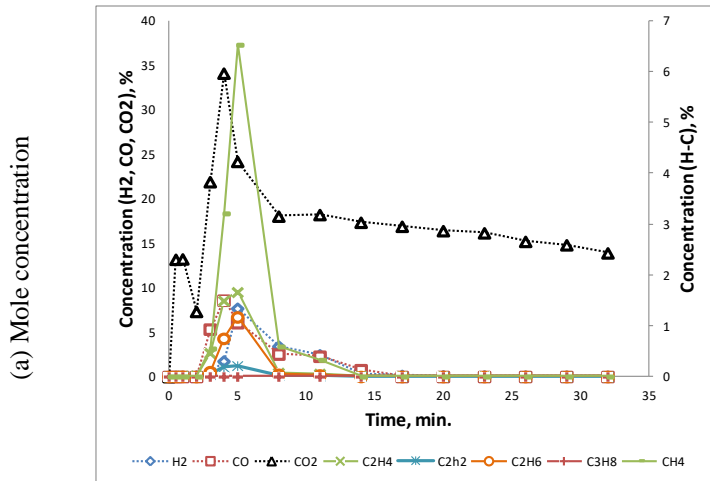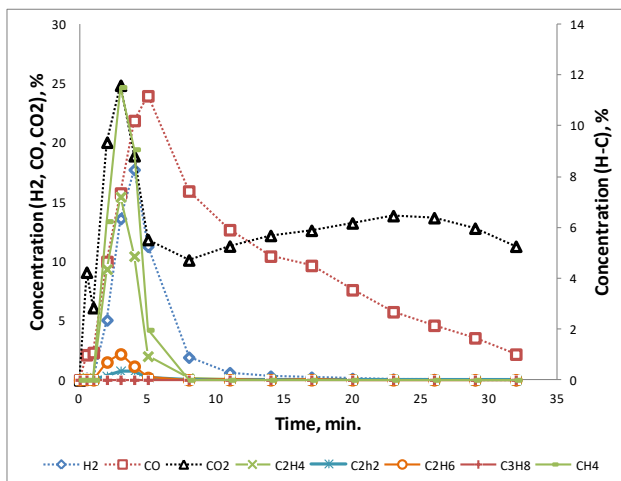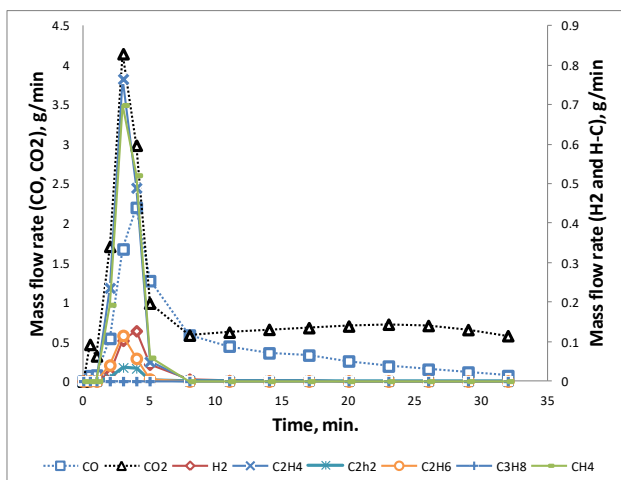
Figure 5-35 : The evolution of different gases at 1000°C, case 3

5.4.2 The effect of temperature on the evolution of different gases:

Figure 5-6 : The effect of temperature on the evolution of H2, case 0. H_2 is exclusively produced during the early Pyrolysis stage, and no important concentrations were detected after the first 10 min. at any temperature. As the temperature increases the total production and peak magnitude increases, while the peak time decreases.
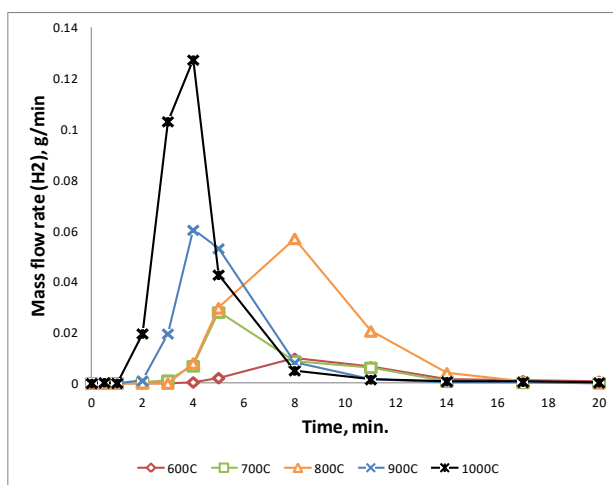
Figure 5-36 : The effect of temperature on the evolution of H_2, case 3

CO was produced at the highest flow rates and after the first 10 minutes it was the only significant syngas component. Reactions (5-1) and (5-2) as well as the dissociation of the produced CO_2 are the prime movers of the conversion of char into gas. Figure 5-37, shows the progress of the mass flow rate of CO as the temperature increases. As the temperature increases the equilibrium concentrations of eq. (5-6) favor the production of CO and thus the peak values of CO increases.
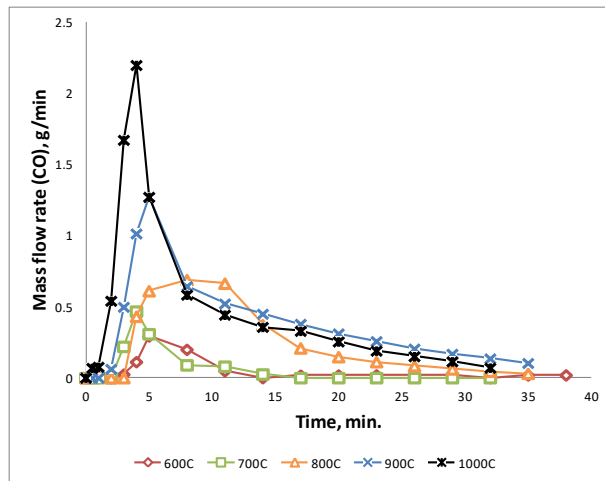
Figure 5-37 : The effect of temperature on the evolution of CO, case 3

The mass flow rate of carbon dioxide contributed by at least 50% of the total mass flow rate of the product gas all the time and close to 100% when the conversion was near its end. Similar to other gases the higher the temperature, the higher the mass flow rate peak and the earlier the maximum flow rate is occurring.
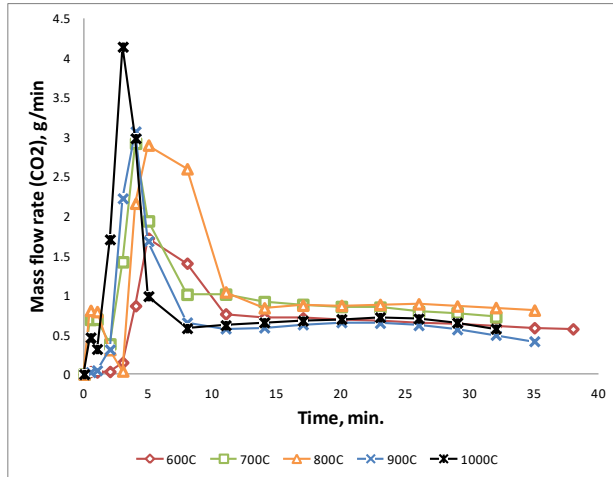
Figure 5-38 : The effect of temperature on the evolution of CO_2, case 3

Figure 5-9 : The effect of temperature on the evolution of syngas, case 0shows the total mass evolution of syngas, the mass flow rate peaked at 3.5 g/min. after 4 minutes from the start of the reaction, at $1000^{o}C$. The peak is two times the peak at $900^{o}C$. The bulk mass of the gas is CO which contributed in the highest mass fraction of all other gases at all the five different temperatures.
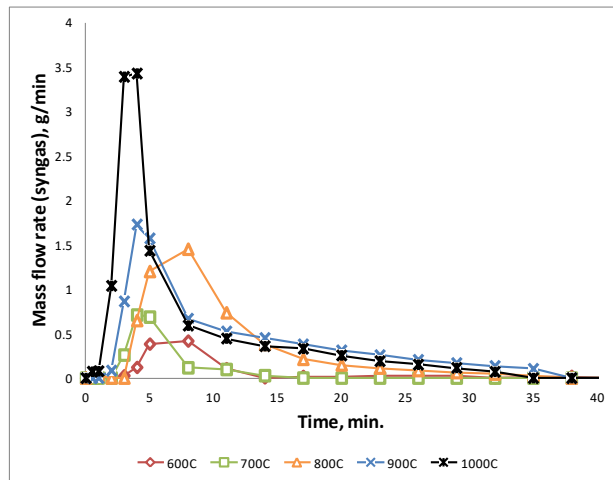
Figure 5-39 : The effect of temperature on the evolution of syngas, case 3

5.4.3 Conversion efficiency:

Figure 5-40 shows the calculated values for carbon and energy conversion efficiencies, both efficiencies increased with the temperature. The efficiency increase was gradual with no sudden increase from one temperature to another. The gradual increase is characteristic for oxygen/air gasification as the main drive of the reactions is the reaction between the fixed carbon and oxygen. The oxidation of carbon takes place at any of tested temperatures, unlike other cases where the driving reaction is only effective at a certain temperature. The carbon conversion is close to unity at 900 and $1000^{o}C$, which indicates a very low tar production. The energy conversion is higher than case 2 when air (21% O_2) was used.
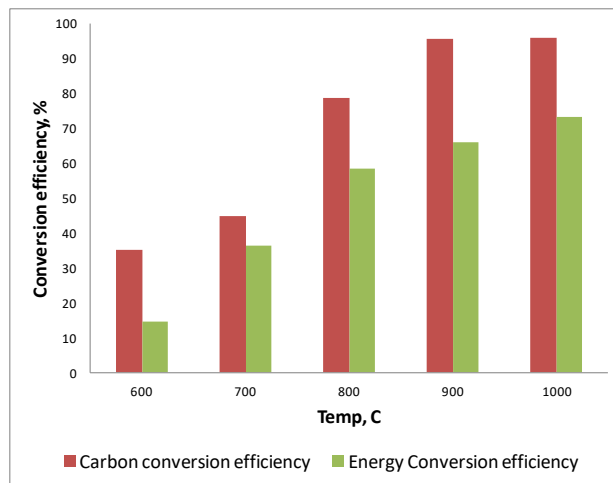
Figure 5-40 : Carbon and energy conversion efficiencies at different temperatures, case 3

5.5 Steam gasification, Case 4

5.5.1 Evolved gas analysis at different temperatures

Figure 5-41 shows, (a) the mole fraction of different gas species in the product gas and (b) the mass flow rate of different species. Both (a) and (b) are for $600^{o}C$, when steam was used

as the gas agent. The mass flow rates of syngas components are lower as compared to higher temperatures. Unlike all the previous cases CO is not the main component in the syngas. Instead, H_2 and CH_4 contribute with the highest concentrations and mass flow rates. In previous cases, the production of H_2 and hydrocarbons was exclusive for the Pyrolysis stage, while when steam is the gas agent CH_4 and H_2 are detected all through the gasification stage at 600^oC. CO, on the other hand, is only detected at the Pyrolysis stage due to the breaking of carboxylic chains in the biomass. Equations (5-3)and (5-4) are controlling the conversion mechanism in steam gasification which explains the evolution of H_2 and the absence of CO. Even at the low temperature of 600^oC; the gasification is active, and it can be observed from the evolution of H_2, CH_4, and CO_2. The gasification reaction rate is slow and the gas evolution is low. The value of the peak of CO_2 is 12% of the total evolving gas volume after 8 minutes from the start of the reaction. CO peaks at the same time as CO_2 with a peak magnitude of 3%. H_2 peak 5 minutes after CO_2 with 3% magnitude a steady H_2 generation 2% is observed after the peak till the end of the reaction. Other hydrocarbons contribute with a lower percentage of the volume; 1.4%, 0.4%, and 0.1% for CH_4, C_2H_6, and C_2H_4 respectively.

(a) Mole concentration
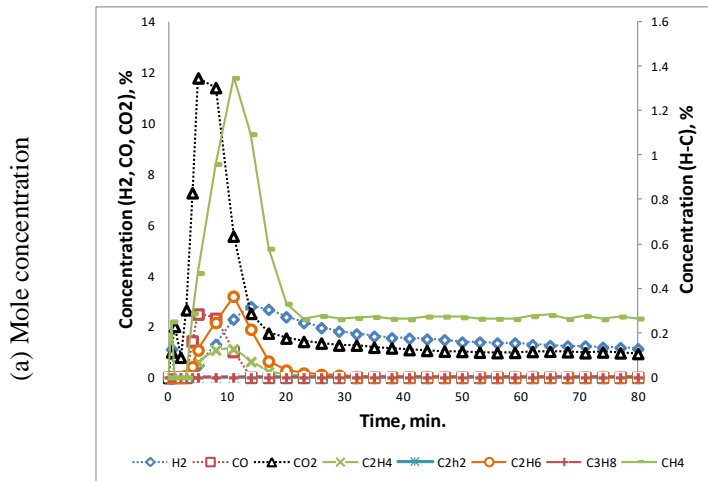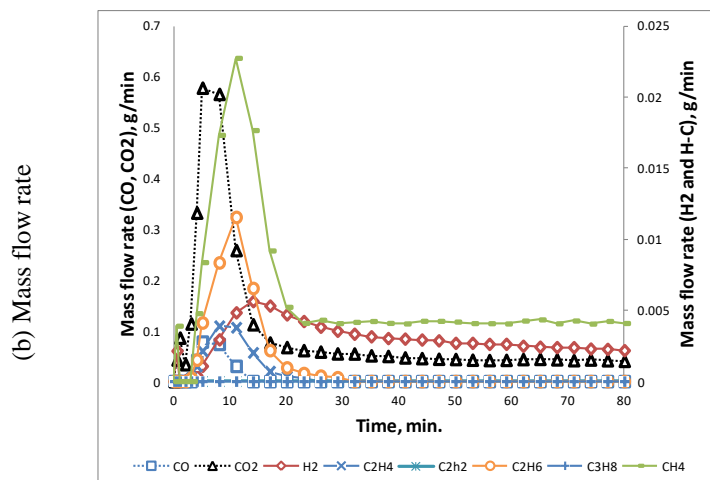
Figure 5-41: The evolution of different gases at 600°C, case 4

As the reaction temperature increases, higher flow rates of the product gases are observed in Figure 5-42 through Figure 5-45.

The peak values increase with temperature while the time at which the peaks occurs decrease. The concentration of H_2 exceeds the concentration of CH_4, but the mass flow rate of CH_4 is higher than that of H_2. At 700°C, the value of the peak of CO_2 is 19% of the total evolving gas volume after 5 minutes from the start of the reaction. CO peaks at the same time as CO_2 with a peak magnitude of 4%. H_2 concentration increases during the first 15 minutes to a maximum value of 11% after which the concentration decreases steadily due to the depletion of char. Other hydrocarbons contribute with a lower percentage of the volume; 2.7%, 0.5%, and 0.6% for CH_4, C_2H_6, and C_2H_4 respectively.
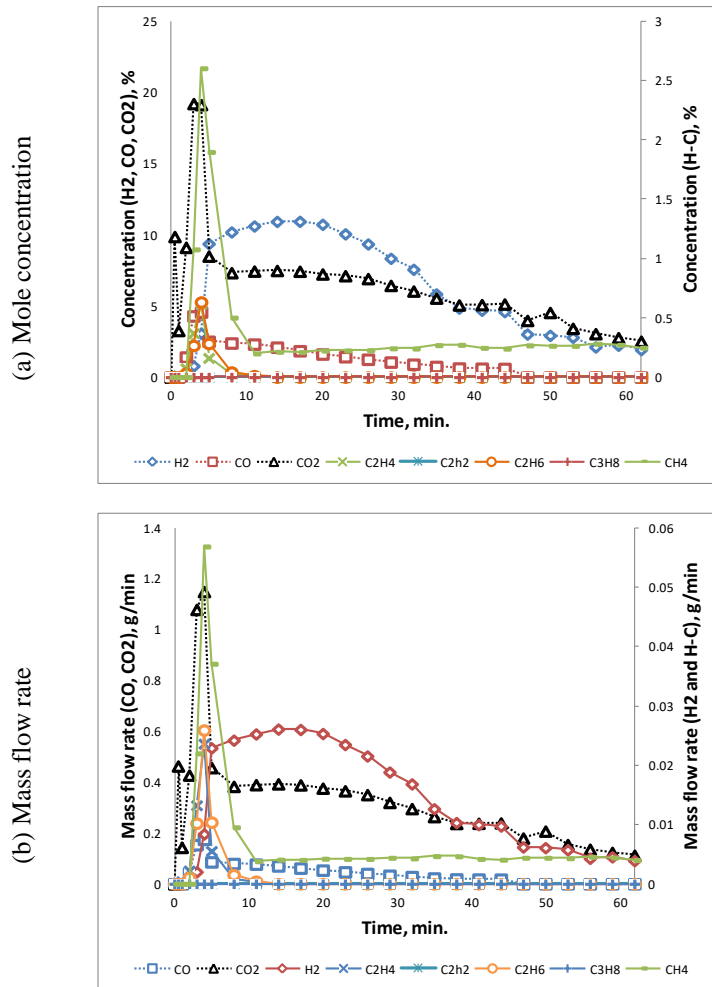
Figure 5-42 : The evolution of different gases at 700°C, case 4

CH$_4$ evolution has one peak during the Pyrolysis stage then the production is steady during the gasification stage. H$_2$ has one peak during the Pyrolysis then another peak at the beginning of gasification. The H$_2$ gasification peak value increases with the increase in temperature faster than the Pyrolysis peak. At 600°C the Pyrolysis peak is larger, while at 800°C the gasification peak is larger. At 800°C, the value of the peak of CO$_2$ is 23% of the total evolving gas volume after 4 minutes from the start of the reaction. CO peaks two times the first one is at the same time as CO$_2$ with a peak magnitude of 6% which is due to Pyrolysis, the second peak is five minutes after, with a 8% value which is a result of gasification. H$_2$ concentration increases during the first 18 minutes to a maximum value of 17% after which the

concentration decreases steadily due to the depletion of char. Other hydrocarbons contribute to a lower percentage of the volume; 4.7%, 1.0%, and 1.6% for CH_4, C_2H_6, and C_2H_4 respectively.

(a) Mole concentration

(b) Mass flow rate
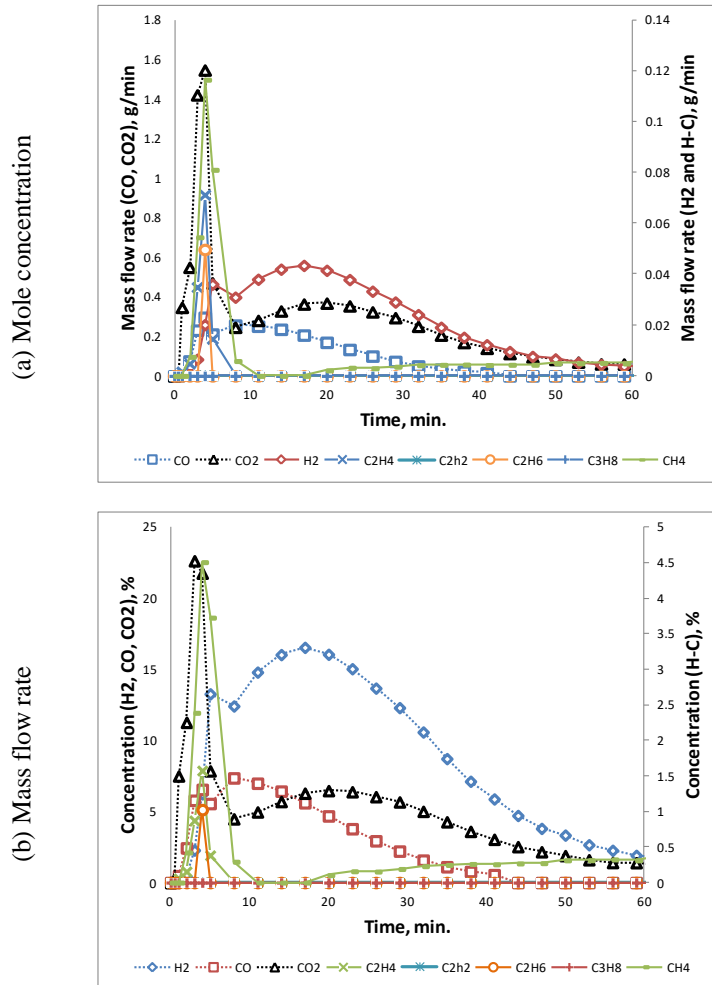
Figure 5-43 : The evolution of different gases at 800°C, case 4

At 900°C the two H_2 peaks overlap, and H_2 has only one evolution peak. CH_4 evolution is different at higher temperatures (800-1000°C). A large peak is detected during the Pyrolysis stage; then the production ceases for few minutes then a steady flow rate is produced until the end of the reaction. At 900°C, the value of the peak of CO_2 is 24% of the total evolving gas volume after 3 minutes from the start of the reaction. CO peaks two minutes after CO_2 with a

peak magnitude of 13% which is an overlap of both Pyrolysis and gasification. H_2 concentration increases during the first 5 minutes to a maximum value of 22% after which the concentration decreases steadily due to the depletion of char. Other hydrocarbons contribute to a lower percentage of the volume; 4.9%, 0.9%, and 1.9% for CH_4, C_2H_6, and C_2H_4 respectively.
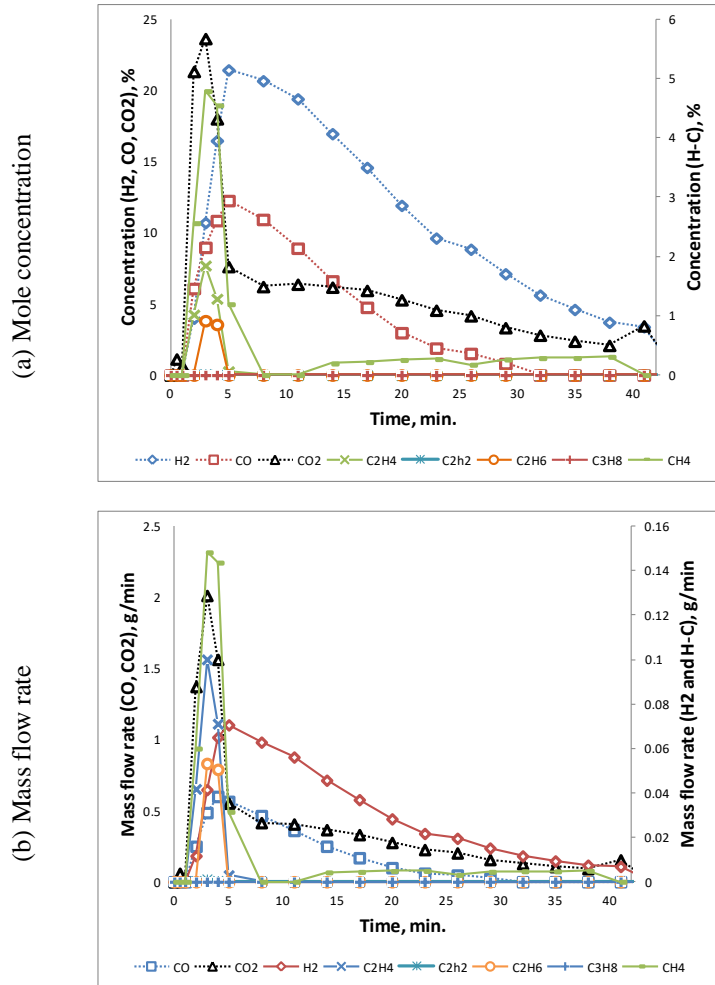
Figure 5-44 : The evolution of different gases at 900°C, case 4

CO concentration and flow rate increases significantly at the higher temperatures due to reactions (5-4) and (5-6). The evolution concentrations of heavier hydrocarbons (C_2 and C_3) decreased by increasing the temperature. At 100°C, the value of the peak of CO_2 decreased

to 18% of the total evolving gas volume after 3 minutes from the start of the reaction. CO peaks one minute after CO_2 with a peak magnitude of 22% which is an overlap of both Pyrolysis and gasification. H_2 concentration increases during the first 4 minutes to a maximum value of 24% after which the concentration decreases rapidly compared to the lower temperature due to the depletion of char. Other hydrocarbons contribute to a lower percentage of the volume; 7.5%, 0.9%, and 4% for CH_4, C_2H_6, and C_2H_4 respectively.

(a) Mole concentration

(b) Mass flow rate
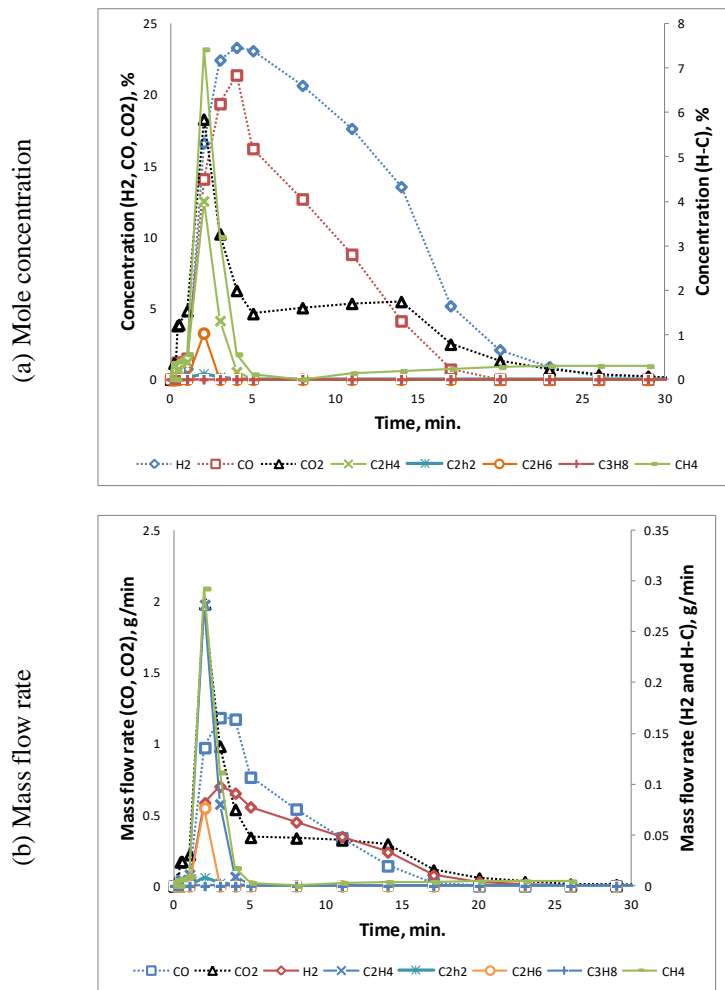
Figure 5-45 : The evolution of different gases at 1000°C, case 4

82

5.5.2 The effect of temperature on the evolution of different gases:

Figure 5-6 : The effect of temperature on the evolution of H2, case 0. H_2 contributed by the highest concentration in the syngas produced by steam gasification. High concentrations of hydrogen improve the syngas flammability and thus its desirability for power generation. H_2 was generated the during all of the reaction time unlike all other cases when it was produced mainly during the Pyrolysis process.
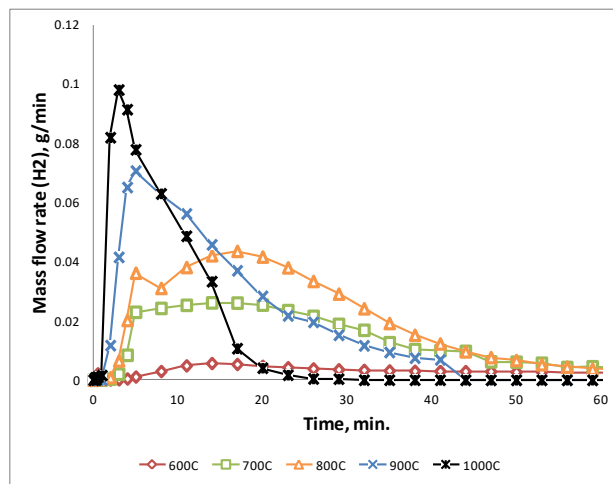
Figure 5-46 : The effect of temperature on the evolution of H_2, case 4

CO was produced at the highest flow rates, and after the first 10 minutes, it was the only significant syngas component. Reactions (5-4) and (5-6) are the prime mover of the conversion of char into gas. Figure 5-47, shows the progress of the mass flow rate of CO as the temperature increases. As the temperature increases the equilibrium concentrations of eq. (5-6) favor the production of CO and thus the peak values of CO increases.
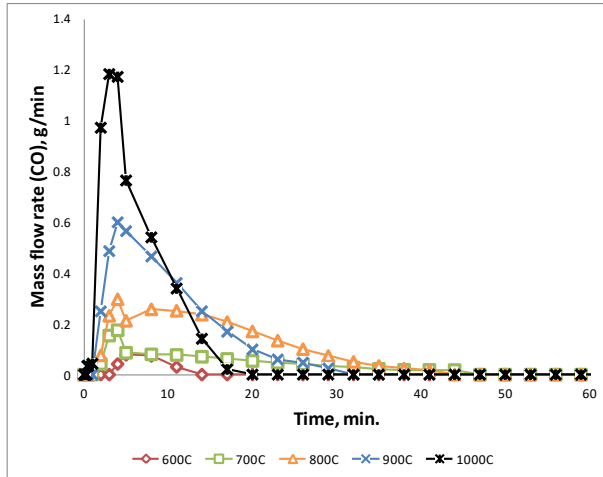
Figure 5-47 : The effect of temperature on the evolution of CO, case 4

The mass flow rate of CO_2 decreased significantly compared to all previous cases. When the temperature increased from $900^{o}C$ to $1000^{o}C$ the total CO_2 production decreased which is the result of high rates of reaction (5-6).
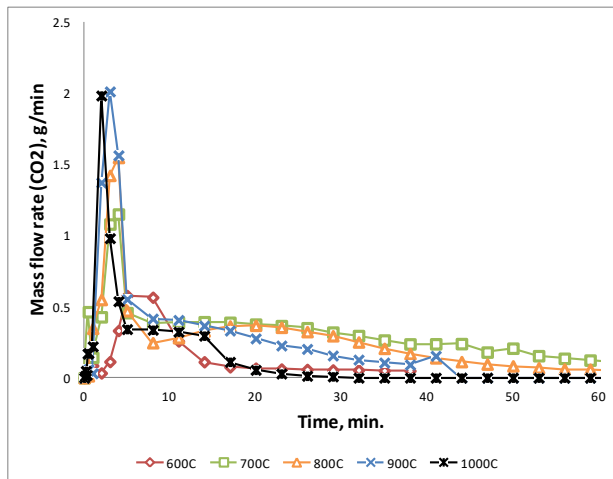
Figure 5-48 : The effect of temperature on the evolution of CO_2, case 4

Figure 5-9 : The effect of temperature on the evolution of syngas, case 0shows the total mass evolution of syngas, the mass flow rate peaked at 1.8 g/min. after 5 minutes from the start

of the reaction, at 1000°C. The peak is 2 times the peak at 900°C. The bulk mass of the gas is CO but H$_2$ contributes in a larger fraction of the energy in the gas.
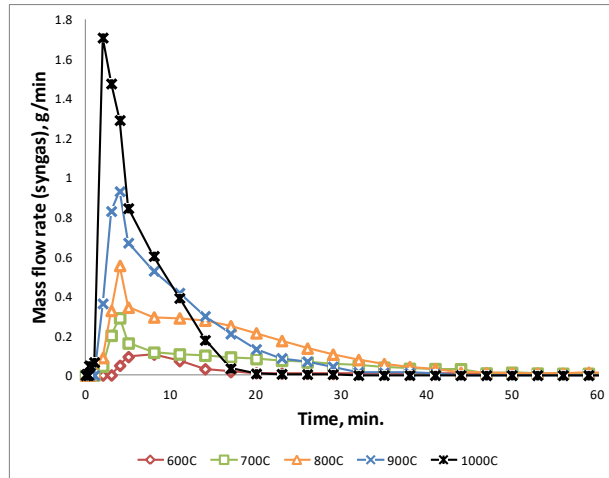
Figure 5-49 : The effect of temperature on the evolution of syngas, case 4

5.5.3 Conversion efficiency:

Figure 5-50 shows the calculated values for carbon and energy conversion efficiencies, both efficiencies increased with the temperature. The efficiency increase was gradual with no sudden increase from one temperature to another. The energy conversion efficiency at 1000°C is approaching the 100%. Reactions (5-3) and (5-4) produce H$_2$, by reducing the steam. The high heating value of hydrogen compared to CO improved the energy conversion efficiency.
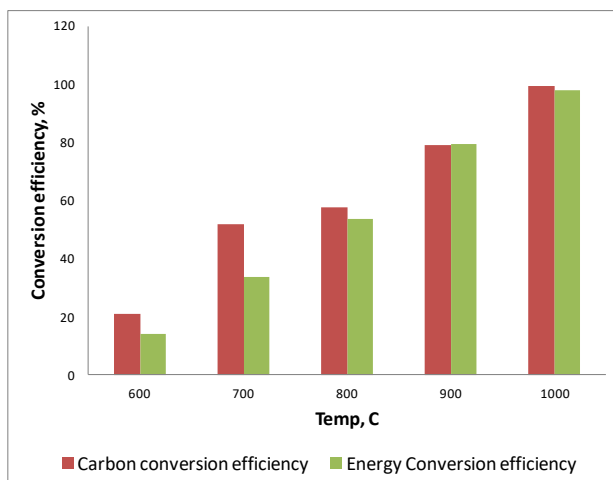
Figure 5-50 : Carbon and energy conversion efficiencies at different temperatures, case 4

5.6 Summary of cases 0-4

The five different cases were compared using the energy and carbon conversion efficiencies

5.6.1 The energy conversion efficiency for different cases:

Figure 5-51 shows the energy conversion efficiency for the five different cases. The general trend is an increase in the efficiency of conversion as the temperature increase. At $600^{o}C$ the highest efficiency was for the air gasification case. At this low temperature, the exothermic reaction due to the oxidation of some of the resulting gases, helps in increasing the conversion rate. CO_2 gasification generated the lowest energy efficiency at the $600^{o}C$ because reactions (5-2) is inactive at this low temperature. 10% O_2 came in the second place as the presence of oxygen promotes the slow reaction while steam came in the third place with a slight improvement over N_2 Pyrolysis. At $700^{o}C$ CO_2 gasification is improved as reaction (5-2) becomes active and CO_2 achieves the highest efficiency at this temperature. 10% O_2 comes second followed by steam. Air gasification did not improve at the same rate as the other cases

due to the combustion of some of the product gases. N_2 Pyrolysis in the last place of all the 5 cases at 700^oC. CO_2 gasification maintains the first place except at 1000^oC when steam provides the highest efficiency. 10% O_2 gasification showed good progression in the efficiency with the increase of temperature except at 1000^oC where the high temperature resulted in the combustion of a larger fraction of the produced gases. N_2 pyrolysis had a steady progression with temperature. Air had the slowest progression starting in first place at 600^oC and ending in the last place at 1000^oC
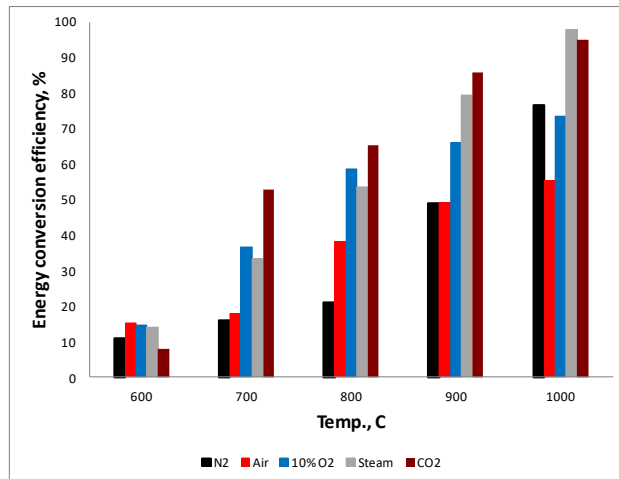
Figure 5-51 : Energy conversion efficiency for different cases

5.6.2 The carbon conversion efficiency for different cases:

Figure 5-52, Shows the carbon conversion efficiency for the 5 different cases. The general trend is an increase in the efficiency of conversion as the temperature increase. At 600^oC the highest efficiency was for the air gasification case which maintained the first place till 1000^oC when steam achieved the highest carbon efficiency. N_2 pyrolysis progressed steadily but was limited by the fixed carbon content in the manure which will not be gasified by Pyrolysis. CO_2

87

gasification had the lowest efficiency at 600°C then the efficiency picked up starting 700°C. 10% O_2 case progressed similarly to the air case.
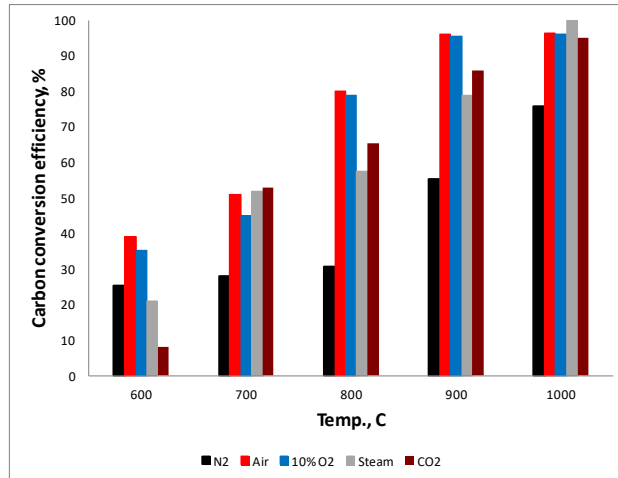
Figure 5-52: Carbon conversion efficiencies for different cases

5.7 Adding low O2 concentrations to steam gasification

Steam gasification showed the highest energy conversion of all of the cases while air gasification had the lowest reaction time. A mixture of steam and oxygen was studied to combine the advantages of each case. All different oxygen concentrations were tested at the same 900°C temperature.

5.7.1 The effect of O_2 concentration on the evolution of different gases:

Figure 5-53 shows the evolution of hydrogen mass flow rate by gasification in steam at various oxygen concentrations. The peak value increased with increase in the percentage of oxygen until 2% then it decreased at 3 and 4% oxygen concentration. Also, the peak location as well as the total gasification time slightly shifted to earlier times, which indicate a faster reaction. The larger peaks and faster reactions can be due to the exothermic reaction of oxygen with the gases providing energy to promote the pyrolytic stage. The further decrease in the peak value for

oxygen concentrations above 2% is attributed to the burning of syngas due to the abundance of oxygen at a rate higher than the positive effect of added oxygen. In the case of 0% oxygen, the peak tends to be flatter, and the hydrogen production continued for a longer period. In general, the total hydrogen fuel gas produced decreased due to the oxygen combustion, but the total reaction time was reduced by 50% when 1% of oxygen was added and by 70% when 4% of oxygen added. With the furnace maintained at 900°C, the overall process efficiency can be improved if some of the gases can be sacrificed to shorten the sample residence time in the reactor.
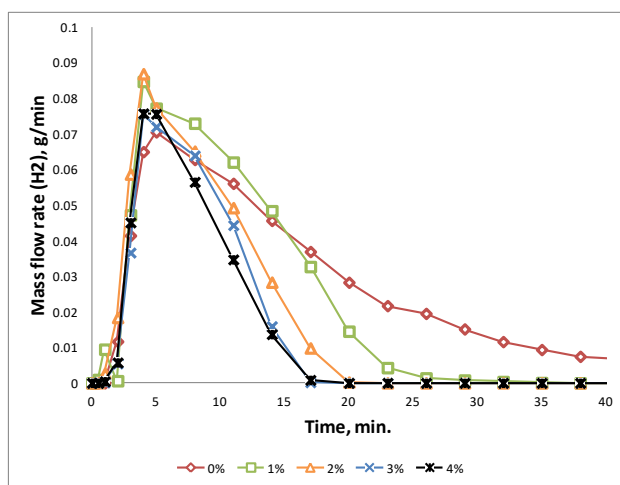
Figure 5-53 : The effect of O_2 concentration on the evolution of H_2

Unlike the hydrogen yield, the methane gas yield shown in Figure 5-54 implies a definite improvement in the methane gas yield with the increase of oxygen concentration. This improvement is less significant compared to the overall decline in hydrogen yield because methane is only produced during the early stages of pyrolysis and for a short period compared to hydrogen. The absolute increase in methane gas yield can be attributed to the exothermic energy available from hydrogen combustion and the lower flammability limits of methane in the presence of such low oxygen concentrations. So, no further decrease in the peak value was

89

observed for the range of oxygen concentrations tested. Another source of methane is from the cracking of tar due to the exothermic reactions that accompany in the presence of oxygen.
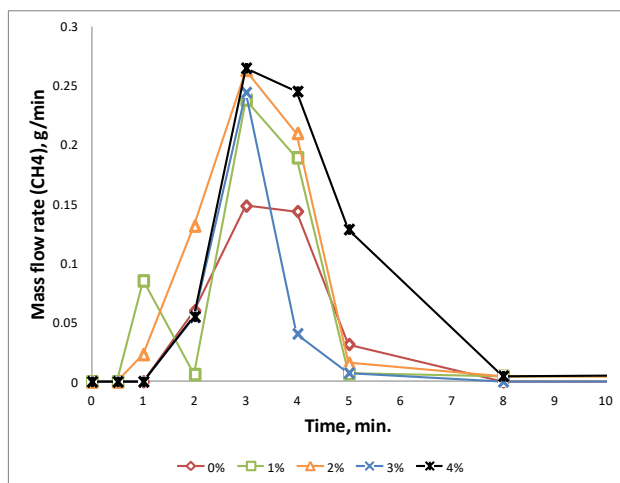
Figure 5-54 : The effect of O_2 concentration on the evolution of CH_4

The carbon monoxide gas yield was significantly increased at up to 9% oxygen concentration, after which the CO production decreased. Carbon monoxide is generated from breaking the organic chains, the dissociation of carbon dioxide (reaction (5-2)), the water gas shift reaction (5-2)and (5-6), the water gas reaction (5-4) and the incomplete combustion of fixed carbon. At the 900°C, reaction (5-3) favors the formation of carbon monoxide. When the oxygen concentration was increased beyond the 3%, a complete combustion took place along with less dissociation in the presence of the extra oxygen. This behavior is evident from Figure 5-56. The total reaction time was also decreased with increase in the oxygen concentration that also supported a comparable yield in hydrogen.
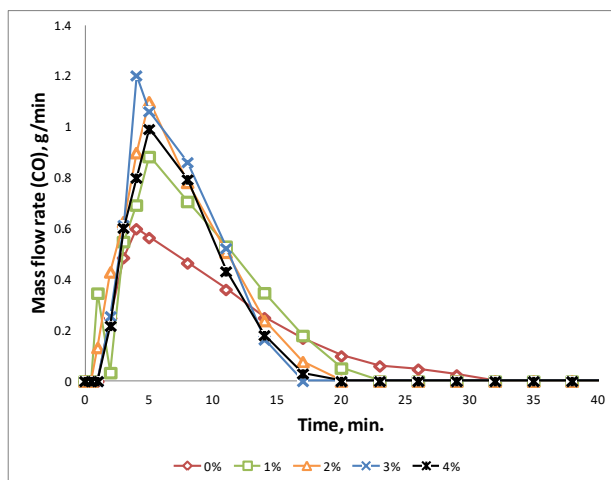
Figure 5-55 : The effect of O_2 concentration on the evolution of CO

Carbon dioxide contributed to 50% of the evolved gas composition most of the time until the process was complete (compare Figure 5-56 and Figure 5-57). The main source of carbon dioxide is the breaking of the carboxylic bonds in the organic manure chains and the complete combustion of char and hydrocarbons. During the first 10 minutes, all the samples responded in a similar manner whether excess oxygen was present or not except for the 4% oxygen sample case. With 4% oxygen the peak value slightly increased compared to all other cases, but a significant increase was observed after the peak (at about 10 minutes into gasification), where the carbon dioxide flow rate was higher by some 40% compared to the 0% oxygen case. During the first 10 minutes, the major CO_2 source is pyrolysis with minor production from char combustion. Therefore, all the samples responded similarly. With complete pyrolysis, the effect of excess oxygen was more noticeable as the CO_2 was mainly produced from the oxidation of char. Figures Figure 5-53through Figure 5-57 show that the gasification reaction was completed faster when oxygen was added to the samples.
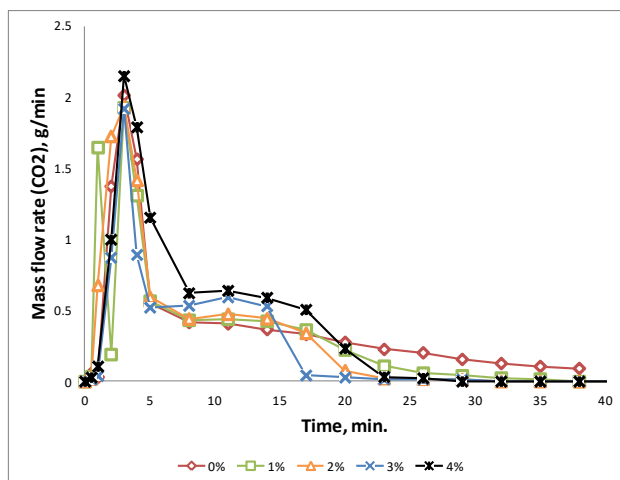
Figure 5-56 : The effect of O_2 concentration on the evolution of CO_2

Figure 5-57 shows the total syngas yield for the different cases. During the first 10 minutes, a significant improvement in the total flow rate of syngas was achieved by adding oxygen to the steam. Five minutes later the syngas yield declines and the 0% case continued to generate gas till the 40th minute while the process was complete in less than 25 minutes when the oxygen was added. Oxygen addition of 2, 3, and 4% had very similar behavior on the total syngas yield flow rate, but the gas composition was different.
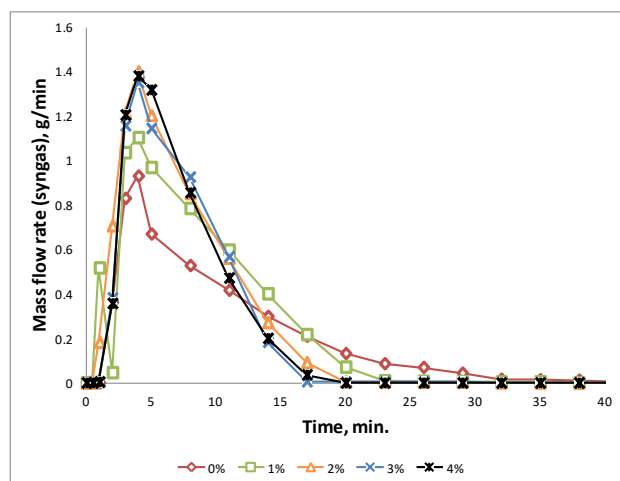
Figure 5-57 : The effect of O_2 concentration on the evolution of syngas

5.7.2 The effect of O_2 concentration on energy and carbon efficiencies

The results shown in all the above figures demonstrated that the conversion reaction was faster with oxygen added to the steam. But to obtain a quantitative assessment of the results, the total energy yield needs to be investigated. The total energy yield was calculated from the determined gas flow rates and heating values. Figure 5-58 and **Error! Reference source not found.** shows the energy and carbon conversion efficiencies for different concentrations of added oxygen. The energy conversion decreased with the increase in oxygen percentage added which was due to the combustion of some of the gases in the presence of an oxidizer and high temperature. Even though Figure 5-57 shows an increase in the total gas yield, the decrease in the total hydrogen yield shown in Figure 5-53 lead to a reduction in the net energy yield. On the other hand, the carbon conversion efficiency increased with the increase in O_2 concentration which indicates a lower tar production.
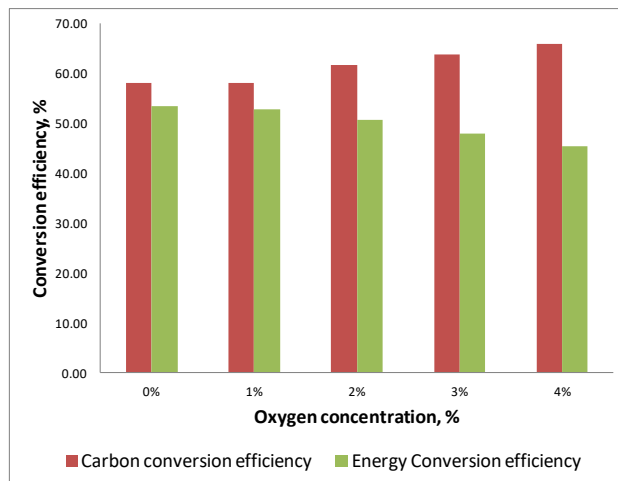
Figure 5-58 : The effect of O_2 concentration on the energy and carbon conversion efficiencies

In order to assess the improvement in the reaction time, an accumulative energy yield was calculated for each case, and the results are shown in Figure 5-59 : The effect of O2

concentration on the cumulative energy yield. After 15 minutes from the start of the reaction, all the cases where oxygen was added have already generated more than 90% of the total gas yield, while the 0% case does not reach this percentage for 11 more minutes. For instance, at the 10th minute, different cases of 0, 1, 2, 3, 4% oxygen addition have generated 144, 173, 203, 201, 193 kJ respectively. Thus, if the residence period was to be reduced to 10 minutes, then adding up to 2% oxygen to the steam improved the energy yield of 62%, even though the total energy yields for full conversion decreased by only 5% for the same case. At 10 minute after the start of gasification, all the cases with added oxygen had yielded more energy than the 0% oxygen case.
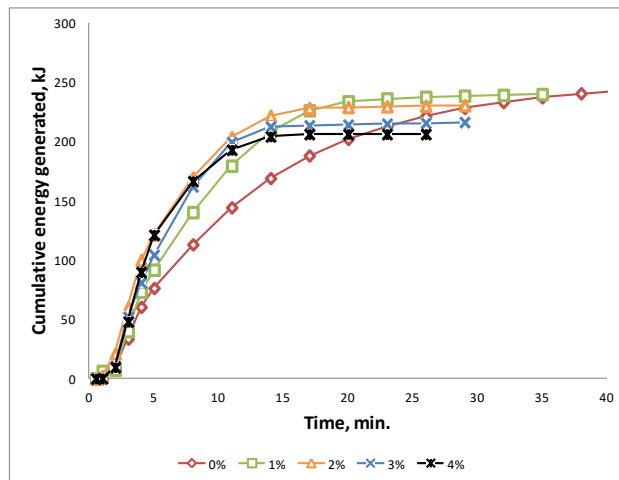
Figure 5-59 : The effect of O_2 concentration on the cumulative energy yield

Chapter 6 -   Conclusions

6.1 TGA and DTA:

The thermo-gravimetric and differential thermal analyses were conducted for chicken manure using three different gasifying media (Nitrogen, air, and carbon dioxide) with eight different heating rates (5, 10, 15, 20, 25, 30, 35, and 40°C/min.) from room temperature to 1000°C. For N_2 and CO_2 the reactions were endothermic and thus energy must be supplied in terms of heating of the sample to maintain the reaction. Air gasification was exothermic, and ignition was observed at 600°. Thus the reaction has the potentials to be self-sustainable with no external heating. The chicken manure thermal degradation implied the presence of the three components; Hemi-cellulose, cellulose, and lignin. The highest reaction rates were observed at temperatures corresponding to known peak characteristics of the three components. The only air had an extra peak for ignition at 600°C. The reaction kinetic parameters for the conversion reaction was calculated for the different medias. The Nitrogen Pyrolysis was divided into two regions at 360°C with the order of reaction of five for both regions. Kinetic parameters for air gasification were calculated using a third order single region reaction. CO_2 had the most complicated mechanism of the three cases and was divided into three regions at 360 and 630°C. The kinetic parameters varied with the heating rate. It is recommended to utilize values generated by the lowest heating rate because the slow heating rate allows a quasi-equilibrium state and thus decreasing the effects of measurements errors due to delay in response or any transient condition error. At the lowest heating rate the chemical kinetic parameters for different cases were as follows:

Table 6-1 Chemical kinetic parameters for different case:

Gasifying agent	Temperature range	Order "n"	log(A/β)	E_a, kJ/mole
N_2	$<360^oC$	5	14.9	84
	$>360^oC$	5	10.9	63.1
Air	All	3	11.2	70.3
CO_2	$<360^oC$	5	9.8	63.2
	$360<T<630^oC$	5	4.3	39
	$>630^oC$	5	72.5	575.5

The chemical kinetic parameters can be used in the simulation of chicken manure using order of reaction mechanism for solid state gasification.

6.2 EGA

Chicken manure Gasification and Pyrolysis was studied using five different gasifying media (Nitrogen, air, 10% oxygen, carbon dioxide, and steam) and at five different temperatures (600, 700, 800, 900, and 1000°C). The energy yield increased by increasing the temperature and the steam produced the highest yield followed by CO_2 then Nitrogen then air. It is discouraged to operate a gasifier at temperatures below 750°C as the tar production increases, or higher than 1050°C to avoid ash fusion difficulties. The evolution of syngas flow rates suggests increased gaseous products yield with an increase in temperature and O_2 content in the gasifying agent. The quality of gases produced was determined from the chemical composition of the gases evolved. Higher O_2 content in gasifying medium produced higher CO_2 content in the syngas at low gasification temperatures. However, at higher temperatures (more than 800°C) CO_2

decomposed into CO by reaction with the char residuals. The gaseous evolution occurred in approximately two stages. They included rapid decarboxylation and cracking of hydrocarbons followed by gasification of residue char formed after devolatilization. The gasification reaction was the fastest in the case of air, decreasing the reaction time by 75% when compared to CO_2, on the expense of the total energy yield which was also decreased by 55% at 1000^oC. Except for N_2, which represents only pyrolysis, the total energy yield was inversely proportional to the total reaction time for different gases at the same temperature. At lower temperature air yielded energy comparable or superior to the other gases as the exothermic reactions provided more energy that helped in the cracking of bonds. The cumulative energy yields showed that gasification by partial oxidation produces more energy compared to pyrolysis and very high temperatures are required for pyrolysis to match the energy yield from air gasification. The results also showed that at higher temperatures, due to better conversion kinetics, higher O_2 content in gasifying medium assists to enhance carbon oxidation. At higher temperatures, due to Boudouard reaction equilibrium, higher CO is favored – more O_2 content produces more CO_2 which then reacts with char to enhance CO yield. Residues after gasification were ash (mineral matter) that is high in chicken manure compared to other biomass feedstocks so that better and corrosive resistant hardware will be required to handle high ash amounts that also has low melting points to provide issues of fouling and deposition on heat exchange equipment in chicken manure-fired feedstock systems. The carbon conversion efficiency which was used as an indication of the possible tar conversion showed better gaseous conversion at a higher temperature. All cases approached the 100% conversion at 1000^oC with steam achieving the highest conversion. At low temperature cases with O_2 concentrations achieved a higher carbon conversion efficiency and the efficiency was directly proportional to the concentration of O_2 in

the gasifying agent. If tar generation is to be minimized while operating at lower temperatures, the addition of controlled O_2 concentrations can help in the reduction of tar but at the expense of the energy yields. The reaction rates were enhanced when small amounts of oxygen were added to steam gasification. Adding oxygen to steam gasification significantly decreased the total reaction time by some 50%. At, 4% of oxygen addition the reaction time decreased by 70%. The total energy yield was reduced by 4-15% depending on the percentage of oxygen added. An accumulative time analysis performed on the results revealed improved accumulative yield by up to 20 minutes for all cases reported here. The addition of oxygen was found to be a favorable economic option to significantly shorten the manure residence time which enabled lesser process energy requirement to generate the gasifying steam.

This study can guide in determining the most feasible gas for gasification depending on the source and availability of the gases, the energy costs, and the design temperature.

Appendix

The values for the conversion efficiencies and total energy for all the cases are tabulated in this chapter. Discussion and figures for the same data are available in 0

Table 0-1: Carbon and energy conversion efficiencies at different temperatures, case 0

temp., ^{o}C	η_c,%	E, kJ	η_E,%
600	25.36253	49.31356	10.83814
700	27.96864	72.73825	15.98643
800	30.57475	96.16293	21.13471
900	55.29581	222.3589	48.87008
1000	75.83568	348.3204	76.55393

Table 0-2: Carbon and energy conversion efficiencies at different temperatures, case 1

temp., ^{o}C	η_c,%	E, kJ	η_E,%
600	8.06	36.4	8.00
700	76.98	240.2	52.80
800	81.43	297.5	65.39
900	85.87	390.5	85.83
1000	100	432.25	95

Table A-3: Carbon and energy conversion efficiencies at different temperatures, case 2

temp., ^{o}C	η_c,%	E, kJ	η_E,%
600	39.12	69.26	15.22
700	50.84	81.52	17.92

800	79.90	174.01	38.24
900	96.00	223.09	49.03
1000	96.31	251.60	55.30

Table A-4: Carbon and energy conversion efficiencies at different temperatures, case 3

temp., ^{o}C	η_c,%	E, kJ	η_E,%
600	35.15	66.53	14.62
700	44.92	166.37	36.56
800	78.81	266.21	58.51
900	95.60	300.00	65.93
1000	96.00	333.80	73.36

Table 0-5: Carbon and energy conversion efficiencies at different temperatures, case 4

temp., ^{o}C	η_c,%	E, kJ	η_E,%
600	20.91	63.97	14.06
700	51.84	152.27	33.46
800	57.47	244.24	53.68
900	78.95	360.60	79.25
1000	99.39	445.45	97.90

Table A-6: Carbon and energy conversion efficiencies at O$_2$ concentrations

O$_2$, %	η_c,%	E, kJ	η_E,%
0%	58.05	243.21	53.45
1%	58.06	240.05	52.76

2%	61.73	230.70	50.70
3%	63.84	218.48	48.02
4%	65.96	206.27	45.33

References

[1] Ahmed, I. I., & Gupta, A. (2010). Pyrolysis and gasification of food waste: Syngas characteristics and char gasification kinetics. *Applied Energy* (87), 101-108.

[2] Ahmed, I., & Gupta, A. (2009). Syngas yield during pyrolysis and steam gasification of paper. *Applied Energy , 86*, 1813-1821.

[3] Arbalo, M., Bahadori, A., Ghiasi, M., & Abbas, A. (2015). A novel modeling approach to optimize oxygen–steam ratios in coal gasification process. *Fuel* , 1-5.

[4] Bahng, M., Mukarakate, C., Robichaud, D., & Nimlos, M. (2009). Current technologies for analysis of biomass thermochemical processing: a review. *Analytical chemistry* , 117-138.

[5] Behavior of inorganic elements in poultry manure during supercritical water gasification. (2008). *Journal of the Japan Institute of Energy* , 731-736.

[6] Boer, K., Woolcock, P., Johnston, P., & Brown, R. (2015). Steam/oxygen gasification system for the production of clean syngas from switchgrass. *Fuel* , 282-292.

[7] Breault, R. W. (2010). "Gasification processes Old and new: A basic review of the Major Technologies". *Energies* , 216-240.

[8] Bridgeman, T. G., Jones, J. M., Shield, I., & Williams, P. T. (2008). "Torrefaction of reed canary grass, wheat straw and willow to enhance solid fuel qualities and combustion properties". *Fuel* (87), 844-856.

[9] Bullushev, D., & Ross, R. (2011). Catalysis for conversion of biomass to fuels via pyrolysis and gasification: A review. *Catalysis today* , 1-13.

[10] Caputo, A., Palumbo, M., Pelgagge, P., & Scacchia, F. (2005). Economics of biomass energy utilization in combustion and gasification plants:effects of logistic variables. *Biomass and Bioenergy* (28), 35-51.

[11] Chatelier, L. (1887). "The action of heat on clays". *Bull. Soc. Franc. Min.* , 204-211.

[12] Collard, F. X., Blin, J., Bensakhria, A., & Valette, J. (2012). Influence of impregnated metal on the pyrolysis conversion of biomass constituents. *Journal of Analytical and Applied Pyrolysis* (95), 213-226.

[13] Dry, M. E. (1996). "Practical and Theoretical aspects of the catalytic Fischer-Tropsch process". *Applied Catalysis A , 138* (2), 319-344.

[14] Glass, H. D. (1954). *Investigation of rank in coal by differential thermal analysis.* Urbana, Illinois: State of Illinois, Department of Registration and education.

[15] Hoogendoorn, J. C., Andrew, s. P., & Schulz, H. (1981). "Motor Fuels and chemicals from coal via the Sasol Synthol Route [and Discussion]". *Philosophical transaction A , 300*, 99-109.

[16] Ibrahim, M. S., & Amano, R. (2015). Simultaneous Differential Thermal and Thermogravimetric Analysis of Chicken Manure Gasification using Nitrogen and carbon dioxide. *7th ISEES International Workshop on Sustainable Energy, Environment & Safety with Railway Centric Theme.* Lucknow, India: Indian institute of Technology, Kanpur.

[17] Ibrahim, M. S., Gupta, A., & Amano, R. (2013). Experimental investigation of gasification of biomass using carbon dioxide. *51ST AIAA Aerospace Sciences Meeting.* Dallas, Texas: AIAA.

[18] Ibrahim, M. S., Gupta, A., Gage, D., Zeamer, A., & Amano, R. (2014). "Chicken Manure Pyrolusis Using Carbon Dioxide". *ASME 2014 International Design Engineering Technical Conferences and Computers and Information in Engineering Conference.* Buffalo, New York: ASME.

[19] Kalinci, Y., Hepbasili, A., & Dincer, I. (2009). Biomass-based hydrogen production: A review and analysis. *International journal of hydrogen energy* , 8799-8817.

[20] Karatas, H., Olgun, H., & Akgun, F. (2012). Experimental results of gasification of waste tire with air&CO2, air&steam and steam in a bubbling fluidized bed gasifier. *Fuel process technology* , 166-174.

[21] Kelleher, B., Leahy, J., & Henihan, A. (2002). Advances in poultry litter disposal technology – a review. *Bioresources technology* , 27-36.

[22] Kim, S., & Agblevor, F. (2007). Pyrolysis characteristics and kinetics of chicken litter. *Waste management* , 135-140.

[23] Kirubakaran, V., Sivaramkrishnan, V., Premalatha, M., & Subramanian, P. (2007). Kinetics of Auto-Gasification of Poultry Litter. *International journal of green energy* , 519-534.

[24] Kissinger, H. E. (1957). "Reaction Kinetics in Differential Thermal Analysis". *Analytical chemistry* , 1702-1706.

[25] Kissinger, H. E. (1956). Variation of peak temperature with heating rate in differential thermal analysis . *Journal of research of the national bureau of standars* .

[26] Kracek, F. C. (1929). "The Polymorphism of Sodium Sulphate. I: Thermal Analysis". *J. Phys. Chem.* , 1281-1303.

[27] Kumar, A., Jones, D., & Hanna, M. (2009). Thermochemical biomass gasification: A review of the current status of the technology. *Energies* , 556-581.

[28] Mansaray, K. G., & Ghaly, A. E. (1999). Determination of kinetic parameters of rice husks in oxygen using thermogravimetric analysis. *Biomass and Bioenergy* (17), 19-31.

[29] Mansaray, K. G., & Ghaly, A. E. (1998). Thermal dgradation of rice husks in Nitrogen atmosphere. *Bioresource Technology* (65), 13-20.

[30] Mermoud, F., Golfier, F., Salvador, S., Van De Steene, L., & Dirion, J. L. (2006). "Experimental and numerical study of steam gasification of a single charcoal particle". *Combustion and Flame* (145), 59-79.

[31] Mermoud, F., Salvador, S., Van de steen, L., & Golfier, F. (2006). Influence of the pyrolysis heating rate on the steam gasification rate of large wood char particles. *Fuel* (85), 1473-1482.

[32] Murphy, C. B. (1958). "Differential thermal analysis". *Analytical chemistry* , 867-872.

[33] NAS. (1983). *"Producer gas: Another fuel for motor transport".* Washington D.C: National Academy Press.

[34] Netherlands, E. r. (n.d.). *Phyllis2*. Retrieved from Database for biomass and waste 2015: https://www.ecn.nl/phyllis2

[35] NETL. (2015). *National Energy technology laboratory*. Retrieved November 11, 2015, from US DOE: http://www.netl.doe.gov/research/coal/energy-systems/gasification/gasifipedia/history-gasification

[36] Norton, F. H. (1925). "Mechanism of spalling". *J. Am. Ceram. So.* , 29-39.

[37] Parthasarathy, P., & Narayanan, K. (2014). Hydrogen production from steam gasification of biomass: Influence of process parameters on hydrogen yield – A review. *Renewable energy* , 570-579.

[38] Partridge, E. (1941). *J. Am. Chem. SOC* , 454.

[39] Pinto, F., Andre, R., Miranda, M., Neves, D., & Varela, F. (2016). Effect of gasification agent on co-gasification of rice production wastes mixtures. *Fuel* , 407-416.

[40] Poletto. (2010). Materials produced from plant biomass: Part I: evaluation of thermal stability and pyrolysis of wood. *Materials Research* , 375-379.

[41] Priadarashan, S., Annamalai, K., Sweeten, J., Holtzapple, M., & Mukhtar, S. (2005). Co-gasification of blended coal with feedlot and chicken litter biomass. *Proceedings of the combustion institute* , 2973-2980.

[42] Puig-Arnavat, M., Bruno, J., & Coronas, A. (2010). Review and analysis of biomass gasification models. *Renewable sustainable energy* , 2841-2851.

[43] Reed, T. B. (1988). *"Handbook of Biomass downdraft gasifier engine systems"*. US DOE: Solar energy research institute.

[44] Ridlington, E. (2016). *Frontier Group*. Retrieved from http://www.frontiergroup.org/reports/unsustainable-path

[45] Saxena, R., Seal, D., Kumar, S., & Goyal, H. (2008). Thermo-chemical routes for hydrogen rich gas from biomass: A review. *Renewable sustainable energy* , 1909-1927.

[46] Sharma, S., & Sheth, P. (2015). Air–steam biomass gasification: Experiments, modeling and simulation. *Energy conversion management* , 307-318.

[47] Song, T., Wu, J., Shen, L., & Xiao, J. (2012). Experimental investigation on hydrogen production from biomass gasification in interconnected fluidized beds. *Biomass and bioenergy* (36), 258-267.

[48] Sutton, D., Kelleher, B., & Ross, J. (2001). Review of literature on catalysts for biomass gasification. *Fuel process technology* , 155-173.

[49] Tanksale, A., Beltramini, J., & Lu, G. (2010). A review of catalytic hydrogen production processes from biomass. *Renewable sustainable energy* , 166-182.

[50] Van de steen, L., Tagutchou, J. P., EscuderoSanz, F. J., & Salvador, S. (2011). Gasification ofwood chip particles:Experimenta land numerical study of char–H2O, char–CO2, andchar–O2 reactions. *Chemical Engineering Science* (66), 4499-4509.

[51] Van Dyk, J. C., Keyser, M. J., & Coertzen, M. (2006). "Syngas production from South African coal sources using Sasol-Lurgi gasifiers". *International Journal of Coal Geology , 65* (3-4), 243-353.

[52] Vold, M. J. (1949). "Differential Thermal Analysis". *Analytical chemistry* , 683-688.

[53] Vold, R. D. (1941). *J. Am. Chem.* , 2915.

[54] Wang, S., Guo, X., Wang, K., & Luo, Z. (2011). Influence of the interaction of components on the pyrolysis behavior of biomass. *Journal of Analytical and Applied Pyrolysis* (91), 183-189.

[55] White, J. E., Catallo, W. J., & Legendre, B. J. (2011). "Biomass pyrolysis kinetics: A comparative critical review with relevant". *Journal of Analytical and Applied Pyrolysis* (91), 1-33.

[56] Woolcock, P., & Brown, R. (2013). A review of cleaning technologies for biomass-derived syngas. *Biomass and bioenergy* , 54-84.

[57] Yanagida, T., Minowa, T., Shimizu, Y., Matsumura, Y., & Noda, Y. (2009). Recovery of activated carbon catalyst, calcium, nitrogen and phosphate from effluent following supercritical water gasification of poultry manure. *Bioresources technology* , 4884-4886.

[58] Yang, H. (2007). Characteristics of hemicellulose, cellulose and lignin pyrolysis. *Fuel* , 1781-1788.

[59] Yanik, J., Stahl, R., Troeger, N., & Sinag, A. (2012). "Pyrolysis of algal biomass". *Journal of Analytical and Applied Pyrolysis* .

Curriculum Vitae

Mohamed Saeed Ibrahim Hussein

3739 S. Packard Ave, St. Francis, Wi, 53235, USA

mmhmdsi@gmail.com / ibrahim3@uwm.edu

Feb., 1985

414-306-0436

Work / Research interests

Mechanical engineering, Computational fluid dynamics using both commercial software and generating codes, Fluid mechanics, Heat transfer, Combustion, Fire protection, Environmental protection, Biomass gasification.

Education

- PhD in engineering from the University of Wisconsin Milwaukee, Accumulative GPA 3.9, Dec. 2016.

- Dissertation: Experimental investigation of chicken manure pyrolysis and gasification.

- M Sc. in mechanical power engineering, Faculty of engineering, Cairo University, 2010 (87%).

- Thesis: Numerical Simulation of Hydrogen-Air Reacting Flows in Rectangular Channels with Catalytic Surface Reactions, 2010

-Graduated from Cairo University, Faculty of Engineering, Mechanical Power department. (Distinction 3rd on my department GPA 3.9).

- Senior design project on Air-conditioning in Cairo University. (Distinction)

Publications

1- K.G. Burra, M.S. Hussein, R.S. Amano, A.K. Gupta, "Syngas evolutionary behavior during chicken manure pyrolysis and air gasification," Applied Energy, Nov.2016, 181, P 408-415.

2- M.S. Hussein, K.G. Burra, R.S. Amano, A.K. Gupta, "Effect of oxygen addition in steam gasification of chicken manure," Fuel, Feb. 2017, 189, P 428-435.

3- M.S. Hussein, K.G. Burra, R.S. Amano, A.K. Gupta, "Chicken Manure Gasification and Pyrolysis using different Gas Media," In progress.

4- Mohamed S. I. Hussein, Madison Morrison , and Ryoichi Amano, "Simultaneous Differential thermal and thermogravimetric analysis of chicken manure gasification using Nitrogen, Air and carbon dioxide," Propulsion and energy 25-27 July 2016, Salt Palace convention center, Salt Lake city, Utah

5- Ryoichi S. Amano, Mohsen M. Abou-Ellail, Samer Elhaw, Mohamed Saeed, "Numerical Simulation of Hydrogen-Air Reacting Flows in Rectangular Channels with Catalytic Surface Reactions", Springer Heat and mass transfer journal, September 2013, Volume 49, Issue 9, pp 1243-1260.

6- Alka Gupta, Mohamed S. Ibrahim, R.S. Amano, "Experimental study of novel passive control methods to improve combustor exit temperature uniformity", Springer Heat and mass transfer journal, June 2014, Volume 51, Issue 1 , pp 23-32

7- Mohamed Ibrahim, Abul Alsultan, Shahoa Shen, Ryoichi Amano, "Advances in Horizontal axis Wind turbine blade design: Introduction of slots and tubercle," ASME Journal of Energy Resources technology, September 2015, Volume 137, Issue 5, 051205.

8- Alka Gupta, Mohamed Ibrahim, Ryoichi Amano, "Effect of Jet-to-Mainstream Momentum Flux Ratio on Mixing Process," Springer Heat and mass transfer journal, 2015, online May 2015.

9- Mohamed Ibrahim, Ryoichi Amano, "Simultaneous Differential Thermal and Thermo-gravimetric Analysis of Chicken Manure Gasification using Nitrogen and Carbon Dioxide," 7th ISEES International Workshop, Sustainable Energy, Environment & Safety with Railway Centric Theme, December 2015, Lucknow, India.

10- Mohamed Ibrahim, Abdul Alsultan, Shahoa Shen, Ryoichi Amano, "Novel Horizontal axis Wind turbine blade designs", 2014 International Conference on New Generation Wind Energy, October 2014, Madrid, Spain (Keynote Paper)

11- Mohamed S. Ibrahim, Alka Gupta, R. S. Amano, "Experimental investigation of Gasification of biomass using carbon dioxide," 51st AIAA Aerospace Sciences Meeting, January, 7-11, 2013, Dallas, Texas.

12- Mohamed Ibrahim, Alka Gupta, Dave Gage, Justin Zeamer, Ryoichi Amano, "Chicken manure Pyrolysis using carbon dioxide", Proceedings of ASME: ASME DFMLC 2014, August 17-20, Buffalo, NY

13- And other conferences papers

Professional Experience

- August 2011 till December 2016 as a researcher in CEAS of the University of Wisconsin Milwaukee, USA.
-Fall 2012 till December 2016 as an Instructor and teaching assistant in the mechanical department at the Univ. of Wisconsin Milwaukee. Teaching courses of Fundamentals thermodynamics, Heat Transfer, air-conditioning and Fluid mechanics labs.
- August 2007 till August 2011 as a teaching assistant in the Mechanical power department, Faculty of Engineering, Cairo University, teaching courses of Thermodynamics, Combustion, Energy conservation, Environmental protection, Laboratories and measurements.
- May 2008 till August 2011 as a part time technical office engineer in the engineering company for project services (ProService contracting) working on Air conditioning, fire protection systems, and plumbing

Skills
-Arabic   (Mother tongue)
- English   (Fluent)
- French   (Minimal)
-Star CCM+   (Very good)
-ANSYS Fluent   (Very good)
- AutoCAD   (Very good)
- Microsoft office   (Very good)

Activities and Awards

-Distinguished graduate student award from the University of Wisconsin Milwaukee 2015
-Organizer, secretary and speaker in the "International conference for new generation wind turbines", October 2014, Madrid, Spain.
-Reviewer for the ASME IDETC 2014 international conference
-Volunteering in the CEAS volunteer tutor center in UWM for 2013 and 2012.
-Vice president of the AIAA student organization in UWM.
-Chancellor Award Fall 2012-Spring 2015